

Optical and Electronic Properties of Functional Polythiophenes

by

Tamara Katherine Kunz

Hon. B.Sc., Chemistry (Co-op)
University of Victoria, 2003

A THESIS SUBMITTED IN PARTIAL FULFILLMENT OF
THE REQUIREMENTS FOR THE DEGREE OF

DOCTOR OF PHILOSOPHY

in

The Faculty of Graduate Studies
(CHEMISTRY)

THE UNIVERSITY OF BRITISH COLUMBIA

(Vancouver)

December 2009

© Tamara Katherine Kunz, 2009

Abstract

The synthesis and characterization of a series of functionalized head-to-tail regioregular poly-3-alkylthiophenes are reported. The influences of the structure and functional groups on the optical and electronic properties are investigated with NMR, absorption, emission and infrared spectroscopy, gel permeation chromatography, and cyclic voltammetry.

A regioregular poly-3-alkylthiophene (**Poly-1**) was synthesized via Grignard Metathesis polymerization conditions. **Poly-1** contains bromide groups as sites of latent reactivity along the polymer backbone through which additional reactions were carried out post-polymerization. The bromide was converted to an azide group (**Poly-2**) which was further functionalized via Click chemistry with a variety of functional groups.

Click chemistry was carried out using the Huisgen 1,3-dipolar cycloaddition reaction. Post-polymerization functionalization of **Poly-2** provided a facile method for preparing a variety of related functional polymers, each with identical average chain length, average polydispersity and average distribution of monomers. Preparation of **Poly-3a**, **-3b**, and **-3c**, demonstrated the utility of the Click reaction for modifications with a variety of functional groups.

A series of poly-3-alkylthiophene analogs (**Poly-1 - Poly-11**) were characterized by absorption and emission spectroscopies and the spectra were found to be dependant on regioregularity along the polymer backbone. The UV-vis absorption maxima, varied with the percentage of head-to-tail couplings in relation to the extent of conjugation.

The series of dithienylethene functionalized oligo- (**71**) and polymer analogs (**Poly-4**, **Poly-7** and **Poly-11**) displayed fluorescence quenching capabilities upon

photoinduced ring closing of the dithienylethene moiety via energy transfer. The extent of quenching was determined to be dependent on both the length and structure of the backbone. Extended conjugation contributed to amplified fluorescence quenching as observed by complete fluorescence quenching of **Poly-4**.

The functionalization of the **Poly-2** with the stable free nitroxide radical 2,2,6,6-tetramethylpiperidine-1-oxyl is described. The resulting polymer, **Poly-12**, was characterized with cyclic voltammetry and IR spectroscopy. Electrochemical deposition of thin films of **Poly-12** onto various working electrodes is described. The thin films were investigated for potential charge storage via galvanostatic charge/discharge cycles. IR spectroscopy revealed that the nitroxide radical had sensitized the polythiophene backbone to oxidation, resulting in irreversible damage to the polymer and reduced charge storage capacity.

Chart 0-1

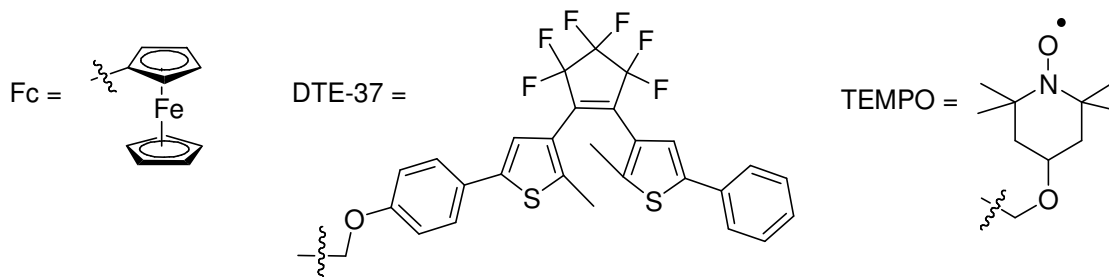
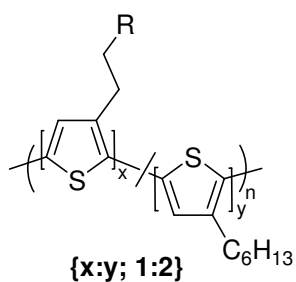


Chart 0-2



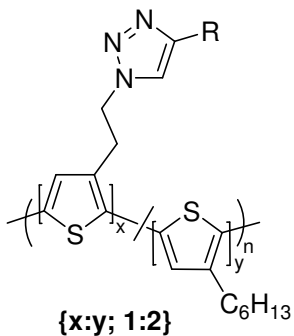
Poly-1 R = Br

Poly-2 R = N₃

{x:y; 2:3}

Poly-5 R = Br

Poly-6 R = N₃



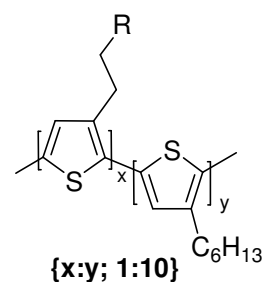
Poly-3a R = (CO)OMe

Poly-3b R = Fc

Poly-3c R = CH₂NH₂

Poly-4 R = DTE-37

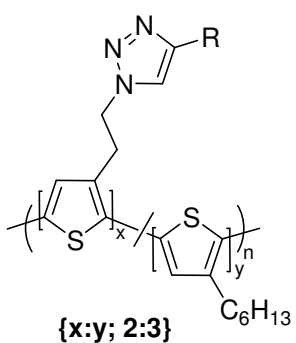
Poly-12 R = TEMPO



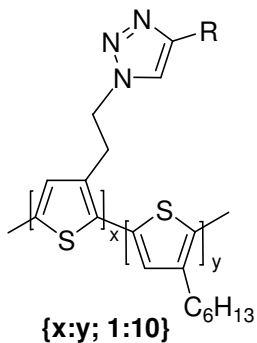
Poly-8 x = 0

Poly-9 R = Br

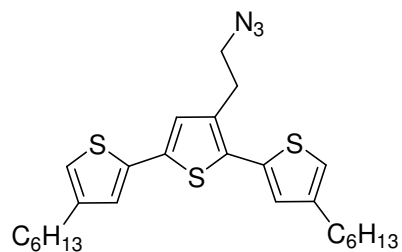
Poly-10 R = N₃



Poly-7 R = DTE-37



Poly-11 R = DTE-37



70 R = N₃

71 R = DTE-37

Table of Contents

Abstract.....	ii
Table of Contents.....	v
List of Tables.....	viii
List of Figures.....	ix
List of Charts.....	xiii
List of Schemes.....	xiv
List of Equations.....	xvi
List of Symbols and Abbreviations.....	xvii
Acknowledgements.....	xxiii
Dedication.....	xxv
Co-Authorship Statement.....	xxvi
CHAPTER 1 Introduction.....	27
1.1 Overview.....	27
1.2 Polymer Fundamentals.....	29
1.2.1 Definitions.....	29
1.2.2 Polymerization Methods.....	31
1.3 Conjugated Polymers.....	33
1.3.1 Electronic Structure.....	33
1.3.2 Polythiophene.....	34
1.3.3 Regioregularity.....	36
1.3.4 Synthetic Methods.....	38
1.4 Polymer Functionalization.....	40
1.4.1 Post-Polymerization.....	41
1.4.2 Click Chemistry.....	42
1.4.3 Huisgen 1,3-Dipolar Cycloaddition.....	43
1.5 Pendant Groups.....	44
1.5.1 Dithienylethenes.....	45
1.5.2 Stable Nitroxyl Free Radical: TEMPO.....	50
1.6 Goals and Scope.....	53
1.7 References.....	54

CHAPTER 2 Synthesis of Random Co-Polythiophenes Using GRIM Polymerization and Functionalization Via Huisgen 1,3-dipolar Cycloaddition	62
2.1 Introduction.....	62
2.2 Experimental.....	67
2.2.1 General.....	67
2.2.2 Procedures.....	68
2.3 Results and Discussion	77
2.3.1 Monomer Synthesis and Spectroscopy	77
2.3.2 Polymer Synthesis and Spectroscopy	79
2.3.3 Monomer Click Reaction and Spectroscopy.....	85
2.3.4 Polymer Click Reactions and Spectroscopy	88
2.4 Conclusions.....	92
2.5 References.....	93
 CHAPTER 3 Synthesis and Characterization of Dithienylethene Modified Oligo- and Polythiophenes	 97
3.1 Introduction.....	97
3.2 Experimental.....	100
3.2.1 General.....	100
3.2.2 Procedures.....	101
3.3 Results and Discussion	114
3.3.1 Synthesis	114
3.3.2 NMR spectroscopy.....	120
3.3.3 Size Exclusion Chromatography.....	128
3.4 Conclusions.....	130
3.5 References.....	131
 CHAPTER 4 Reversible Amplified Fluorescence Quenching of Dithienylethene Functionalized Polythiophene.....	 135
4.1 Introduction.....	135
4.2 Experimental.....	138
4.2.1 General.....	138
4.3 Results and Discussion	139
4.3.1 Absorption and Emission Studies.....	139
4.3.2 Fluorescence Quenching and Amplification.....	150
4.4 Conclusions.....	158
4.5 References.....	159

CHAPTER 5 Electrodeposition of TEMPO Functionalized Polythiophene Thin Films.161

5.1	Introduction.....	161
5.2	Experimental.....	163
5.2.1	General.....	163
5.2.2	Procedures.....	165
5.3	Results and Discussion	166
5.3.1	Synthesis and Characterization	166
5.3.2	Electron Spin Resonance Studies.....	169
5.3.3	Cyclic Voltammetry Studies	170
5.3.4	Capacity and Charge/Discharge Studies	175
5.3.5	Backbone Oxidation.....	177
5.4	Conclusions.....	180
5.5	References.....	181

CHAPTER 6 Conclusions and Future Work185

6.1	General Conclusions	185
6.2	Suggestions for Future Work.....	187
6.3	References.....	192

List of Tables

Table 2-1. Absorption and emission data comparisons for Poly-1 and Poly-2	85
Table 3-1. SEC comparative data for polymer series.	128
Table 4-1. UV-vis absorption and emission data from different polymer species	143

List of Figures

Figure 1-1. Examples of common π -CPs; polyacetylene (PA , 1), polyaniline (PANI , 2), poly(p-phenylenevinylene) (PPV , 3), polypyrrole (PPy , 4), and polythiophene (PT , 5).....	28
Figure 1-2. Oxidation (p-doping) of 1 with iodine.	33
Figure 1-3. Simplified molecular orbital diagram for a CP.	34
Figure 1-4. A schematic representation of (a) rr-HT coupling, with planar arrangement of the thiophene rings, and (b) steric interactions of the alkyl side chains due to HH/TT mis-couplings causing twisting of the PT backbone.....	37
Figure 1-5. Typical UV-vis absorption spectra of photoinduced reaction between two isomers A and B	47
Figure 1-6. Simplified energy diagram for photo-induced ring closing reaction of 1,3,5- hexatriene.....	49
Figure 2-1. ^1H NMR spectra of Poly-1 (black), 60 (red), and 63 (green). X = residual CHCl_3 in the deuterated solvent.	82
Figure 2-2. ^1H NMR spectra of Poly-1 (black) and Poly-2 (red). X = residual CHCl_3 and H_2O in the deuterated solvent.....	83
Figure 2-3. ATR-IR spectra of Poly-1 (black) and Poly-2 (red).	84
Figure 2-4. ^1H NMR spectra isomers 65 (black) and 66 (red). X = residual CHCl_3 in the deuterated solvent.	86
Figure 2-5. ^1H - ^1H NMR NOE difference spectrum (red) and ^1H NMR spectrum (black) of 65 . X = residual CHCl_3 in the deuterated solvent.	87
Figure 2-6. ^1H NMR spectra of 65 (black) and Poly-3a (red).	89
Figure 2-7. Cyclic voltammogram of Poly-3b on a Pt button electrode in dry CH_2Cl_2 containing 0.1 M $[\text{n-Bu}_4\text{N}]\text{PF}_6$. Scanned from +0.2 to +1.2 V vs. SCE, scan rate = 100 mVs^{-1}	91
Figure 3-1. Typical absorption spectra of the ring-open (black) and ring-closed (red) isomers of substituted DTE.....	98

Figure 3-2. ^1H NMR spectrum 68 dissolved in C_6D_6 (400 MHz). X = residual C_6H_6 in the deuterated solvent.	121
Figure 3-3. ^1H NMR spectra of a C_6D_6 solution of 68o as a function of irradiation time (a) 0 min, (b) 10 min, (c) 90 min, (d) 145 min (400 MHz). Irradiation with UV-lamp at 302 nm.	122
Figure 3-4. ^1H NMR spectrum of Poly-4 dissolved in C_6D_6 (300 MHz). X = residual CHCl_3 present in the deuterated solvent.	124
Figure 3-5. ^1H NMR spectra for Poly-8 (black) and Poly-9 (red) dissolved in CDCl_3 (400 MHz). X = residual CHCl_3 and water in the deuterated solvent.	126
Figure 3-6. ^1H NMR spectrum of Poly-11 dissolved in CDCl_3 (300 MHz). Inset shows the magnified baseline. X = residual CHCl_3 in the deuterated solvent.	127
Figure 4-1. Demonstration of amplified fluorescence quenching along a polymer backbone through binding of a quencher (●) to a receptor (☀).	136
Figure 4-2. (a) Absorption spectra of 68o (black dashed) and 68c (red dashed) and (b) absorption (black) and emission (red) spectra of Poly-2	140
Figure 4-3. UV-vis absorption spectra of a C_6H_6 solution of Poly-4 , with irradiation at 310 nm.	141
Figure 4-4. Emission spectra of a C_6H_6 solution of Poly-4 , with irradiation at 310 nm.	142
Figure 4-5. (a) Absorbance spectra of 68o (black dashed) and 68c (red dashed) and (b) absorbance (black) and emission (red) of 70	144
Figure 4-6. (a) UV-vis absorption and (b) emission spectra of the photo-induced ring closing reaction of a C_6H_6 solution of 71 upon irradiation with a 302 nm lamp.	145
Figure 4-7. Monitoring the change in absorbance and emission intensity of 71 over 11 ring-opening and ring-closing cycles. Absorbance monitored at 298 nm (■), and 595 nm (●). Emission monitored at 440 nm (□).	146
Figure 4-8. (a) UV-vis absorption and (b) emission spectra of the photo-induced ring closing reaction of a C_6H_6 solution of Poly-7 upon irradiation with a 302 nm lamp.	147

Figure 4-9. (a) UV-vis absorption and (b) emission spectra of the photo-induced ring closing reaction of a C ₆ H ₆ solution of Poly-11 upon irradiation with a 302 nm lamp.....	149
Figure 4-10. (a) Absorption and (b) emission spectra of Poly-4 (open: black solid lines, closed: black dotted line) and Poly-2/DTE-37 (open: red solid lines, closed: red dotted line).	150
Figure 4-11. Changes in absorbance ($\lambda_{\max} = 595$ nm) of Poly-4c (■) and Poly-2/DTE-37c (□), and changes in emission ($\lambda_{\max} = 575$ nm) of Poly-4o (●) and Poly-2/DTE-37o (○) upon approaching the PSS.	151
Figure 4-12. Normalized emission, F/F_0 ($\lambda_{\max} = 575$ nm), as a function of normalized absorbance, A/A_{PSS} ($\lambda_{\max} = 595$ nm), for the C ₆ H ₆ solutions of Poly-4 (■) and Poly-2/DTE-37 (■).	153
Figure 4-13. Initial induction of fluorescence quenching experienced by Poly-4 with shorter irradiation times. ²⁹	154
Figure 4-14. Comparison of amplified fluorescence quenching for Poly-4 (■), Poly-2/DTE-37 (■), Poly-7 (▲), Poly-11 (◆) and 71 (●).	156
Figure 5-1. IR spectra of Poly-12 (green), Poly-2 (red), and 74 (black) displaying the fingerprint region. (*) indicates the $\nu(\text{NO}\cdot)$ stretching frequency.	167
Figure 5-2. Absorption and emission spectra of CH ₂ Cl ₂ solutions of Poly-2 (black) and Poly-12 (red).	168
Figure 5-3. X-band ESR spectrum of Poly-12 in C ₆ H ₆ solution at 22 °C. Modulation Frequency: 20.00 kHz. Modulation Amplitude: 0.02 G. Time Constant: 2.56 s. Gain: 60 dB. Sweep Width: 150.6 G.	170
Figure 5-4. (a) Initial scan and (b) polymerization of Poly-12 on ITO. 0.1 M [<i>n</i> -Bu ₄ N]PF ₆ in CH ₂ Cl ₂ on ITO coated glass working electrodes. Scan rate = 50 mVs ⁻¹	171
Figure 5-5. Cyclic voltammograms of the growth of Poly-12 vs. Poly-2 . 0.1 M [<i>n</i> -Bu ₄ N]PF ₆ in CH ₂ Cl ₂ solutions growth on ITO coated glass electrodes. Scan rate = 50 mVs ⁻¹	172
Figure 5-6. Degradation of Poly-12 on ITO working electrode. 0.1 M [<i>n</i> -Bu ₄ N]PF ₆ in ACN. Scan rate = 100 mVs ⁻¹	173
Figure 5-7. Cyclic voltammogram of Poly-12 on carbon paper with increasing scan rate (Propylene carbonate, mVs ⁻¹): 25, 50, 100, 150, 200.	174

Figure 5-8. Typical galvanostatic charge-discharge curve of Poly-12 scanned at 0.1 mA in propylene carbonate with 0.1 M $[n\text{-Bu}_4\text{N}]\text{PF}_6$ supporting electrolyte. Scanned between 0.8 – 1.2 V.....	176
Figure 5-9. ATR-IR spectra of (a) Poly-12 before (black) and after (green) isolation from the CV solution and (b) Poly-12 (black) and Poly-2 (red) isolated from the polymerization reaction.....	178
Figure 6-1. Schematic of a gated sensor based on DTE photoinduced ring-closing fluorescence quenching in which DTE (👉) can only undergo the ring-closing reaction upon binding of the analyte (👈).....	189

List of Charts

Chart 0-1	iii
Chart 0-2	iv
Chart 1-1	29
Chart 1-2	30
Chart 1-3	35
Chart 1-4	37
Chart 1-5	40
Chart 1-6	50
Chart 6-1	190
Chart 6-2	191

List of Schemes

Scheme 1-1	32
Scheme 1-2	36
Scheme 1-3	39
Scheme 1-4	43
Scheme 1-5	44
Scheme 1-6	45
Scheme 1-7	50
Scheme 1-8	51
Scheme 1-9	52
Scheme 2-1	63
Scheme 2-2	64
Scheme 2-3	66
Scheme 2-4	77
Scheme 2-5	80
Scheme 2-6	86
Scheme 2-7	88
Scheme 3-1	114
Scheme 3-2	115
Scheme 3-3	116
Scheme 3-4	118
Scheme 3-5	119
Scheme 3-6	120

Scheme 5-1	161
Scheme 5-2	162
Scheme 5-3	166
Scheme 5-4	179
Scheme 6-1	188
Scheme 6-2	190
Scheme 6-3	191

List of Equations

$M_w = DP \cdot M_{ru}$	Eq. 1-1.....	30
$I-I \rightarrow 2 I \cdot$	Eq. 1-2.....	32
$I \cdot + M \rightarrow I-M \cdot$	Eq. 1-3.....	32
$I-M \cdot + nM \rightarrow I-[M]_n-M \cdot$	Eq. 1-4.....	32
$I-[M]_n-M \cdot + S \rightarrow I-[M]_n-M + (S^*)$	Eq. 1-5	32
$PSS (\%) = B_{eq} / A_i \times 100$	Eq. 1-6.....	48
$A^* + Q \rightarrow A + Q$	Eq. 4-1.....	152
$A^* + Q \rightarrow A + Q^*$	Eq. 4-2.....	152
$C(Ah/kg) = \frac{N_A \times e}{3600 \times \left(\frac{MW}{1000} \right)}$	Eq. 5-1.....	175

List of Symbols and Abbreviations

Abbreviation	Description
α	methylene group; directly attached to aromatic ring
A	Ampere; chromophore: generic ring-open isomer (DTE)
A_i	initial concentration of open isomer (DTE)
ACN	acetonitrile
AFM	atomic force microscopy
AFP	amplified fluorescent polymer
ATR	attenuated total reflectance
β	methylene group; once removed from aromatic ring
B	generic ring-closed isomer (DTE)
br	broadened (NMR)
BDE	bond dissociation energy
BPP	bis(<i>p</i> -phenylene)-34-crown-10
B_{eq}	equilibrium concentration of closed isomer (DTE)
χ	methylene spacer (DTE)
c	ring closed isomer
C	Coulomb (A s)
°C	degrees Celsius
cm^{-1}	wavenumber (IR)
CP	conjugated polymer
Co-op	Cooperattive Education

CV	cyclic voltammetry
Calcd	calculated
δ	chemical shift (ppm)
d	doublet (NMR)
dB	decibel
dd	doublet of doublets (NMR)
dppe	diphenylphosphinoethane
dppp	diphenylphosphinopropane
DMF	N,N-dimethylformamide
DP	degree of polymerization
\overline{DP}_w	weight average degree of polymerization
DTE	dithienylethene
ϵ	molar absorptivity ($\text{L mol}^{-1} \text{cm}^{-1}$)
e	electron charge
E_{red}	peak potential, reduction process (V)
EI	electron impact
ESI	electrospray ionization
ESR	electron spin resonance
EtOAc	ethyl acetate
ϕ	methyl groups (DTE)
Φ	quantum yield
F	Farad (A s V^{-1}); fluorescence intensity measured at time t
Fc	ferrocene

FET	field effect transistor
FT	Fourier transform
G	Gauss
GHz	gigahertz
GRIM	Grignard Metathesis
h	hour
h	Planck's constant
HPLC	high-pressure liquid chromatography
HOMO	highest occupied molecular orbital
HH	head-to-head
HR	high resolution
HT	head-to-tail
Hz	Hertz
<i>i</i> -	iso: equal
I	quantum spin-spin coupling constant
I·	initiator
ITO	indium tin oxide
J	NMR coupling constant (Hz)
k_o	heterogeneous rate constant
k_{ex}	self exchange rate constant
kHz	kilohertz
kJ	kilojoules
λ_{max}	wavelength at band maximum (nm)

L-	left handed enantiomeric form
LCD	liquid crystal display
LUMO	lowest unoccupied molecular orbital
m	multiplet (NMR)
M	molarity (mol L ⁻¹); molecular weight of molecule (MS)
<i>M</i>	monomer
M ⁺	molecular ion
<i>M_{ru}</i>	molecular weight of the repeat unit
\bar{M}_n	number average molecular weight
<i>M_w</i>	molecular weight
\bar{M}_w	weight average molecular weight
MW	equivalent mass of polymer (g)
<i>m/z</i>	mass-to-charge ratio
mA	milliampere
MHz	megahertz
min	minute
mmol	millimole
mol	mole
MS	mass spectrometry
mV	millivolts
v	frequency
n	number
<i>n</i> -	normal

N _A	Avogadro's number
NBS	N-bromosuccinimide
NOE	nuclear overhauser effect
NR	nitroxyl radical
Nu	nucleophile
o	ring open isomer
<i>o</i> -	ortho: arene substitution pattern, next to each other
OLED	organic light emitting diode
OPV	organic photovoltaics
<i>p</i> -	para: arene substitution pattern, opposite from each other
P3AT	poly(3-alkylthiophene)
P3HT	poly(3-hexylthiophene)
PA	polyacetylene
PANI	polyaniline
PDI	polydispersity index
PPE	poly(phenylene ethynylene)
ppm	parts per million
PPV	poly(<i>p</i> -phenylenevinylene)
PPy	polypyrrole
PSS	photostationary state
PT	polythiophene
PTI	Photon Technology International
Q	quencher

R	generic chemical moiety / end group
$R\cdot$	neutral radical
R^+	oxidized radical / cation
R^-	reduced radical / anion
R_f	retention factor
rr	regioregular
r.t.	room temperature
s	second; singlet (NMR)
S^*	activated species from chain transfer
SAM	self assembled monolayer
SCE	saturated calomel electrode
SEC	size exclusion chromatography
S/N	signal-to-noise
θ	twist angle departure from coplanarity
t	triplet (NMR)
<i>t</i> -	tertiary
TEMPO	2,2,6,6-tetramethylpiperdine-1-oxyl
THF	tetrahydrofuran
TLC	thin layer chromatography
TT	tail-to-tail
V	Volt
vis	visible

Acknowledgements

First and foremost, I have to thank my supervisor Dr. Mike Wolf. Thank you for giving me an option when things were uncertain and thank you even more for standing behind my decision to finish what I started. You gave me the opportunity to prove something to myself, and for that I am forever thankful.

I would like to extend my appreciation to Dr. Colin Fyfe for reading this thesis in its entirety. On that note, I am also especially grateful to Marek Majewski, without whom, I may never have shown a chapter to Mike. Thank you for reading my entire thesis, some chapters twice, and always with thorough and thoughtful editing. I am indebted to you. I would like to thank all members, past and present, of the Wolf and MacLachlan groups. It has been such a pleasure to work with such a warm, intelligent and entertaining group of people. It will be hard to leave such a fantastic work environment. Some days, it was definitely the people that I came into work for.

This thesis would have never been possible without the help and guidance that I received from the chemistry support staff. In particular, David Wong, for weighing out multiple samples of carbon paper, with the promise that this was the last time, only for me to show up again the following week; Brian Ditchburn, for repairing the electrochemistry cell, time and again after I broke it; and finally, Zorana Danilovic, for laughing at me when caught talking to myself. I would also like to thank all members of chemistry acquisitions, the mechanical shop, electronics, and secretarial staff for the help and humour that they provided to me during the course of my work here at UBC.

A special thank you goes to both Prof. Neil Branda and Dr. Jeremy Finden, my collaborators on the DTE project. Thank you for all of the thoughtful discussions and

hard work that made that project come to light. I must also thank Prof. Steven Holdcroft for the use of his SEC instrument, and thank you to UBC for funding.

Acknowledgments must also be made to Dr. Peter Wassell and Angelo Ariganello for believing in my teaching abilities. The encouragement and opportunities I have received from you both will never be under appreciated.

To all of my friends, I count myself blessed because I have too many to mention individually. I hope you all know that this thesis would never have been possible without the support and laughter that I gained from each and every one of these friendships. That being said, there are a few names that I must mention: Agostino Pietrangelo, Toby Astill, and Marek Majewski. Thank you all for the ‘tough love’. To my closest girlfriends, Elektra Jordan and Sylvia Lymburner, I can never thank you enough, just for being there.

My final words of appreciation go to my family. This trip has not been smooth sailing and I cannot thank them enough for being, at the same time, both my shoulder to cry on, and my legs to walk on (literally) during the last six years. To Cindy, Lee, and my beautiful new niece, Jorja, thank you for helping me find my smile. To the Jordans, my extended family, thank you for providing me with a home away from home. And to my wonderful, supportive, and loving parents, Fred and Wendy, thank you for EVERYTHING.

Dedication

To my family at Mahony & Sons.

Co-Authorship Statement

A version of Chapter 2 will be submitted for publication. Kunz, T. K.; Stott, T. L.; Wolf, M. O., Functionalized Polythiophenes via “Click Chemistry”. The work presented in this chapter was done in collaboration with Dr. Tracey L. Stott, at the University of British Columbia. I am the principal investigator and primary author of this work under the supervision of Prof. Michael Wolf. Compounds **60** and **Poly-1** were both prepared by Dr. Tracey L. Stott.

A version of Chapters 3 and 4 has been published. Finden, J.; Kunz, T. K.; Branda, N. R.; Wolf, M. O., *Adv. Mater.* **2008**, 20, (10), 1998-2002. The work presented in these chapters was done in collaboration with Prof. Neil R. Branda and Dr. Jeremy Finden at Simon Fraser University. I was one of the principal investigators and primary authors of this work under the supervision of Prof. Michael O. Wolf. Dr. Jeremy Finden, contribution to this work includes: (1) the synthesis of **DTE-37**, (2) the absorbance and emission studies of the C₆H₆ solution of precursors **Poly-2/DTE-37**, (3) the rate data of **Poly-4** and **Poly-2/DTE-37**, (4) the shorter irradiation time experiment of **Poly-4**, and (5) collaborative efforts towards quantum yield (Φ) measurements of **Poly-4** and **Poly-2/DTE-37**.

A version of Chapter 5 will be submitted for publication. Kunz, T. K. and Wolf, M. O., Electrochemical Thin Film Deposition of TEMPO Functionalized Polythiophenes. I am the principal investigator and primary author of this work under the supervision of Prof. Michael Wolf.

CHAPTER 1 Introduction

1.1 Overview

In October of 2007, Sony® introduced a new state-of-the-art flat screen OLED (organic light emitting diode) television.^{1,2} The OLED technology in this TV is based on emission from small organic molecules sandwiched between two conductive plates and demonstrates the ultimate goal of commercial application for thin-film organic devices. The 3-mm thick screen boasts unparalleled picture quality with an amazing contrast ratio (1,000,000:1), outstanding brightness, exceptional colour reproduction, and a rapid response time when compared to liquid crystal display (LCD) technology.

The interest in marrying small organic molecules, and in particular, conjugated polymers (CPs), with inorganic semiconductor technology stems from a variety of promising benefits. As successfully predicted by Moore's law over the past few decades the number of components on an integrated circuit will double every one to two years.^{3,4} At this rate, a fundamental size regime limit of solid state integrated circuitry will be reached. A significant benefit offered by organic materials is the ability to move beyond this limit into nanometer scale electronics. Soluble organic polymers open the possibility of depositing thin organic films on a variety of very-low-cost substrates (glass or plastic) through an assortment of innovative processing techniques (spin coating,^{5,6} stamping,⁷ and ink-jet deposition⁸⁻¹⁰). Such films can be processed at room temperature, over large areas, into desired shapes and with optical quality. The ease of polymer processing offers potential for large cost-savings in comparison to traditional semiconductor technology. Additionally, organic compounds can be synthetically engineered to tailor and optimize

the desired functions and properties that are useful in electronic devices. Thus, research relating to CPs is almost exclusively dedicated towards electronic applications such as OLEDs,¹¹⁻¹³ field effect transistors (FETs),¹⁴⁻¹⁶ organic photovoltaics (OPV),¹⁷⁻¹⁹ and sensors.^{20,21}

CPs (Figure 1-1), also referred to as 'synthetic metals',^{22,23} are polymers that possess the electronic, magnetic and optical properties of a metal while retaining the mechanical properties and processibility commonly associated with conventional polymers. Specifically, the materials' ability to conduct electricity, stability observed upon partial oxidation or reduction (doping), and strong absorption (and emission) in the UV-vis spectrum are features observed because of the delocalization of π -electrons.²³⁻²⁵

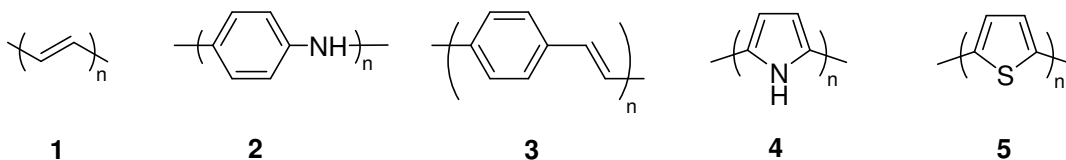


Figure 1-1. Examples of common π -CPs; polyacetylene (**PA**, **1**), polyaniline (**PANI**, **2**), poly(p-phenylenevinylene) (**PPV**, **3**), polypyrrole (**PPy**, **4**), and polythiophene (**PT**, **5**).

The extent of delocalization of the π -electrons is known to be strongly dependent on the coplanarity of the conjugated system.^{26,27} Understanding the influence of substituents on this structural characteristic is an essential facet in the study of the structure-property relationships in CP materials. The aim of this work was to prepare π -CPs with defined backbone structure and to investigate the influence of different functional groups on the optical and electronic properties.

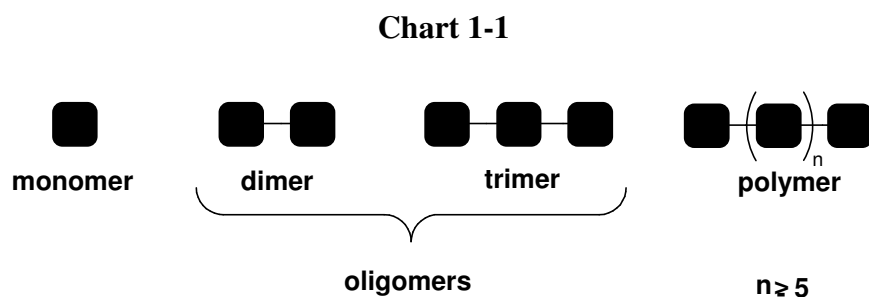
This thesis describes the synthesis and characterization of regioregular poly(3-alkylthiophenes) (rr-P3ATs) prepared under Grignard Metathesis (GRIM) polymerization conditions. These polymers are prepared with latent functionality to allow post-

polymerization modification through the employment of Click chemistry. The effect of the side groups on the polymer properties, as well as the utility of this approach is discussed. Potential applications of these materials arising from the displayed characteristics are also considered.

1.2 *Polymer Fundamentals*

1.2.1 Definitions

Polymers are macromolecular structures that consist of a minimum of several hundred covalently linked atoms and have molecular weights above 10^3 g mol^{-1} .²⁸ A polymer is also defined as a substance that consists of multiple repetitions of one or more species. These species may be atoms or groups of atoms which are individually referred to as constitutional or repeat units. When the number of repeat units within a chain is low, from two (dimers) up to approximately seven (heptamers),²⁹⁻³¹ the resulting structures are referred to as oligomers (Chart 1-1). The term monomer refers to the unreacted species from which the polymer is derived.



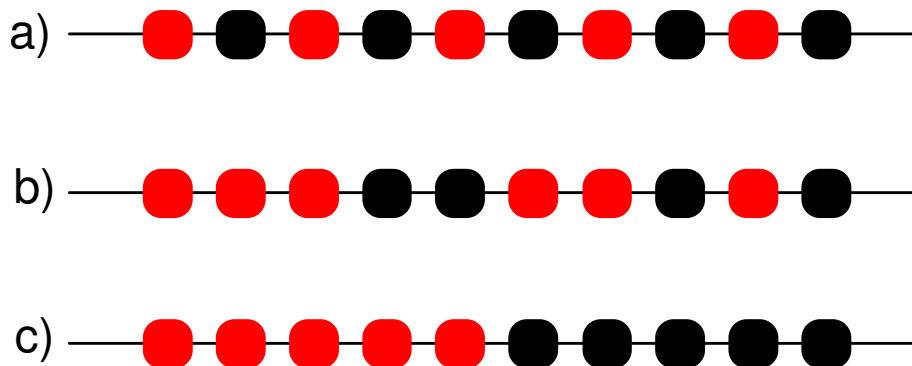
Synthesis of a polymer rarely results in molecules of identical structure. Instead, mixtures of macromolecules are obtained that contain similar structures but differ in degree of polymerization (DP). The degree of polymerization is a measure of how many

monomer units are incorporated into the polymer chain and can be related to the molecular weight (M_w) according to Eq. 1-1, where M_{ru} is the molecular weight of the repeat unit. Molecular weight is important because it determines many of the physical properties.^{32,33} These mixtures are referred to as polydisperse with Gaussian distribution and as a result, the values of DP and M_w are generally reported as average values \overline{DP}_w and \overline{M}_w .

$$M_w = DP \cdot M_{ru} \quad \text{Eq. 1-1}$$

Polymer backbones that consist of a single type of repeat unit are termed homopolymers. When a polymer is synthesized from two or more different types of monomers, they are referred to as copolymers. Additional distinctions are made according to the spacial arrangement of monomers within the backbone. This arrangement includes the forms: (a) alternating, (b) random, and (c) block copolymers (Chart 1-2).

Chart 1-2



1.2.2 Polymerization Methods

In general, polymerization reactions afford high molecular weight chains of repeat monomer units. Depending on the nature of the reactive site on the monomer unit, these chains may be linear, branched, or cross-linked. The chemical process of chain elongation occurs by two main mechanisms; chain growth or step growth.³⁴

Chain Growth Polymerization

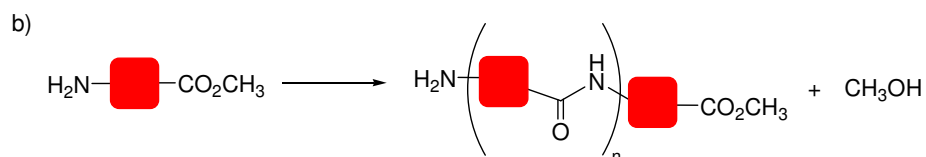
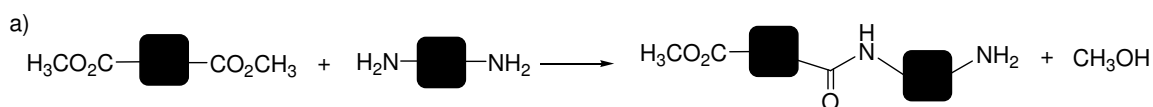
There are three main steps through which a chain growth polymerization reaction proceeds. These steps are referred to as the initiation (Eq. 1-2 and Eq. 1-3), propagation (Eq. 1-4) and termination steps (Eq. 1-5). Initiation occurs with the addition of an initiator ($I\cdot$) or activated species that adds to a monomer (M) in such a way that the monomer becomes the new activated center that is able to react further (Eq. 1-3). The activated species is usually generated as the result of a homolytic bond cleavage from a metal complex, or from strongly polar (or ionic) molecules to form two radicals (Eq. 1-2). The chain growth proceeds as a cascade reaction (Eq. 1-4), where the number of growing chains is directly related to the concentration of initiators in the reaction mixture. Chain growth will proceed until the reactive centers have been terminated or a transfer step has occurred (Eq. 1-5). In a chain transfer reaction, the active center is transferred to a new species (S^*) (solvent, initiator, monomer, etc.) that can polymerize further, while resulting in termination of growth for the original polymer chain. Chain growth reactions are characterized by the immediate formation of high molecular weight species and the reaction time generally has no influence on the average molecular weight, only the yield.



Step Growth Polymerization

In a step growth mechanism, there is no cascade reaction and there is no need for an activated center to initiate or progress the reaction. Instead, the monomers are linked together via conventional organic synthetic methods such as the formation of an amide linkage via the reaction of an ester and amine (Scheme 1-1). In these reactions, the monomers must contain two functional groups, which may be the same or complementary functionality, in order for polymerization to occur. Step growth is dependant on the sequential collisions/reactions of these complementary groups. In a reaction between two different monomers, stoichiometry is crucial for obtaining high molecular weight species. The mechanism of a step growth reaction is characterized by the immediate formation of low molecular weight species (dimers, trimers, etc.), followed by longer oligomers and towards the end of the reaction time, high molecular weight polymers.

Scheme 1-1



1.3 Conjugated Polymers

1.3.1 Electronic Structure

Conjugated polymers (CP)s are known to be electrically insulating, or at best semiconductors in their undoped state.²³ The discovery by Heeger, MacDiarmid and Shirakawa, which demonstrated that oxidatively doped polyacetylene (PA) (**1**, Figure 1-2) displays up to 12 orders of magnitude increase in conductivity relative to undoped PA³⁵ sparked the increased interest in CPs for electronic applications.

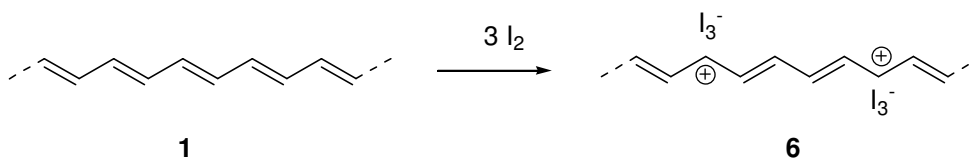


Figure 1-2. Oxidation (p-doping) of **1** with iodine.

The characteristic feature of a CP is the alternating single and multiple (double or triple) bonds along the polymer backbone leading to an extended π -electron system. PA, the prototypical conducting polymer, has the molecular formula $(-\text{CH}=\text{CH}-)_n$ with two π -electrons per formula unit, implying a metallic state.³⁵ True PA has localized π -electrons as a result of Peierls instability leading to alternate single and double carbon-carbon bonds.^{24,25} The localization resulting from lattice distortions removes the degeneracy of the π -orbitals, splitting them into π and π^* bands. Since each band can hold $2n$ electrons, the π band is filled and the π^* band is empty. Displayed in the simplified molecular orbital diagram of the valence π -orbitals (Figure 1-3), increasing the number of repeat units increases the number of orbitals and results in bringing the HOMO and LUMO energy levels closer together. An infinite chain, representative of a CP has a molecular

orbital diagram that resembles that of a semiconductor; it consists of a continuum of energy levels which form both a conduction band and a valence band. The energy difference between the highest occupied state (HOMO) and the lowest unoccupied state (LUMO) is the π - π^* energy gap, or band gap.

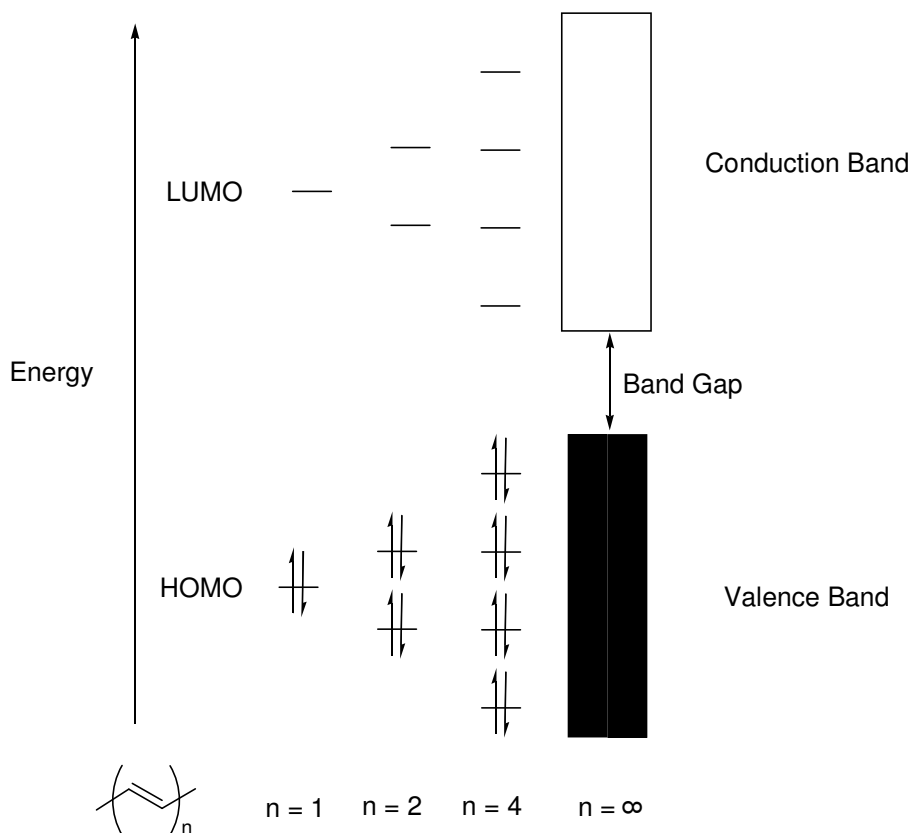


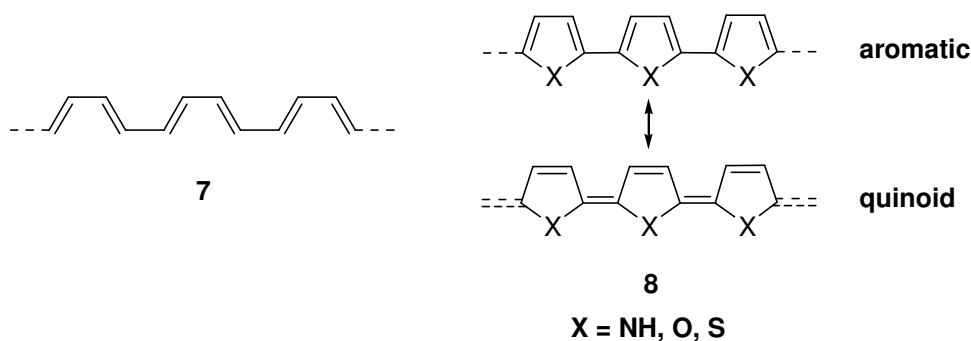
Figure 1-3. Simplified molecular orbital diagram for a CP.

1.3.2 Polythiophene

Analogous in structure to *cis*-polyacetylene (**7**, Chart 1-3), poly(heterocycles) (**8**, Chart 1-3) are stabilized by the presence of a heteroatom such as sulfur, nitrogen or oxygen. The additional stabilization compared to **7**, results from a non-degenerate ground state corresponding to two energetically non-equivalent resonance structures, aromatic

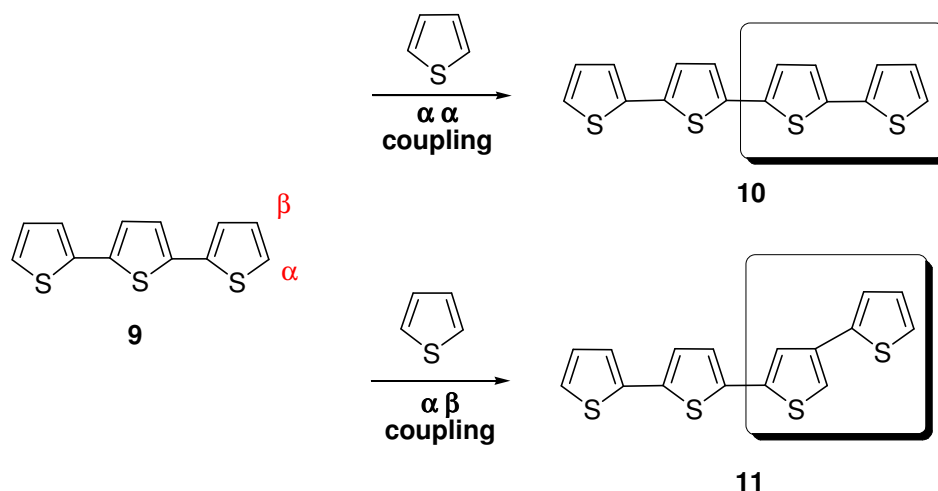
and quinoidal (Chart 1-3)³⁶ In particular, PT (PT) (**5**, Figure 1-1) is one of the most extensively studied CPs.³⁷ With exhibited structural versatility, PT also has a relatively high environmental stability in both the doped and undoped states. There have been reports of synthesized PT displaying conductivity values as high as 10^3 S cm^{-1} ¹² and as such, PT is actively investigated for its conductivity, electrochemistry, and optical properties for material applications³⁸ (electrode materials, electrochromic devices and energy storage).

Chart 1-3



Early syntheses of unsubstituted PT produced polymers with low solubility and processibility, contributing to difficulties in full characterization of the prepared material. Attachment of a flexible alkyl side chain to the conjugated backbone in the 3-position was demonstrated to improve solubility and enhance processibility.³⁹ Additionally, it has been identified that effective conjugation is a crucial parameter in achieving high electrical conductivity.⁴⁰⁻⁴² Extended π -conjugation in PT is only possible when the repeat units are 2,5-linked.⁴³ Since thiophene monomers can couple at the α -(2/5-) or β -(3/4-) positions (Scheme 1-2), introduction of side chains at the 3-position also produced a decrease in the number of α - β mis-couplings (**11**).^{44,45}

Scheme 1-2



1.3.3 Regioregularity

With the incorporation of alkyl substituents at the 3-position, the asymmetry of the thiophene monomer leads to three regioisomers upon coupling. As displayed in Chart 1-4, head-to-tail (HT), head-to-head (HH) and the corresponding tail-to-tail (TT) orientations are possible. Alkyl chains influence thiophene rotation along the chain; HH and/or TT interactions create sterically driven twisting of the polymer backbone. This disrupts the effective conjugation length of a CP as orbital overlap varies approximately with the twist angle (θ) departure from coplanarity.^{26,27,46,47} Clearly, HT couplings lead to the most favourable *trans*-coplanar arrangement of the thiophene rings to minimize gauche interactions and a higher degree of conjugation (Figure 1-4).

Chart 1-4

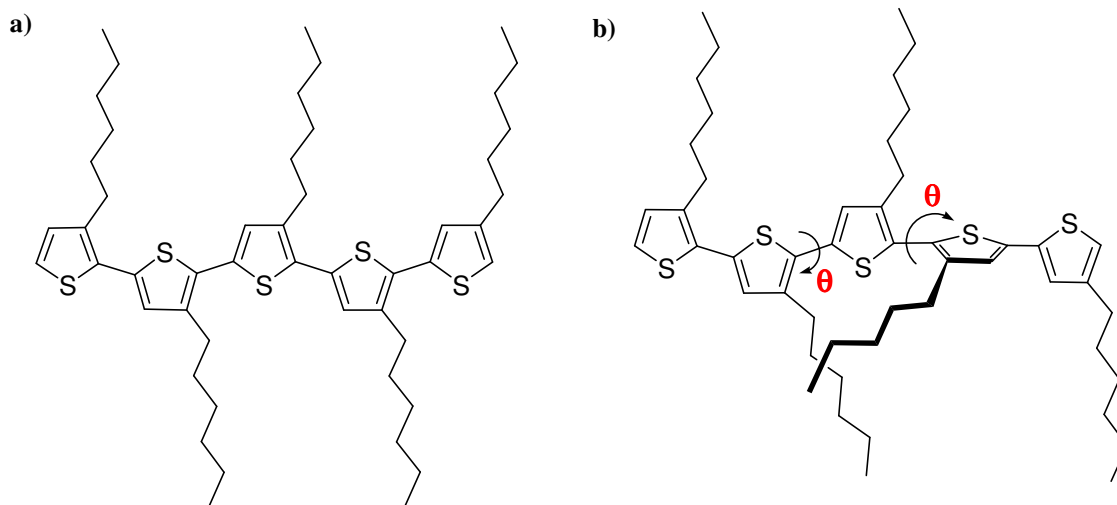
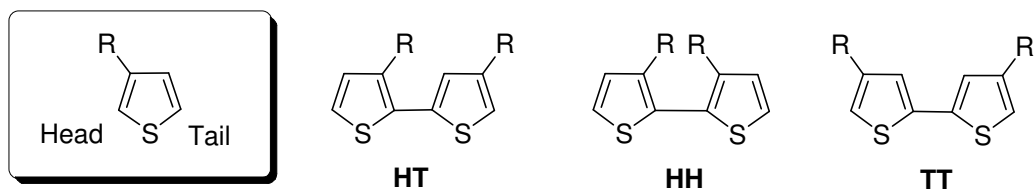


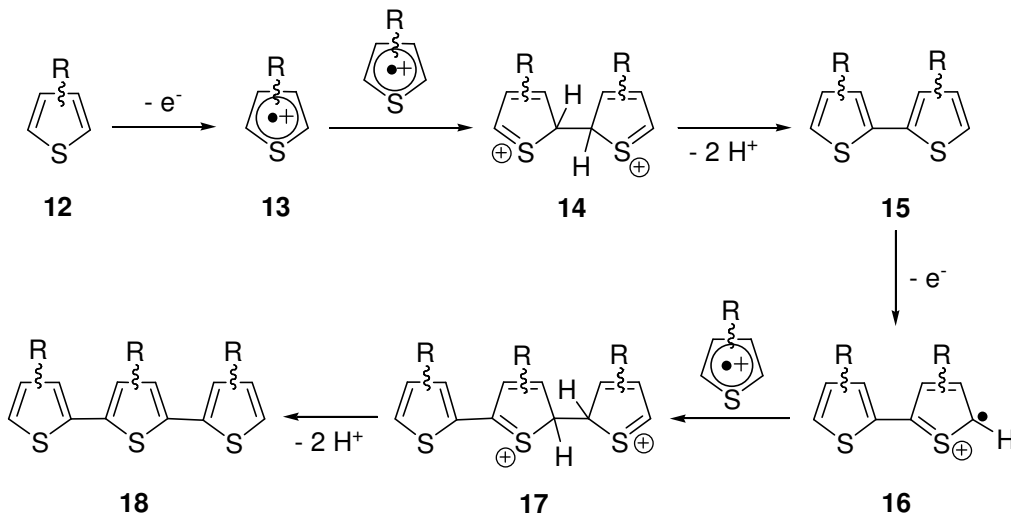
Figure 1-4. A schematic representation of (a) rr-HT coupling, with planar arrangement of the thiophene rings, and (b) steric interactions of the alkyl side chains due to HH/TT mis-couplings causing twisting of the PT backbone.

1.3.4 Synthetic Methods

The synthesis of P3AT is carried out via one of three general methodologies: electrochemical oxidation, chemical oxidative polymerization, or metal catalyzed cross-coupling of 2,5-dihalo-3-alkylthiophenes. The most straightforward method of polymerization is chemical oxidation of 3-alkylthiophene monomers through oxidants such as FeCl_3 .^{48,49} This technique generally produces a significant number of regiochemical defects, such as α - β couplings, and is appropriate only when the regioregularity is of no concern. One example of regio-control employing chemical oxidation was demonstrated with the slow addition of FeCl_3 to 3-(4-octylphenyl)thiophene.⁵⁰

Electrochemical routes provide a convenient and controllable way to prepare thin films on a conducting surface. Electrochemical polymerization (Scheme 1-3) is proposed^{36,51} to proceed via the coupling of two radical cations (**13**) generated by oxidation of a thiophene monomer (**12**). Rearomatization of the bithiophene intermediate is the driving force to the dihydro dimer (**15**). The dimer, with lower oxidation potential, is more easily oxidized and now undergoes coupling with **13**. The electropolymerization continues with subsequent addition of **13** until the polymer precipitates onto the electrode surface due to its insolubility in the electrolytic solution. Electrochemical polymerization of a number of 3-alkylthiophenes, including 3-methylthiophene and 3-ethylthiophene results in fewer α - β linkage defects than found through chemical oxidation reactions, but the polymers obtained have regiorandom structure.

Scheme 1-3



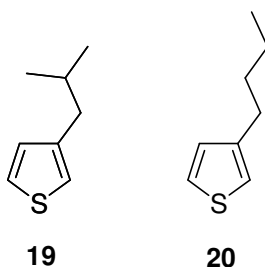
The high stability of thiophene provides easy access to multiply substituted thiophenes and tolerance to a variety of cross-coupling reactions. Traditionally, transition metal catalyzed cross-coupling reactions did not lend themselves to regioselective polymerization.^{52,53} A few representative examples that achieve regioregularities close to 100% HT coupling are based on the selective formation of an organometallic group at the α -position of the thiophene ring. McCullough *et al.*⁵⁴ developed a synthesis based on the regiospecific lithiation of 2-bromo-3-alkylthiophene at the 5-position followed by metal exchange to form the Grignard reagent. Polymerization follows with the addition of Ni(dppp)Cl₂ (dppp = diphenylphosphinopropane) as the catalyst. Independent studies by Rieke *et al.*⁵⁵ developed a methodology that forms the regiospecific organozinc compound by reaction of dibromo-3-alkylthiophene with highly reactive Zn⁰, which is subsequently polymerized with a Ni(dppe)Cl₂ (dppe = diphenylphosphinoethane) catalyst. Additionally, McCullough *et al.*⁵⁶ developed a more general synthesis towards rr-P3AT. This method, known as GRIM polymerization, depends on the regiospecific

generation of the Grignard reagent, 2-bromo-5-(bromomagnesio)-3-alkylthiophene, from the dibromo starting material. Polymerization is carried out *in situ* using the Ni(dppp)Cl₂ catalyst. These methods and others are discussed in greater detail in Chapter 2.

1.4 Polymer Functionalization

The initial reason for the incorporation of side chains, and in particular, flexible hydrocarbon chains, onto a PT backbone was to improve polymer solubility. However, it was also observed that the electron donor properties of the alkyl substituent lowers the oxidation potential of the monomers and increases the stability of the resulting polymer to overoxidation.⁵⁷ Longer alkyl substituents (beyond 7-9 carbons) also strongly influence the co-planarity of the molecules, leading to an increase in mean conjugation length and electrochemical reversibility.^{56,58} In general, variation of the ratio, electronics and size of the side groups help to tailor and tune the electronic and optical properties of the polymer in combination with the structural modifications. This can be demonstrated with a simple comparison between poly-(3-isobutyl)thiophene (**19**) and poly-3-butylthiophene (**20**) (Chart 1-5). The bulky, branched structure of the isobutyl side chain induces a coil like structure in solution making it quite soluble, however, this produces a deleterious break in conjugation and a corresponding blue shift in peak absorption compared to **20**.⁵⁹

Chart 1-5



1.4.1 Post-Polymerization

An ongoing research goal has been the reduction of the energy bandgap of the CP.⁶⁰ A smaller bandgap should facilitate the ease of doping, improve photoconductivities, and is likely to afford material that would be transparent in the doped state. The most direct approach towards this goal is by the covalent grafting of functional groups onto the monomers prior to polymerization. This requires a detailed comprehension of the effects of substitution (inductive or steric) on the monomer for subsequent reaction. For instance, while strong electron-withdrawing groups on the thiophene monomer will lower the LUMO, effectively reducing the bandgap, this raises the oxidation potential and prevents electropolymerization.^{45,61}

It is also important for the functionality of the monomer to remain compatible with the polymerization conditions. Grignard reagents are incompatible with alcohol functional groups and as a result, protection of such side groups is required during polymerization, potentially adding steps to the synthetic procedure.^{62,63}

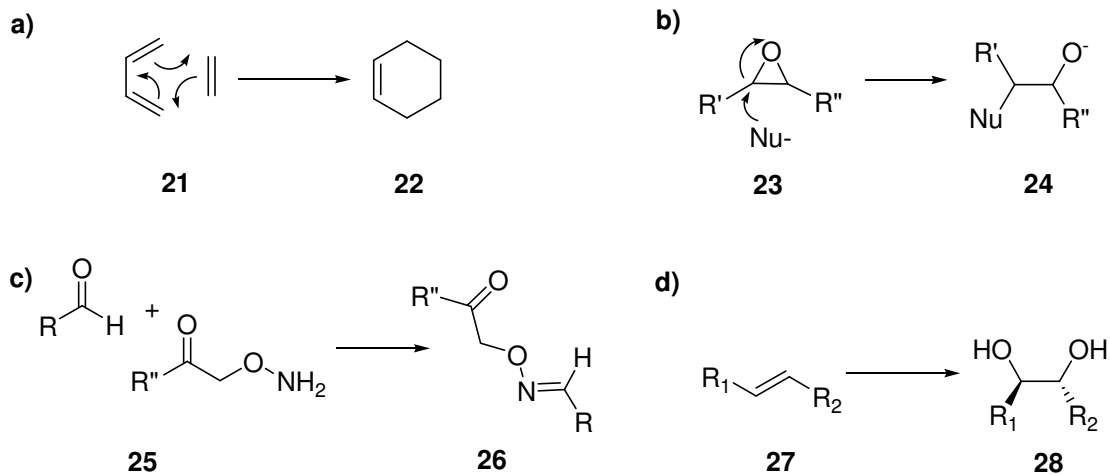
An alternate method to prepare polymers bearing functional pendant groups is to incorporate latent functionality into the polymer backbone, which can be modified post-polymerization.⁶⁴⁻⁶⁶ In addition to removing potential complications during polymerization, this provides a facile method to generate a series of related polymers bearing a diverse library of functionality. The ability to perform these modifications via ‘simple’ chemical reactions (i.e. reactions that do not require complex work-up or purification) is highly desirable. “Click” reactions, a moniker coined by Sharpless *et al.*,⁶⁷ are a family of reactions that are powerful in their simplicity and utility for chemical modifications.

1.4.2 Click Chemistry

Click reactions have been used extensively in a broad spectrum of applications such as surface engineering, synthesis of macromolecular structures, and in the modification of biological molecules.^{68,69} However, in order to be deemed a Click reaction, a stringent list of criteria must be met.⁶⁷ The reaction must give quantitative yields (100% product). They must have high functional group tolerance (avoiding protecting group strategies), and generate only inoffensive by-products which can be easily removed with non-chromatographic techniques. Reaction conditions must be simple; ideally insensitive to oxygen and water, be carried out in all solvents irrespective of their protic/aprotic or polar/nonpolar nature, require readily available starting materials and reagents, and be carried out at ambient temperature.

There are four broad classes of reaction that fit the Click chemistry paradigm (Scheme 1-4). These include (a) cycloadditions; 1,3-dipolar cycloaddition and the Diels-Alder [4+2] cycloaddition, (b) nucleophilic substitution/ring opening reactions, (c) carbonyl chemistry of the 'non-aldol' type, and (d) addition to carbon-carbon multiple bonds. In each of these reactions, the driving force is a thermodynamic gain of usually greater than 84 kJ mol^{-1} .⁶⁷ The reagents of a Click reaction are necessarily highly reactive, but have very narrow reaction trajectories, that is, they produce a single product with high yields and exclusive stereospecificity.

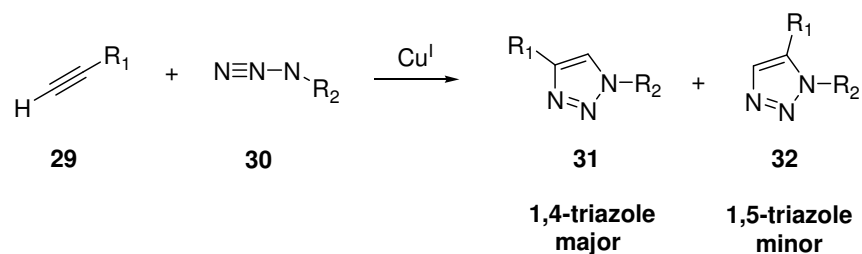
Scheme 1-4



1.4.3 Huisgen 1,3-Dipolar Cycloaddition

The Huisgen 1,3-dipolar cycloaddition^{70,71} (the reaction between a terminal alkyne (**29**) and an azide group (**30**), Scheme 1-5), has emerged as the method of choice among the many available types of Click reactions. This reaction is a pure fusion reaction, meaning the molecular formula of the product is the combined formulae of the reactants. While there are concerns about the explosive nature of the azide moiety,^{72,73} it is ideal for standard organic synthesis because of its inactivity towards a wide variety of conditions and reagents⁷⁴ rendering it ‘invisible’ and preserving it through a reaction sequence until needed. Furthermore, the triazole ring is a thermally and hydrolytically stable conjugated linkage.^{75,76}

Scheme 1-5



Initial studies of the cycloaddition between aryl/alkyl azides and strongly activated alkynes proceeded at moderate temperatures reaching yields of 90-100%.^{67,77,78} Further to the purely thermal process, it was discovered that Cu^I salts accelerated the cycloaddition reaction to result in quantitative yields at 25 °C.⁷⁹ Finally, it was observed that the formation of the 1,4-triazole (**31**) was regioselectively preferred through a Cu^I catalyzed Huisgen reaction between non-activated alkynes and aryl/alkyl azides (Scheme 1-5).⁸⁰

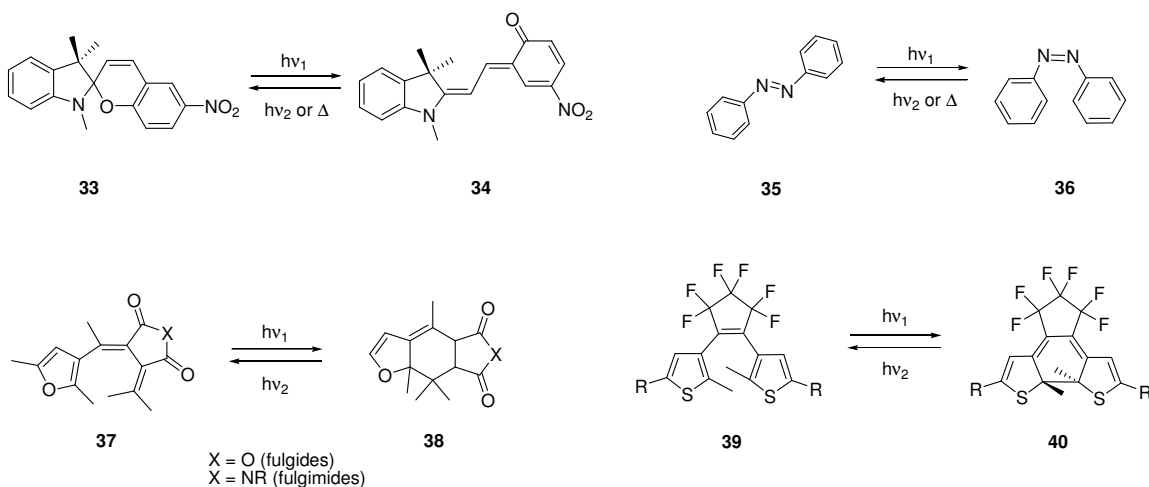
1.5 Pendant Groups

Molecules that respond to external stimuli such as light, electricity, or chemical reagents are potentially useful for application in organic electronic devices.⁸¹ The use of light (photons) and electricity (electrons) are particularly promising stimulants. They can influence a system response without any extraneous waste (by-products from chemical reactions), they behave as stoichiometric triggers, and can be focused to localized areas without affecting the surrounding area. In the two next sections, two molecular moieties will be described and their desirable properties with application towards modification of the CP will be outlined. In this thesis, a light activated switch (dithienylethene (DTE)) and a redox active group (2,2,6,6-tetramethylpiperdine-1-oxyl (TEMPO)) are both investigated for their influence on a rr-P3AT.

1.5.1 Dithienylethenes

Compounds that change colour and reversibly interconvert between two isomers upon the absorption of light, in which each isomer displays unique absorption spectra, are classified as photochromic compounds.⁸² There are several main classes of organic photochromic compounds including spiropyrans (**33**→**34**), azo compounds (**35**→**36**) and fulgides/fulgimides (**37**→**38**) (Scheme 1-6). In particular, dithienylethene (DTE, **39**→**40**) is a commonly studied photochromic compound that displays thermal irreversibility. DTE and its derivatives display a colouration/decolouration fatigue resistance of more than 10^4 cycles, in addition to their thermal stability, making them highly appealing for applications to molecular electronics.^{83,84}

Scheme 1-6



In general, irradiation of an open isomer (**A**) with one wavelength ($h\nu_1$) will induce a photoisomerization reaction to produce a closed isomer (**B**).⁸⁵ The reverse reaction is accomplished by irradiating **B** with a different wavelength ($h\nu_2$). The wavelengths of irradiation are dependant on the absorption spectra of the two isomers. Ideally, the two isomers, **A** and **B**, would absorb light in well separated regions of the absorption spectrum, allowing for the independent irradiation of each compound. Frequently, however, the two isomers have absorption bands in the same region of the spectrum where light is used to induce one of the photochemical transformations.

As seen in a typical absorption spectrum (Figure 1-5), irradiation of isomer **A** with $h\nu_1$ results in a decrease of **A**'s absorption band and the corresponding increase of the absorption band of isomer **B** located in the visible region of the spectrum. It can be observed that formation of isomer **B** does not fully reduce the absorption in the region up to approximately 350 nm.

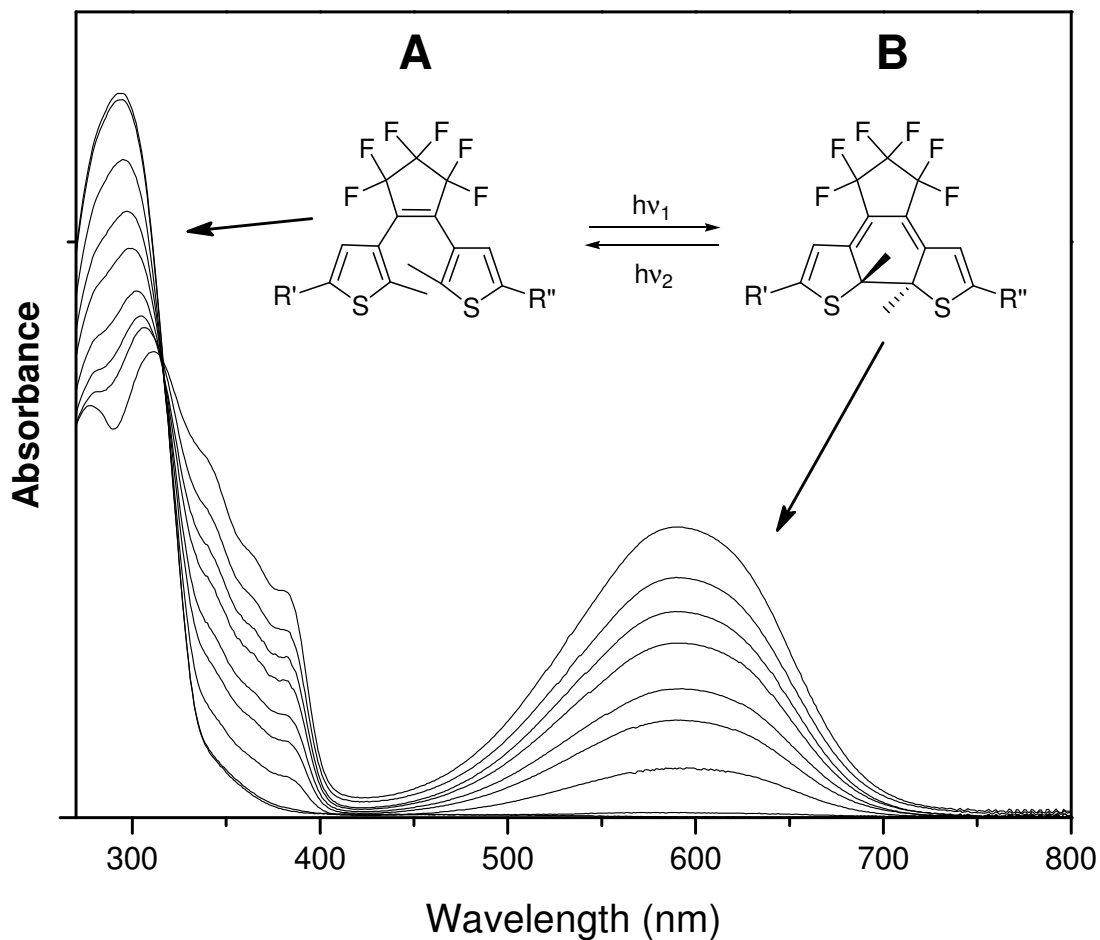


Figure 1-5. Typical UV-vis absorption spectra of photoinduced reaction between two isomers **A** and **B**.

Irradiation into this region of spectral overlap (~ 350 nm) results in two competing photoisomerization reactions (i.e. $\mathbf{A} \rightarrow \mathbf{B}$ and $\mathbf{B} \rightarrow \mathbf{A}$), and sets up an equilibrium between the forward and reverse reactions. The point at which the equilibrium is reached is termed the photostationary state (PSS).⁸⁶ The PSS can be calculated by determining the amount (or concentration) of isomer **B** at equilibrium (B_{eq}) in relation to the initial amount (or concentration) of isomer **A** (A_i) and is usually reported as a percentage according to Eq. 1-6. The equilibrium between the two isomers,

and therefore the PSS, is governed by the quantum yields (Φ) of the forward and reverse reactions, the concentrations and the molar absorptivities (ϵ) of the two isomers at the irradiation wavelength.

$$\text{PSS (\%)} = \mathbf{B_{eq} / A_i \times 100} \quad \text{Eq. 1-6}$$

The backbone of DTE is based on a 1,3,5-hexatriene moiety. According to the Woodward-Hoffmann⁸⁷ rules of pericyclic reactions, a system with $4n + 2 \pi$ -electrons will ring close in a conrotatory fashion from the excited state and in a disrotatory fashion from the ground state. The relative ground state energy differences between the open and closed states of a disrotatory ring closure are very large. This energy difference practically prohibits cyclization from the ground state. There is no large energy barrier between the open and closed states of a conrotatory ring closure, ensuring that cyclization will only occur from the excited state. The frontier molecular orbitals of the hexatriene system are shown in Figure 1-6. Absorption of light promotes an electron from the HOMO to the LUMO and based on the symmetry of the excited state, the ring closing reaction must occur in a conrotatory fashion.^{84,88}

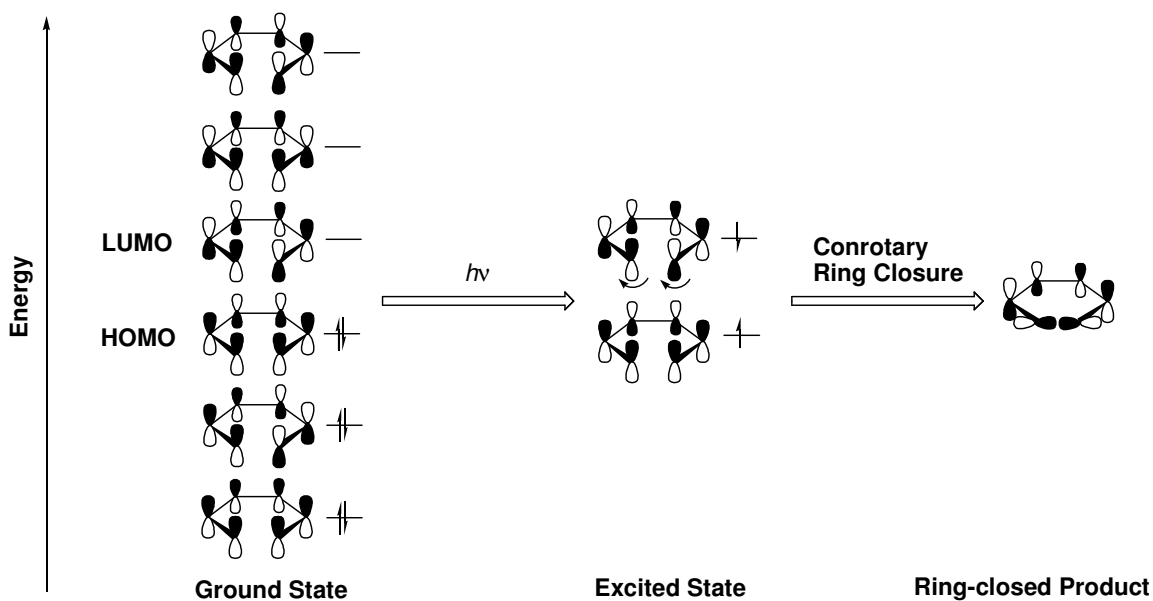
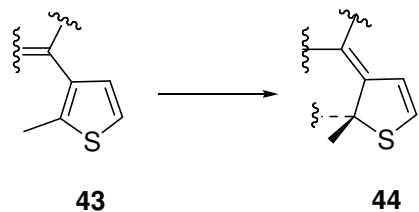


Figure 1-6. Simplified energy diagram for photo-induced ring closing reaction of 1,3,5-hexatriene.

The stability of the photo-generated product depends on the energy barriers associated with the cycloreversion reaction. If the energy difference between the open and closed isomers is large, the reaction barrier becomes small and the reaction readily takes place. However, if the energy difference between the open and closed isomers is small, the reaction barrier is large and the cycloreversion is not expected to occur. The ground state energy difference is related to the aromaticity change between the open and closed isomers (Scheme 1-7). The energy difference between **43** and **44** is determined to be $\sim 2 \text{ kJ mol}^{-1}$ which is one of the lowest aromatic stabilization energies.^{84,88} These energy considerations demonstrate the thermal irreversibility of ring opening/closing in DTE.

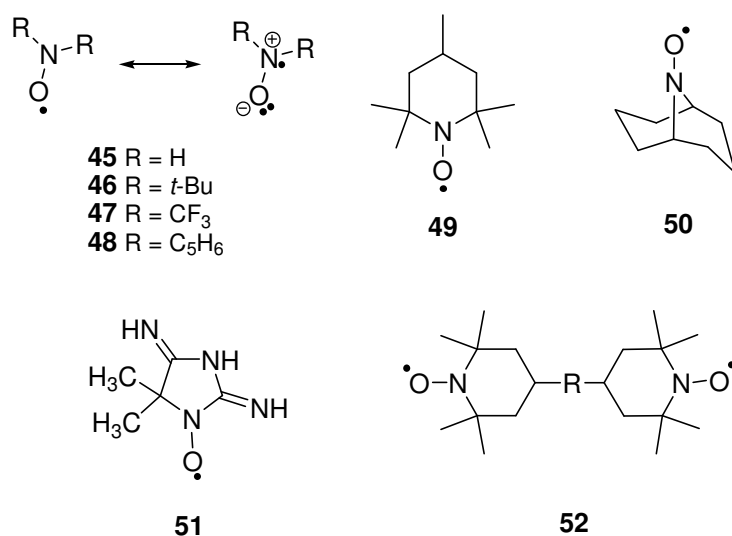
Scheme 1-7



1.5.2 Stable Nitroxyl Free Radical: TEMPO

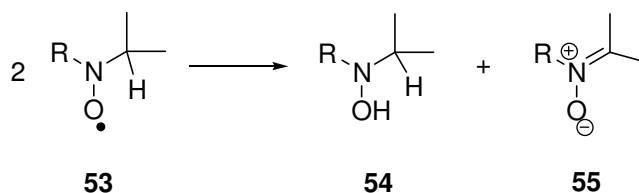
Since the first example of a stable organic nitroxyl radical (NR) was prepared by Piloty and Schwerin,⁸⁹ a variety of NRs have been prepared (Chart 1-6).⁹⁰ Besides the parent compound (**45**), NRs bearing primary, secondary, and tertiary alkyl groups, aryl, alkoxy and amino groups are all known. The characteristic feature of a NR is the presence of a single unpaired electron delocalized over an N-O group, conceived as the superposition of two resonance structures.

Chart 1-6



Several NRs demonstrate remarkable stability.⁹⁰ They do not decompose over long periods of time, do not show any tendency to dimerize, and persist in both polar and non-polar solvents to form brightly coloured solutions. The absence of α -hydrogen atoms is an essential element with regards to the observed stability. The presence of one or more α -H atoms will allow disproportionation of the species to the hydroxylamine (**54**) and the corresponding nitron (**55**) (Scheme 1-8).

Scheme 1-8

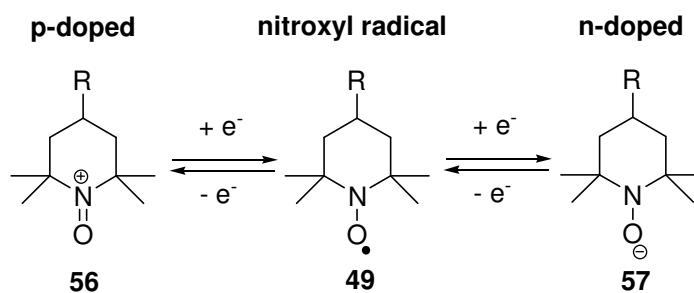


The relative stability of these radicals can also be explained based on several thermodynamic parameters. The energy of delocalization of the unpaired electron over the N-O bond has been estimated at $\sim 125 \text{ kJ mol}^{-1}$ for heterocyclic NRs.⁹¹ The N-OH bond dissociation energy (BDE) of the parent hydroxylamine is also considered a key characteristic in accounting for the stability of the obtained radical. In particular, TEMPO (**49**, Chart 1-6), has been reported to have a BDE of 292 kJ mol^{-1} .⁹² To quantify this value, the ability of TEMPO to affect hydrogen abstraction would be highly endothermic based on the determined BDE. As a result of this unprecedented stability, TEMPO radicals are in practical use to monitor/mediate redox reactions^{93,94}, antioxidants,^{95,96} and as charge transfer salts with 1,4-benzoquinone derivatives.⁹⁷

The TEMPO radical has also been heavily investigated for its rich electrochemistry and remarkably fast electrode kinetics. The neutral radical can be both

oxidized (p-doped) and reduced (n-doped) via rapid, reversible and stoichiometric $1e^-$ transfer processes (Scheme 1-9). For example, the TEMPO/TEMPO⁺ redox couple displays a hetero-geneous rate constant of $k_0 = 8.4 \times 10^{-1} \text{ cm s}^{-1}$ and an electron self exchange rate of $k_{\text{ex}} \sim 10^8 \text{ M}^{-1} \text{ s}^{-1}$ in solution.^{98,99} The impressive rate of electron transfer is accounted for by very little structural change coupled with the available flexibility of the six-membered ring.¹⁰⁰ These properties of the TEMPO radical have generated considerable interest for applications in organic based batteries.¹⁰⁰⁻¹⁰³

Scheme 1-9



1.6 Goals and Scope

The goals of this thesis are: (1) to synthesize HT rr-P3AT, (2) to functionalize the prepared polymers post-polymerization, and (3) to investigate the electronic and optical properties of these functionalized polymers for possible materials applications. The first goal of this study was to prepare PT copolymers with HT regioregularity via GRIM polymerization conditions, to ensure optimal conjugation along the polymer backbone. Using variations of the GRIM conditions, different copolymer backbone motifs (random vs. block) were prepared to study the effect of monomer arrangement throughout the polymer chain. The second goal involved functionalization of the polymer backbone post-polymerization via Click chemistry. The ease and utility of the Huisgen 1,3-dipolar cycloaddition reaction was exploited to attach several different pendant groups to a parent PT derivative. Additionally, the employment of post-polymerization modification facilitated purification of the different functionalized polymers. The final goal of the thesis was investigation of the influence of pendant groups on the optical and electronic properties of the parent polymer for potential applications towards organic material based devices. In particular, DTE and TEMPO were the pendant groups of choice. DTE was attached to the PT backbone to investigate the influence of the ring closing reaction on the luminescent properties of the polymer, and TEMPO was attached to study the potential increase in charging/doping of the polymer backbone.

1.7 References

1. Sonystyle Canada Home Page. <http://www.sonystyle.ca/commerce/servlet/HomepageView?storeId=10001&langId=-1&catalogId=10001>. XEL-1 OLED TV. <http://www.sonystyle.ca/commerce/servlet/ProductDetailDisplay?storeId=10001&catalogId=10001&langId=-1&productId=1004843> (accessed Sept 14 2009).
2. Sony Homepage. http://www.sony.ca/view/press_494.htm#. Sony Corporation Press Release. <http://www.sony.ca/view/homepage.htm> (accessed Sept 14 2009).
3. Moore, G. E., *Electronics* **1965**, 38, (8).
4. CNET Homepage. www.cnet.com. New Life for Moore's Law. http://news.cnet.com/New-life-for-Moores-Law/2009-1006_3-5672485.html
5. Cui, H. N.; Teixeira, V.; Zhang, J.; Lee, H., *Thin Solid Films* **2006**, 515, (1), 301-306.
6. DeLongchamp, D. M. et al., *Chem. Mater.* **2005**, 17, (23), 5610-5612.
7. Kumar, A.; Whitesides, G. M., *Appl. Phys. Lett.* **1993**, 63, (14), 2002-2004.
8. Aernouts, T. et al., *Appl. Phys. Lett.* **2008**, 92, (3), 33306 (3 pages).
9. Jahn, S. F. et al., *Langmuir* **2009**, 25, (1), 606-610.
10. Wood, V. et al., *Adv. Mater.* **2009**, 21, (21), 2151-2155.
11. Burroughes, J. H. et al., *Nature* **1990**, 347, (6293), 539-541.
12. Friend, R. H.; Greenham, N. C., Electroluminescence in Conjugated Polymers. In *Handbook of Conducting Polymers*, Skotheim, T. A., Elsenbaumer, R. L., Reynolds, J. R., Eds. Marcel Dekker: New York, 1986; pp 823-845.

13. Perepichka, I. F.; Perepichka, D. F.; Meng, H., Thiophene-based Materials for Electroluminescent Applications. In *Handbook of Thiophene-Based Materials: Applications in Organic Electronics and Photonics*, Perepichka, I. F., Perepichka, D. F., Eds. John Wiley & Sons: Chichester, 2009; Vol. 1, pp 695-756.
14. Facchetti, A., Electroactive Oligothiophenes and Polythiophenes for Organic Field Effect Transistors. In *Handbook of Thiophene-Based Materials: Applications in Organic Electronics and Photonics*, Perepichka, I. F., Perepichka, D. F., Eds. John Wiley & Sons: Chichester, 2009; Vol. 1, pp 595-646.
15. McCulloch, I.; Heeney, M., Thienothiophene Copolymers in Field Effect Transistors. In *Handbook of Thiophene-Based Materials: Applications in Organic Electronics and Photonics*, Perepichka, I. F., Perepichka, D. F., Eds. John Wiley & Sons: Chichester, 2009; Vol. 1, pp 647-672.
16. Halik, M. et al., *Nature* **2004**, 431, (7011), 963-966.
17. Dennler, G.; Scharber, M. C.; Brabec, C. J., *Adv. Mater.* **2009**, 21, (13), 1323-1338.
18. Xiao, S. Q.; Stuart, A. C.; Liu, S. B.; You, W., *ACS App. Mater. & Inter.* **2009**, 1, (7), 1613-1621.
19. Kim, B. J.; Miyamoto, Y.; Ma, B. W.; Fréchet, J. M. J., *Adv. Funct. Mater.* **2009**, 19, (14), 2273-2281.
20. Ho, H.-A.; Leclerc, M., Chemical and Biological Sensors Based on Polythiophene. In *Handbook of Thiophene-Based Materials: Applications in Organic Electronics and Photonics*, Perepichka, I. F., Perepichka, D. F., Eds. John Wiley & Sons: Chichester, 2009; Vol. 1, pp 813-832.

21. Thomas, S. W.; Joly, G. D.; Swager, T. M., *Chem. Rev.* **2007**, 107, (4), 1339-1386.
22. MacDiarmid, A. G., *Synth. Met.* **2001**, 125, (1), 11-22.
23. MacDiarmid, A. G., *Angew. Chem. Int. Ed.* **2001**, 40, (14), 2581-2590.
24. Heeger, A. J., *Angew. Chem. Int. Ed.* **2001**, 40, (14), 2591-2611.
25. Roncali, J., *Chem. Rev.* **1997**, 97, (1), 173-205.
26. Brédas, J. L.; Street, G. B.; Themans, B.; Andre, J. M., *J. Chem. Phys.* **1985**, 83, (3), 1323-1329.
27. Mulliken, R. S., *Phys. Rev.* **1941**, 59, (11), 873-889.
28. Braun, D. et al., Introduction. In *Polymer Synthesis: Theory and Practice: Fundamentals, Methods, Experiments*, 4 ed.; Berlin, A. G., Ed. Springer Berlin Heidelberg: New York, 2005; pp 17-54.
29. Bäuerle, P.; Segelbacher, U.; Maier, A.; Mehring, M., *J. Am. Chem. Soc.* **1993**, 115, (22), 10217-10223.
30. Donat-Bouillud, A. et al., *Chem. Mater.* **1997**, 9, (12), 2815-2821.
31. Özen, A. S.; Atilgan, C.; Sonmez, G., *J. Phys. Chem. C* **2007**, 111, 16362-16371.
32. Homenick, C. M.; Sivasubramaniam, U.; Adronov, A., *Polym. Int.* **2008**, 57, (8), 1007-1011.
33. Chronakis, I. S.; Alexandridis, P., *Macromolecules* **2001**, 34, (14), 5005-5018.
34. Braun, D. et al., Methods and Techniques for Synthesis, Characterization, Processing and Modification of Polymers. In *Polymer Synthesis: Theory and Practice: Fundamentals, Methods, Experiments*, 4 ed.; Berlin, A. G., Ed. Springer Berlin Heidelberg: New York, 2005; pp 55-172.

35. Chiang, C. K. et al., *Phys. Rev. Lett.* **1977**, 39, (17), 1098-1101.
36. Roncali, J., *Chem. Rev.* **1992**, 92, (4), 711-738.
37. Handbook of Oligo- and Polythiophenes. Wiley-VCH Verlag GmbH: Weinheim, 1998.
38. Handbook of Thiophene-Based Materials: Applications in Organic Electronics and Photonics. Perepichka, I. F.; Perepichka, D. F., Eds. John Wiley & Sons: Chichester, 2009; Vol. 2.
39. Jen, K. Y.; Miller, G. G.; Elsenbaumer, R. L., *J. Chem. Soc., Chem. Commun.* **1986**, (17), 1346-1347.
40. Delabouglise, D.; Garreau, R.; Lemaire, M.; Roncali, J., *New J. Chem.* **1988**, 12, (2-3), 155-161.
41. Roncali, J.; Lemaire, M.; Garreau, R.; Garnier, F., *Synth. Met.* **1987**, 18, (1-3), 139-144.
42. Furukawa, Y.; Akimoto, M.; Harada, I., *Synth. Met.* **1987**, 18, (1-3), 151-156.
43. Feast, W. J. et al., *Polymer* **1996**, 37, (22), 5017-5047.
44. Tourillon, G.; Garnier, F., *J. Phys. Chem.* **1983**, 87, (13), 2289-2292.
45. Waltman, R. J.; Bargon, J.; Diaz, A. F., *J. Phys. Chem.* **1983**, 87, (8), 1459-1463.
46. Barbarella, G.; Bongini, A.; Zambianchi, M., *Adv. Mater.* **1991**, 3, (10), 494-496.
47. Barbarella, G.; Zambianchi, M.; Bongini, A.; Antolini, L., *Adv. Mater.* **1994**, 6, (7-8), 561-564.
48. Leclerc, M.; Diaz, F. M.; Wegner, G., *Makromol. Chem.* **1989**, 190, (12), 3105-3116.
49. Osterholm, J. E. et al., *Synth. Met.* **1989**, 28, (1-2), C435-C444.

50. Andersson, M. R. et al., *Macromolecules* **1994**, 27, (22), 6503-6506.
51. Genies, E. M.; Bidan, G.; Diaz, A. F., *J. Electroanal. Chem.* **1983**, 149, (1-2), 101-113.
52. Mao, H. Y.; Xu, B.; Holdcroft, S., *Macromolecules* **1993**, 26, (5), 1163-1169.
53. Mao, H. Y.; Holdcroft, S., *Macromolecules* **1992**, 25, (2), 554-558.
54. McCullough, R. D.; Lowe, R. D., *J. Chem. Soc., Chem. Commun.* **1992**, (1), 70-72.
55. Chen, T. A.; Rieke, R. D., *J. Am. Chem. Soc.* **1992**, 114, (25), 10087-10088.
56. McCullough, R. D.; Lowe, R. D.; Jayaraman, M.; Anderson, D. L., *J. Org. Chem.* **1993**, 58, (4), 904-912.
57. Somanathan, N.; Radhakrishnan, S., *Int. J. Mod. Phys. B* **2005**, 19, (32), 4645-4676.
58. McCullough, R. D., *Adv. Mater.* **1998**, 10, (2), 93-116.
59. Roncali, J. et al., *J. Phys. Chem.* **1987**, 91, (27), 6706-6714.
60. Chan, H. S. O.; Ng, S. C., *Prog. Polym. Sci.* **1998**, 23, (7), 1167-1231.
61. Waltman, R. J.; Bargon, J., *J. Can. J. Chem.* **1986**, 64, (1), 76-95.
62. Curtis, M. D.; McClain, M. D., *Chem. Mater.* **1996**, 8, (4), 936-944.
63. Denmark, S. E.; Hammer, R. P.; Weber, E. J.; Habermas, K. L., *J. Org. Chem.* **1987**, 52, (1), 165-168.
64. Zhai, L. et al., *Macromolecules* **2003**, 36, (1), 61-64.
65. Benanti, T. L.; Kalaydjian, A.; Venkataraman, D., *Macromolecules* **2008**, 41, (22), 8312-8315.

66. Li, Y. N.; Vamvounis, G.; Holdcroft, S., *Macromolecules* **2002**, 35, (18), 6900-6906.
67. Kolb, H. C.; Finn, M. G.; Sharpless, K. B., *Angew. Chem. Int. Ed.* **2001**, 40, (11), 2004-2021.
68. Binder, W. H.; Kluger, C., *Curr. Org. Chem.* **2006**, 10, (14), 1791-1815.
69. Nandivada, H.; Jiang, X. W.; Lahann, J., *Adv. Mater.* **2007**, 19, 2197-2208.
70. 1,3-Dipolar Cycloaddition Chemistry. Padwa, A., Ed. John Wiley & Sons: New York, 1984; Vol. 1.
71. Gothelf, K. V.; Jørgensen, K. A., *Chem. Rev.* **1998**, 98, (2), 863-909.
72. Hassner, A.; Stern, M.; Gottlieb, H. E.; Frolow, F., *J. Org. Chem.* **1990**, 55, (8), 2304-2306.
73. Brase, S.; Gil, C.; Knepper, K.; Zimmermann, V., *Angew. Chem. Int. Ed.* **2005**, 44, (33), 5188-5240.
74. Saxon, E.; Bertozzi, C. R., *Science* **2000**, 287, (5460), 2007-2010.
75. Katritzky, A. R. et al., *Arkivoc* **2006**, 43-62.
76. Katritzky, A. R. et al., *Tetrahedron Lett.* **2006**, 47, (43), 7653-7654.
77. Demko, Z. P.; Sharpless, K. B., *Angew. Chem. Int. Ed.* **2002**, 41, (12), 2110-2113.
78. Demko, Z. P.; Sharpless, K. B., *Angew. Chem. Int. Ed.* **2002**, 41, (12), 2113-2116.
79. Tornøe, C. W.; Christensen, C.; Meldal, M., *J. Org. Chem.* **2002**, 67, (9), 3057-3064.
80. Rostovtsev, V. V.; Green, L. G.; Fokin, V. V.; Sharpless, K. B., *Angew. Chem. Int. Ed.* **2002**, 41, (14), 2596-2599.
81. Molecular Switches. Feringa, B. L., Ed. Wiley-VCH GmbH: Weinheim, 2001.

82. Bouas-Laurent, H.; Dürr, H., *Pure Appl. Chem.* **2001**, 73, (4), 639-665.
83. Irie, M., Photoswitchable Molecular Systems Based On Diarylethenes. In *Molecular Switches*, Feringa, B. L., Ed. Wiley-VCH GmbH: Weinheim, 2001; pp 37-61.
84. Irie, M., *Chem. Rev.* **2000**, 100, (5), 1685-1716.
85. Organic Photochromic and Thermochemical Compounds. Crano, J. C.; Gugliemetti, R. J., Eds. Plenum New York, 1999; Vol. 2.
86. Yokoyama, Y., Molecular Switches with Photochromic Fulgides. In *Molecular Switches*, Feringa, B. L., Ed. Wiley-VCH GmbH: Weinheim, 2001; pp 107-122.
87. Hoffmann, R.; Woodward, R. B., *J. Am. Chem. Soc.* **1965**, 87, (9), 2046-2048.
88. Nakamura, S.; Irie, M., *J. Org. Chem.* **1988**, 53, (26), 6136-6138.
89. Piloty, O.; Schwerin, B. G., *Chem. Ber.* **1901**, 34, 1870-1887.
90. Aurich, H. G., Nitroxides. In *Nitrones, nitronates and nitroxides*, Patai, S., Rappoport, Z., Eds. John Wiley & Sons: Chichester, 1989; Vol. 2, pp 313-370.
91. Rozantsev, E. G., In *Free Nitroxyl Radicals*, Ulrich, H., Ed. Plenum Press: New York - London, 1970.
92. Mahoney, L. R.; Mendenhall, G.; Ingold, K. U., *J. Am. Chem. Soc.* **1973**, 95, (26), 8610-8614.
93. Sheldon, R. A.; Arends, I., *Adv. Synth. Catal.* **2004**, 346, (9-10), 1051-1071.
94. Sheldon, R. A.; Arends, I., *J. Mol. Catal. A: Chem.* **2006**, 251, (1-2), 200-214.
95. Krishna, M. C. et al., *Proc. Natl. Acad. Sci. USA* **1992**, 89, (12), 5537-5541.
96. Krishna, M. C. et al., *J. Med. Chem.* **1998**, 41, (18), 3477-3492.

97. Nobusawa, M.; Akutsu, H.; Yamada, J. I.; Nakatsuji, S., *Chem. Lett.* **2008**, 37, (7), 788-789.
98. Nishide, H. et al., *Electrochim. Acta* **2004**, 50, (2-3), 827-831.
99. Oyaizu, K.; Suga, T.; Yoshimura, K.; Nishide, H., *Macromolecules* **2008**, 41, (18), 6646-6652.
100. Oyaizu, K.; Nishide, H., *Adv. Mater.* **2009**, 21, (22), 2339-2344.
101. Suga, T. et al., *Adv. Mater.* **2009**, 21, (16), 1627-1630.
102. Qu, J. Q. et al., *J. Polym. Sci., Part A: Polym. Chem.* **2007**, 45, (23), 5431-5445.
103. Suga, T.; Konishi, H.; Nishide, H., *Chem. Commun.* **2007**, (17), 1730-1732.

CHAPTER 2 Synthesis of Random Co-Polythiophenes Using GRIM Polymerization and Functionalization Via Huisgen 1,3-dipolar Cycloaddition*

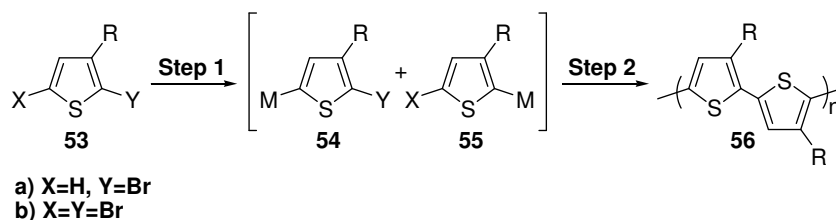
2.1 Introduction

Regioregular polythiophenes (rr-PTs) demonstrate improved optoelectronic properties such as higher mobilities¹⁻⁵ and conductivities⁶⁻¹¹ as compared to their regioirregular counterparts. The structural regularity of the polymer backbone gives rise to a more coplanar arrangement of the individual thiophene rings which results in more extended conjugation and thus smaller band-gaps resulting from the increased π -overlap along the chain.¹²

In 1992, McCullough *et al.* introduced a synthetic method that generates almost exclusively HT rr-poly(3-alkylthiophene) (P3AT).^{8,9} The key step in this method is the regiospecific generation of a 2-bromo-5-bromomagnesio-thiophene. Scheme 2-1 outlines the general synthesis of rr-P3AT, starting from 2-bromo-3-alkylthiophene (**53a**) which is selectively activated with lithium diisopropylamide (LDA) in the 5-position generating intermediate **54** (intermediate **55** is only produced in a 1-2% yield, as demonstrated by quenching studies).⁹ Addition of Ni(dppp)Cl₂ catalyzes the polymerization *in situ* via a cross-coupling reaction and leads to the desired HT rr-P3AT (Step 2). The number average molecular weights (\overline{M}_n) are typically 20000 – 40000 g mol⁻¹ with polydispersities (PDI) of 1.4.

* A version of this chapter will be submitted for publication. Kunz, T. K.; Stott, T. L.; Wolf, M. O., Functionalized Polythiophenes via “Click Chemistry”.

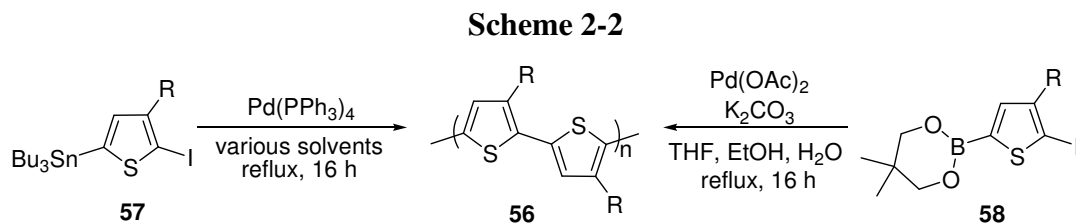
Scheme 2-1



An alternative synthetic route to HT rr-P3AT was developed by Rieke *et al.* where 2,5-dibromo-3-alkylthiophenes (Scheme 2-1, **53b**) are treated with the highly reactive “Rieke zinc” (Zn*), a high surface area zinc powder, to afford the two isomeric intermediates (**54** and **55**) in a ratio of 9:1.^{7,13} The polymerization reaction is performed *in situ* using Ni(dppe)Cl₂ as the catalyst. It was observed in the Rieke method that while highly reactive, the Zn* does not form any of the bis(bromozincio)thiophene, eliminating the need to stoichiometrically lithiate and quench the thiophene as in the McCullough method; however, the highly reactive Zn* leads to metallation that is slightly less selective for isomer **54** and still requires cryogenic temperatures. The typical values of \overline{M}_n for the Rieke method are observed in the range of 24000 - 34000 g mol⁻¹ with a PDI of 1.4.

Several other methods have also been developed to prepare HT rr-P3AT. For example, modified Stille and Suzuki-Miyaura reactions were used for the palladium catalyzed cross-coupling of stannane and boronate intermediates respectively (Scheme 2-2). In 1998, Iraqi *et al.* used 2-iodo-3-alkyl-5-(tri-*n*-butylstannyl)thiophene derivatives (**57**) to generate HT rr-P3AT with greater than 96% HT coupling.¹⁴ Also in 1998, Guillerez *et al.* used 3-octyl-2-iodo-5-boronatothiophene (**58**) to achieve rr-P3AT with 96-97% regioregularity.¹⁵ Both of these methods, however, require cryogenic temperatures to obtain the organometallic monomers which in turn require purification

prior to subsequent reactions and afford much lower number average molecular weights (~ 10000 - 16000 g mol⁻¹).



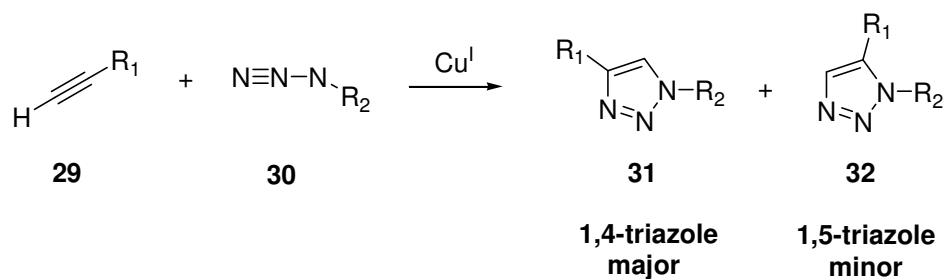
In 1999, a new method for preparing rr-P3ATs was developed whereby a Grignard reagent is generated *in situ* at room temperature or reflux and then addition of a nickel catalyst affords the rr-P3AT.¹⁶ This method (known as the Grignard Metathesis (GRIM) polymerization) offers one paramount advantage over other methods as it does without the highly reactive metals that are required to generate the regio-specific 2-bromo-5-bromomagnesio-3-alkylthiophene intermediate. This eliminates the need for cryogenic temperatures, thus making feasible kilogram scale reactions that still result in high molecular weight rr-P3AT. Starting from 2,5-dibromo-3-alkylthiophene (Scheme 2-1, **53a**), addition of one equivalent of a Grignard reagent affords a mixture of the intermediates **54** and **55**, with the desired isomer **54** formed in 75-85% percent yield. While the ratio of desired (**54**) to undesired (**55**) isomer is not as high as in the McCullough and Rieke methods, this ratio is obtained independent of the Grignard reagent used, the length of reaction time, or reaction temperature. It also still affords polymers with greater than 99% HT couplings and typical \overline{M}_n values of 20000 – 35000 g mol⁻¹ with low PDI of 1.2-1.4.¹⁷

Incorporation of side chains onto the PT backbone was first used to improve polymer solubility, but was also observed to modify the electronic properties of the

polymer. The introduction of electron donating groups or electron withdrawing groups was observed to decrease or increase the bandgap respectively as observed through shifts in the absorption spectrum of the polymer.^{6,7,9,11,13} Additionally, shifts in the absorption of the polymer are related to the oxidation/reduction potentials of the polymer. These potentials determine how readily the polymer may be doped and the stability of doped polymer. This is important for applications in light-emitting devices,¹⁸⁻²⁰ field effect transistors,^{21,22} and solar cells.²³⁻²⁵

Typical modifications to a polymer backbone via side-chain elaboration are installed by changes to the monomer species prior to polymerization. While the GRIM polymerization is compatible with a variety of side chain functionalities,²⁶ obtaining narrow polydispersity materials is still labour intensive, generally requiring repeated Soxhlet extractions. Post-polymerization modification is an alternate method to prepare a series of related polymers bearing a variety of side chains. The work discussed herein demonstrates side chain elaboration through the incorporation of an azide functionality into the polymer backbone. The azide is reacted with a terminal acetylene via a Cu^I catalyzed Huisgen 1,3-dipolar cycloaddition 'Click' reaction, forming the stable triazole ring as shown in Scheme 2-3 below. Advantages of this reaction include its irreversibility and high yield.²⁷ In addition, the acetylene (**29**) and azide (**30**) starting materials do not react with themselves and are known to be tolerant of many different functional groups.²⁸

Scheme 2-3



In this chapter, the synthesis and characterization of a HT rr-P3AT using GRIM conditions and containing latent functionality within the backbone is reported. A parent copolymer is prepared which contains hexyl side chains to maintain solubility and azide groups to provide reactive sites for further functionalization post-polymerization. The feasibility of post-polymerization functionalization will be demonstrated with the generation of a several new functionalized copolythiophenes.

2.2 Experimental

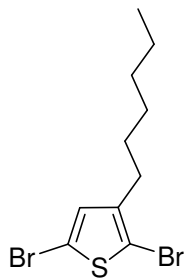
2.2.1 General

All reagents and solvents were used as received except where noted. Tetrahydrofuran (THF) was distilled from Na/benzophenone. Anhydrous dimethylformamide (DMF) was obtained from Aldrich. ^1H NMR spectra were obtained in CDCl_3 either on a Bruker AV- 400 Inverse, a Bruker AV- 400 Direct, or a Bruker AV- 300 spectrometer. Chemical shifts (δ) are reported in ppm, referenced to residual chloroform (CHCl_3) (δ 7.27). Coupling constants (J) are reported in Hertz. Integration of ^1H NMR spectra shows slight variations from batch to batch of similarly prepared GRIM polymers. Consistency between samples was maintained by preparing all subsequent samples from a single precursor polymer. ATR-IR spectra were recorded on a Thermo Scientific Nicolet 6700 FT-IR spectrometer as neat powders or oils. Electronic absorption spectra were obtained on a Varian Cary 5000 UV-vis spectrometer in HPLC grade CH_2Cl_2 and CHCl_3 . Fluorescence measurements were carried out on a PTI Quantamaster spectrometer in the same solvents used for UV-vis measurements. Molecular weight distribution curves of polymers were determined by size exclusion chromatography (SEC) was performed using a Waters SEC equipped with 3 μg -Styrgel columns against polystyrene standards. Polymers were dissolved, filtered and eluted with THF at a flow rate of 1.0 mL/min and monitored with a UV-vis detector (Waters 2487). Data was acquired and analyzed using an IBM personal computer and custom-written software. Electrochemical measurements were conducted on a Autolab PGSTAT12 using a Pt disk working electrode, Pt mesh counter electrode, and a Ag wire reference electrode. These

measurements were made in CH₂Cl₂ passed through an alumina column. An internal reference (decamethylferrocene) was added to correct the measured potentials with respect to saturated calomel electrode (SCE). The 0.1 M [*n*-Bu₄N]PF₆ supporting electrolyte was purified by triple recrystallization from ethanol and dried at 90 °C under vacuum for 3 days.

2.2.2 Procedures

2,5-Dibromo-3-hexylthiophene. (60)



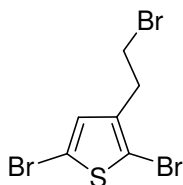
This compound was prepared via a modified literature procedure.²⁹ A solution of 3-hexylthiophene (5.0 g, 30 mmol), and N-bromosuccinimide (NBS) (10.5 g, 59.5 mmol) was prepared in DMF (50 mL). The flask was covered with Al foil and heated to 40 °C under N₂ for 16 hours. The solution was poured into cold water (100 mL) and extracted with diethyl ether (5 × 25 mL). The organic layer was then washed with water, decolourized with activated carbon, filtered, dried (Na₂SO₄) and filtered a second time. The solvent was removed under reduced pressure and purified by column chromatography through silica gel (hexanes) to yield a colourless oil. Yield: 8.76 g (90%). ¹H NMR (400 MHz, CDCl₃, δ): 6.79 (s, 1H), 2.52 (t, 2H), 1.56 (m, 2H), 1.32 (m, 6H), 0.92 (t, 3H).

3-(2'-Bromoethyl)thiophene. (62)



This compound was prepared via modified literature procedures.^{30,31} 2-(3'-thienyl)ethanol (2.0 mL, 18 mmol) and CBr₄ (7.29 g, 21.7 mmol) were dissolved in CH₂Cl₂ (125 mL). The solution was cooled to 0 °C and PPh₃ (7.13 g, 27.2 mmol) was added in one portion. The solution became pale yellow in color, and the reaction was allowed to warm to room temperature and stirred overnight. The solution was filtered through a silica plug (× 2) using CH₂Cl₂ to remove the yellow colour and PPh₃O. The solvent was removed under reduced pressure to yield the crude product, which was purified by column chromatography on silica gel (hexanes). Removal of the solvent gave **62** as a colourless oil. Yield: 3.44 g (99%). ¹H NMR (300 MHz, CDCl₃, δ): 7.34 (dd, 1H), 7.13 (m, 1H), 7.04 (dd, 1H), 3.62 (t, 2H), 3.62 (t, 2H).

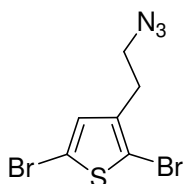
2,5-Dibromo-3-(2'-bromoethyl)thiophene. (63)



This compound was prepared via a modified literature procedure.³² Compound **62** (1.0 g, 5.2 mmol) was dissolved in DMF (25 mL), the solution was deaerated with N₂ and cooled to 0 °C. The round bottom flask was then covered with Al foil. A solution of NBS (2.04 g, 11.5 mmol) in N₂ deaerated DMF (25 mL) was added, the resultant solution

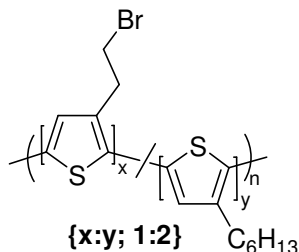
heated to 40 °C and left overnight. The solution was removed from heat and poured into cold water (100 mL). The organics were extracted with diethylether (3 × 50 mL), washed with 1 M aqueous NaHCO₃, dried (Na₂SO₄) and filtered. The solvent was removed under reduced pressure and was purified by column chromatography through silica gel (hexanes). Yield: 1.57 g (86%). ¹H NMR (300 MHz, CDCl₃, δ): 6.87 (s, 1H), 3.50 (t, 2H), 3.11 (t, 2H).

2,5-Dibromo-3-(2'-azidoethyl)thiophene (64)



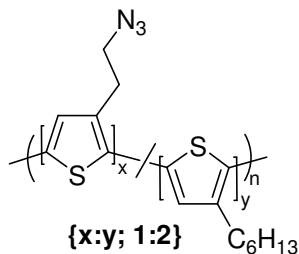
Compound **63** (1.03 g, 2.98 mmol) and NaN₃ (0.29 g, 4.5 mmol) were dissolved in N₂ purged 1-propanol (25 mL). The solution was then heated to reflux overnight. The cooled solution (slightly yellow in color) was extracted with CHCl₃, washed with water, dried (Na₂SO₄) and filtered. The product was isolated as an oil via column chromatography (silica, hexanes, R_f = 0.21) Yield: 0.73 g (88%). ¹H NMR (400 MHz, CDCl₃, δ): 6.85 (s, 1H), 3.46 (t, *J* = 7.0 Hz, 2H), 2.82 (t, *J* = 7.0 Hz, 2H). ¹³C NMR (100.5 MHz, CDCl₃, δ): 138.2, 130.7, 111.0, 109.7, 50.3, 29.0. EI-MS (*m/z*): M⁺ 310. ATR-IR (ν, cm⁻¹): 2956, 2867, 2086 (νN₃), 1541, 1455, 1417, 1345, 1262, 1001, 825, 631, 475. UV-vis (CH₂Cl₂): λ_{max} = 251 nm (ε, L mol⁻¹ cm⁻¹: 8.6×10⁴). Anal. Calcd for C₆H₅Br₂N₃S (%): C, 23.17; H 1.62; N, 13.51. Found: C 23.28; H 1.78; N 13.23.

Poly-3-hexylthiophene-co-3-(2'-bromoethyl)thiophene (Poly-1).



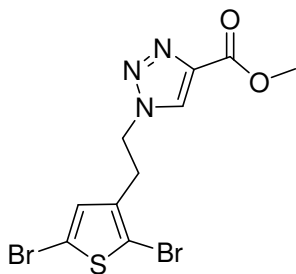
To a round bottom flask containing 100 mL of dry THF, 2,5-dibromo-3-(2'-bromoethyl)thiophene (2.03 g, 5.83 mmol) and 2,5-dibromo-3-hexylthiophene (1.90 g, 5.83 mmol) were added. Methyl magnesium bromide (1.4 M in THF/toluene) (8.33 ml, 8.96 mmol) was added and the solution was heated to reflux for 3 hours during which time the color changed from colorless to orange. The solution was then cooled slightly and 2 mol% of Ni(dppp)Cl₂ was added in one portion. The color changed rapidly to dark red with yellow fluorescence and the solution was heated to reflux overnight. The reaction mixture was then allowed to cool to room temperature and the dark purple polymer precipitated from vigorously stirred methanol. The solid was purified by sequential overnight Soxhlet extractions (24 h CH₃OH, 24 h hexanes, 4 h CHCl₃). Yield: 1.12 g (24%). ¹H NMR (400 MHz, CDCl₃, δ): 7.01 (s), 3.65 (s, -CH₂CH₂Br), 3.41 (s, -CH₂CH₂Br), 2.82 (s, -CH₂CH₂(CH₂)₃CH₃), 1.72 (s, -CH₂CH₂(CH₂)₃CH₃), 1.45–1.35 (m, -CH₂CH₂(CH₂)₃CH₃), 0.93 (s, -CH₂CH₂(CH₂)₃CH₃). ATR-IR (ν, cm⁻¹): 2952, 2921, 2852, 1558, 1507, 1452, 1376, 1302, 1263, 1207, 1102, 1061, 821, 722, 610, 562. UV-vis (CHCl₃) λ_{max}: 442 nm. Fluorescence (CHCl₃) λ_{max}: 572 nm. SEC: \overline{M}_w = 15000 g mol⁻¹, \overline{M}_n = 7000 g mol⁻¹, PDI = 1.8.

Poly-3-hexylthiophene-co-3-(2'-azidoethyl)thiophene (Poly-2).

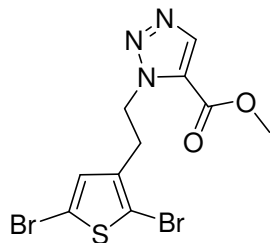


Poly-1 (0.363 g, 0.69 mmol) was placed in a round bottom flask in N_2 purged DMF (150 mL). Under positive N_2 pressure, NaN_3 (0.664 g, 10 mmol) was added in one portion and the reaction was heated to 120 °C and left overnight. The solution was filtered warm to remove any insoluble mass and cooled to room temperature prior to being precipitated from vigorously stirred methanol (150 mL). The resulting dark purple solid was purified by re-precipitation from methanol twice more. Yield: 0.14 g (63%). 1H NMR (400 MHz, $CDCl_3$, δ): 7.00 (s), 3.61 (s, $-CH_2CH_2N_3$), 3.13 (s, $-CH_2CH_2N_3$), 2.80 (s, $-CH_2CH_2(CH_2)_3CH_3$), 1.70 (s, $-CH_2CH_2(CH_2)_3CH_3$) 1.45-1.27 (m, $-CH_2CH_2(CH_2)_3CH_3$) 0.93 (s, $-CH_2CH_2(CH_2)_3CH_3$). ATR-IR (ν , cm^{-1}) 2952, 2922, 2853, 2091(N_3), 1560, 1509, 1454, 1376, 1259, 1087, 1016, 800, 723, 669, 447. UV-vis ($CHCl_3$) λ_{max} : 434 nm. Fluorescence ($CHCl_3$) λ_{max} : 572 nm. SEC: $\overline{M}_w = 12000$ g mol $^{-1}$, $\overline{M}_n = 5800$ g mol $^{-1}$, PDI = 2.1.

Methyl 1-(2-(2,5-dibromothiophen-3-yl)ethyl)-1H-1,2,3-triazole-4-carboxylate (65)



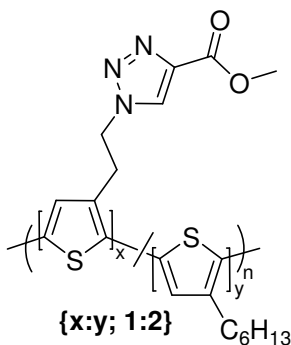
Compound **64** (0.31 g, 1.0 mmol), methylpropiolate (0.10 mL, 1.2 mmol), L-ascorbic acid (10 mol%) and $\text{CuSO}_4 \cdot 5\text{H}_2\text{O}$ (1 mol%) were each dissolved in a 1:1 mixture of *t*-BuOH:H₂O (50 mL). Approximately 10 mL of CHCl_3 was added after several hours to aid in dissolving **64**. The reaction mixture was heated to reflux, and left overnight with vigorous stirring. The solution was cooled, and extracted (3 × 25 mL) with CHCl_3 and washed (3 × 25 mL) with distilled water. It was then dried over MgSO_4 , filtered, and the solvent was removed under reduced pressure. The 1,4-isomer (**65**) was purified by column chromatography (silica, CH_2Cl_2 , $R_f = 0.04$). Yield 0.12 g (30%). ¹H NMR (300 MHz, CDCl_3 , δ): 7.92 (s, 1H), 6.67 (s, 1H), 4.60 (t, $J = 7.0$, 2H), 3.96 (s, 3H), 3.20 (t, $J = 7.0$, 2H). ¹³C NMR (100.5 MHz, CDCl_3): δ 161.0, 140.0, 136.7, 130.4, 127.6, 111.9, 110.6, 52.2, 49.8, 30.3. ESI-MS (m/z): $[\text{M} + \text{Na}]^+$ 418. ATR-IR (ν , cm^{-1}): 3137, 3099, 3076, 3037, 2951, 1723(C=O) 1546, 1524, 1465, 1452, 1434, 1422, 1370, 1317, 1216, 1112, 1051, 1036, 999, 970, 951, 925, 849, 810, 778, 698, 627, 578, 512, 471. UV-vis (CHCl_3) λ_{max} : 250 nm (ϵ , $\text{L mol}^{-1} \text{cm}^{-1}$: 3.4×10^5), 256 nm (ϵ , $\text{L mol}^{-1} \text{cm}^{-1}$: 3.7×10^5), 261 nm (ϵ , $\text{L mol}^{-1} \text{cm}^{-1}$: 3.6×10^5). Anal. Calcd for $\text{C}_{10}\text{H}_9\text{Br}_2\text{N}_3\text{O}_2\text{S}$ (%): C, 30.40; H 2.30; N, 10.64. Found: C, 30.79; H, 2.69; N, 10.68.



The 1,5-isomer (**66**) was isolated by column chromatography on silica gel (CH_2Cl_2 , $R_f = 0.13$). Yield: 0.017 g (4.2%). $^1\text{H NMR}$ (400 MHz, CDCl_3): δ 8.12 (s, 1H), 6.74 (s, 1H), 4.92 (t, $J = 7.2$ Hz, 2H), 3.93 (s, 3H), 3.16 (t, $J = 7.2$ Hz, 2H). ESI-MS (m/z): $[\text{M} + \text{Na}]^+$ 418.

Poly-3-hexylthiophene-co-3-(2-(methyl-1H-1,2,3-triazole-4-carboxylate)ethyl)thiophene

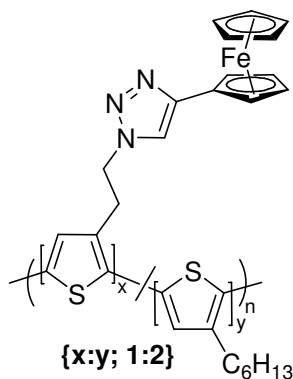
(Poly-3a)



Poly-2 (27 mg, 0.085 mmol) and methylpropiolate (8.5 mg, 0.102 mmol) were dissolved in DMF (25 mL). The solution turned orange and was deaerated with N_2 for ~15 min. L-ascorbic acid (10 mol%) and $\text{CuSO}_4 \cdot 5\text{H}_2\text{O}$ (1 mol%) were each added in one portion and the reaction mixture was slightly heated to dissolve the polymer. The reaction was left overnight under vigorous stirring. The solution was cooled, and the polymer precipitated from methanol, isolated with vacuum filtration and washed via Soxhlet extraction (24 h CH_3OH , 24 h hexanes, 4 h CHCl_3). Yield: 0.017 g (53%). $^1\text{H NMR}$ (400

MHz, CDCl₃, δ) 8.00 (m), 6.94-7.00 (m), 4.75 (s, -CH₂CH₂N₃), 3.92 (s, -OCH₃), 3.49 (s, -CH₂CH₂N₃), 2.80 (s, -CH₂CH₂(CH₂)₃CH₃), 1.71 (s, -CH₂CH₂(CH₂)₃CH₃), 1.44-1.26 (m, -CH₂CH₂(CH₂)₃CH₃), 0.92 (s, -CH₂CH₂(CH₂)₃CH₃). ATR-IR (ν, cm⁻¹): 2953, 2919, 2850, 1724, 1542, 1434, 1367, 1226, 1203, 1102, 1082, 1044, 1026, 807, 774, 720, 697, 665, 504. UV-vis (CHCl₃) λ_{max}: 439 nm. Fluorescence (CHCl₃) λ_{max}: 571 nm. SEC: \overline{M}_w = 11000 g mol⁻¹, \overline{M}_n = 6300 g mol⁻¹, PDI = 1.7.

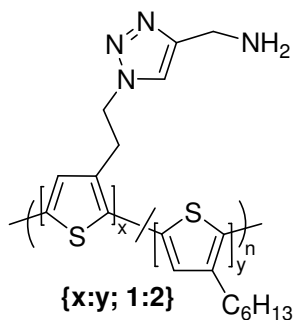
Poly-3-hexylthiophene-co-3-(2-(1H-1,2,3-triazole-4-ferrocene)ethyl)thiophene (Poly-3b)



Poly-2 (0.0364 g, 0.115 mmol) and ethynylferrocene (0.0241 g, 0.115 mmol) were dissolved in DMF (15 mL). The solution turned orange and was deaerated with N₂ for ~ 15 min. L-ascorbic acid (10 mol %) and CuSO₄·5H₂O (1 mol%) were each added in one portion and the reaction mixture was slightly heated to assist in dissolving the polymer. The reaction was left overnight with vigorous stirring. The solution was then cooled, and the polymer precipitated from methanol, isolated with vacuum filtration and washed via sequential Soxhlet extraction (24 h CH₃OH, 24 h hexanes, 4 h CHCl₃). Yield: 0.024 g (62%). ¹H NMR (400 MHz, CDCl₃, δ): 7.00-6.92 (m), 4.68 (s), 4.27 (s), 4.02 (s), 3.47 (s), 2.80 (s), 1.71 (s), 1.44-1.27 (m), 0.92 (s). ATR-IR (ν, cm⁻¹): 2959, 2917, 2849,

1462, 1377, 1259, 1086, 1013, 876, 841, 794, 729, 700, 557, 504. UV-vis (CHCl₃) λ_{\max} : 439 nm. Fluorescence (CHCl₃) λ_{\max} : 571 nm. SEC: \overline{M}_w = 15000 g mol⁻¹, \overline{M}_n = 7700 g mol⁻¹, PDI = 2.0.

Poly-3-hexylthiophene-co-3-(2-(1H-1,2,3-triazole-4-amino)ethyl)thiophene (Poly-3c)



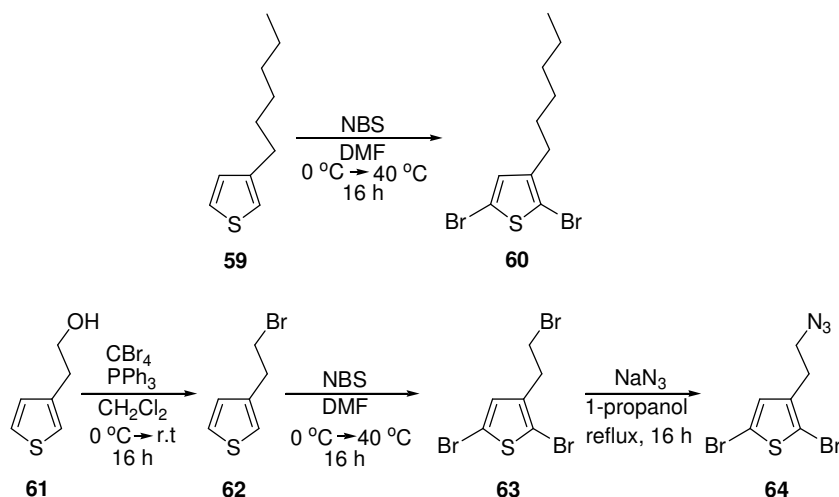
Poly-2 (0.029 g, 0.091 mmol) and 3-aminopropyne (0.01 mL, 0.2 mmol) were dissolved in 15 mL DMF. The solution turned cloudy orange and was deaerated with N₂ for ~ 15 min. L-ascorbic acid (10 mol%) and CuSO₄·5H₂O (1 mol%) were each added in one portion and the reaction mixture heated slightly to help dissolve the polymer. The reaction was left overnight under vigorous stirring. The solution was cooled, the polymer precipitated from vigorously stirred methanol/water (5:1). The solid was isolated with vacuum filtration and washed via sequential Soxhlet extraction (24 h CH₃OH, 24 h hexanes, 4 h CHCl₃). Yield: 0.024 g (71%). ATR-IR (ν , cm⁻¹): 3270, 2922, 2852, 1602, 1433, 1375, 1332, 1046, 822, 722, 609, 443.

2.3 Results and Discussion

2.3.1 Monomer Synthesis and Spectroscopy

Multifunctional polymers for materials applications require careful design. High molecular weight polymers generally require solubilizing groups to maintain processibility. Desired functionality is, in general, afforded through the modification of side chains along the polymer backbone. The synthesis of a multifunctional GRIM polymer was carried out by copolymerization of two different monomers (Scheme 2-4). Poly-3-hexylthiophene (P3HT), is known to remain soluble at high molecular weights,³³ and therefore, 2,5-dibromo-3-hexylthiophene (**60**) was selected as one of the monomers. In order to incorporate the necessary latent functionality on the polymer backbone for post-polymerization functionalization, 2,5-dibromo-3-(2-bromoethyl)thiophene (**63**) was selected as the second monomer. An analogous strategy has been previously used by McCullough *et al.* using 3-(6-bromohexyl)thiophene to make a variety of functional PT derivatives.³⁴

Scheme 2-4



Monomer **60** was synthesized via a modified literature procedure.²⁹ The bromination of 3-hexylthiophene was performed using two equivalents of NBS in dry THF. The solution was left stirring overnight at 40 °C. The small amount of mono-brominated thiophene present was removed via column chromatography to obtain a near quantitative yield of the desired dibromo species **60**.

Monomer **63** was synthesized via a two step procedure, adapted from literature.³⁰⁻³² The bromination of 2-(3-thienyl)ethanol was first carried out using phosphonium bromide generated *in situ* from carbon tetrabromide and tri-phenylphosphine. The phosphine oxide generated as a side product during this reaction made isolation of **62** by column chromatography difficult due to the insolubility of the oxide in hexanes, clogging the silica column used for purification. To solve the aforementioned problem, it was necessary to run the methylene chloride (CH₂Cl₂) solution containing impure product twice through a short silica plug using CH₂Cl₂ as the eluent. Once the oxide had been removed, the remaining material could be eluted with hexanes on a silica column to isolate the desired product as confirmed by ¹H NMR spectroscopy. In the second step, thiophene **62** was brominated in the α-positions with two equivalents of NBS following the same procedure as for the 3-hexylthiophene derivative. The identity of the desired product, **63**, was confirmed by comparison to the ¹H NMR spectrum of **63** from the literature.³²

In addition to the two monomers, **60** and **63**, synthesized for the copolymerization reaction, **64** was prepared as a model to allow comparison with the appropriate polymers. Compound **64** was prepared by heating **63** to reflux overnight with

sodium azide (NaN_3) in 1-propanol, and isolated by column chromatography as a pale yellow oil.

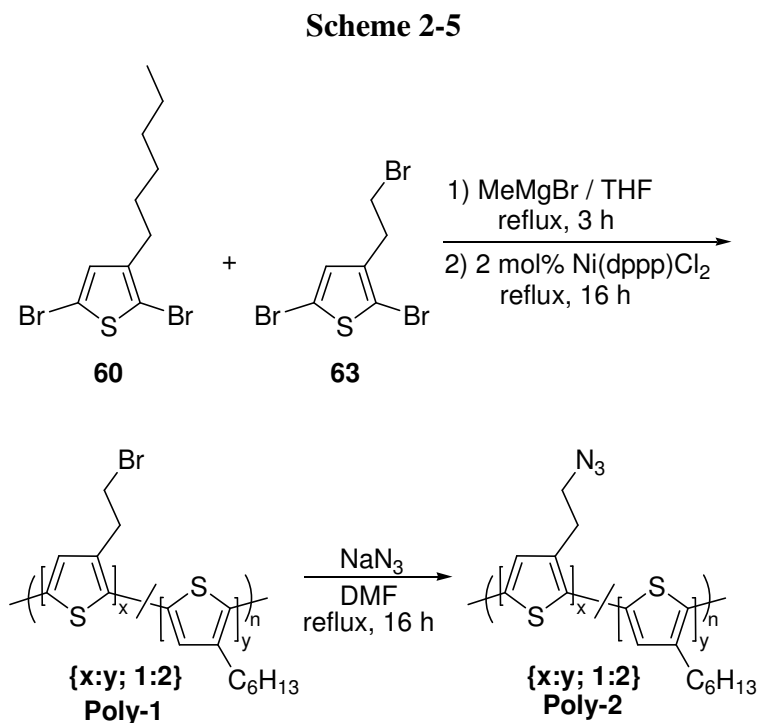
The ^1H NMR spectrum of **64** clearly shows the shift in resonance for the two methylene groups of the ethyl chain upon conversion of the bromide to the azide group. The two triplets at δ 3.11 and 3.50 assigned to the α and β methylene groups of the $-\text{CH}_2\text{CH}_2\text{Br}$, shift to δ 2.82 and 3.46 respectively.

Thiophene **64** was further characterized by mass spectrometry, UV-vis and infrared spectroscopy and elemental analysis. The infrared spectrum was particularly useful for characterization due to the presence of the strong azide stretching band located at 2086 cm^{-1} .

2.3.2 Polymer Synthesis and Spectroscopy

Regioregular HT poly-3-hexylthiophene-*co*-3-(2'-bromoethyl)thiophene (**Poly-1**) was prepared by copolymerization of thiophenes **60** and **63** using the GRIM procedure (Scheme 2-5). Monomers **60** and **63** were dissolved in THF in a 1:1 molar ratio, and an equal molar amount of methyl magnesium bromide was added dropwise. This selectively generated the Grignard reagent at the 5-position of each monomer. The solution was then stirred at reflux for 3 hours, during which time the colourless solution became dark red/orange. The solution was cooled to room temperature and 2 mol% $\text{Ni}(\text{dppp})\text{Cl}_2$ added to initiate the polymerization. The polymerization proceeds via Kumada coupling where the aryl Grignard reagents selectively react with the available aryl halides. The resulting polymer was purified via sequential Soxhlet extractions to yield a purple solid. An overnight methanol extraction was used to remove starting materials and initiator, followed by an overnight hexanes extraction to remove shorter chains and oligomers, and

finally, a chloroform extraction to isolate the soluble polymer from any residual insoluble material.



Regioregular HT poly-3-hexylthiophene-co-3-(2'-azidoethyl)thiophene (**Poly-2**) was prepared by dissolving **Poly-1** in DMF, adding an excess of NaN_3 to the solution and stirring overnight at 120 °C (Scheme 2-5). The following day the dark red-purple solution was filtered hot, to remove any insoluble species. It has been observed previously³⁵⁻³⁸ that elevated temperatures can decompose azides to highly reactive nitrenes. Nitrenes can then insert into single or double bonds, resulting in cross-linking between the polymer chains which may result in insoluble high molecular weight polymers. Purification of **Poly-2** was performed via re-precipitation from vigorously stirred methanol. Here, there

did not appear to be any significant loss of product due to cross-linking as observed by the lack of insoluble material remaining in the filter funnel after purification.

^1H NMR spectroscopy of **Poly-1** and **Poly-2**, showed signals that were characteristically broadened³⁹ compared to the peaks of the corresponding monomeric species. It was observed that polymerization results in several significant shifts in the proton resonances (Figure 2-1). The signals from the α and β methylene groups of the polymer hexyl side chain have shifted to δ 2.82 (α) and 1.72 (β) from δ 2.52 (α'') and 1.56 (β'') respectively, and correspond to chemical shifts observed in rr-P3HT.⁹ The two methylene groups of the polymer ethyl side chain (α' and β') also shifted to higher frequency (δ 3.65 (β') and 3.41(α') from δ 3.50 (β'') and 3.11 (α'')).

Each of the peaks observed in the ^1H NMR spectrum of **Poly-1** were integrated relative to the broad singlet at δ 0.93 (γ) corresponding to the $-\text{CH}_3$ group of the hexyl chain. Comparing the area of this peak to the area of the β' methylene singlet of the ethyl group at δ 3.65, it was determined that the x:y ratio approximates 2:1. While the two monomers **60** and **63** were added to the reaction mixture in the same molar ratio, it is possible that **60** is more reactive, leading to a slightly higher amount being incorporated into the copolymer.

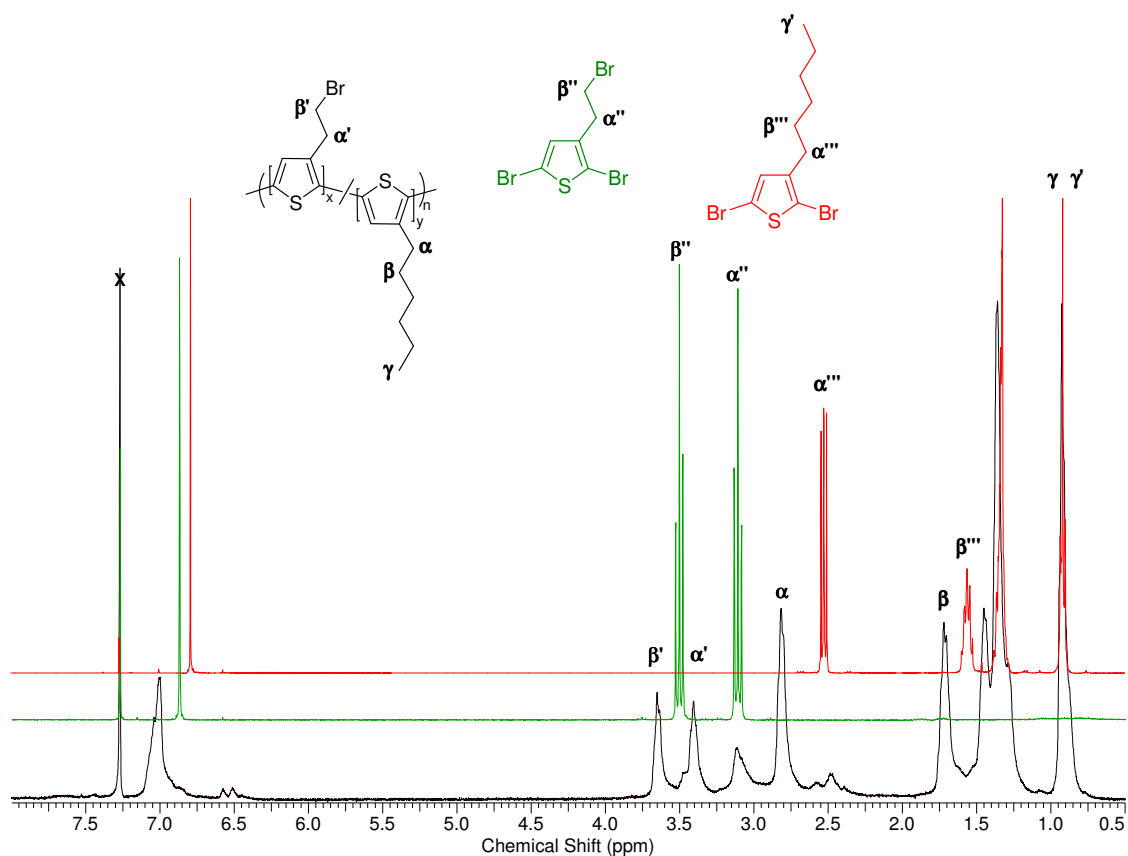


Figure 2-1. ^1H NMR spectra of **Poly-1** (black), **60** (red), and **63** (green). X = residual CHCl_3 in the deuterated solvent.

There are several weak signals in the alkyl ($\sim \delta$ 2.5) and aromatic ($\sim \delta$ 6.5) regions of the ^1H NMR spectrum of **Poly-1**. These signals are a result of imperfections in the regioregularity of the PT backbone, in particular, protons that are influenced by HH/TT couplings within the polymer backbone. This has been previously observed in related polymers.^{9,40} Integration of the two weak signals at δ 2.58 and 2.48 established that **Poly-1** contains $\sim 85\%$ rr-HT couplings.

Conversion of **Poly-1** to **Poly-2** resulted in the shifting of the singlets at δ 3.65 and 3.41 to δ 3.61 and 3.13 in the ^1H NMR spectra respectively (Figure 2-2). These shifts are consistent with those observed in the ^1H NMR spectrum of **64** where shielding

contributes to a shift of approximately δ 0.04 and 0.3 for the β and α protons of the ethyl chain, respectively. The signal that remains at δ 3.41 is assigned to incomplete conversion of the bromide groups.

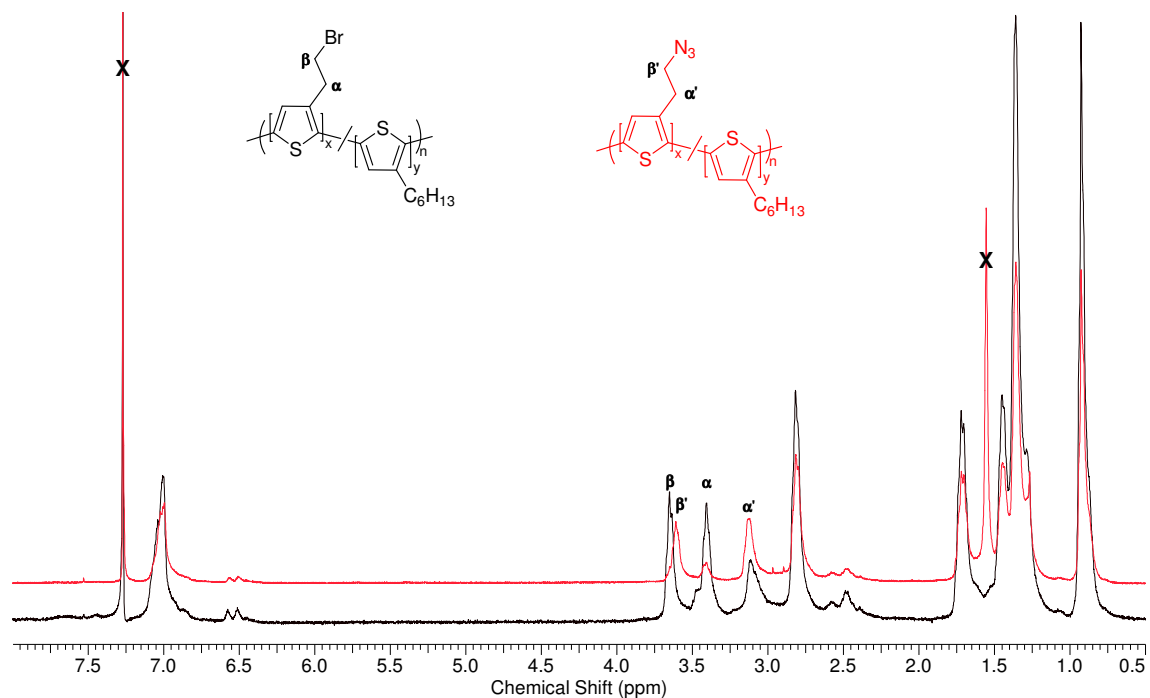


Figure 2-2. ^1H NMR spectra of **Poly-1** (black) and **Poly-2** (red). X = residual CHCl_3 and H_2O in the deuterated solvent.

The conversion of **Poly-1** to **Poly-2** was further confirmed with ATR-IR spectroscopy. As observed in Figure 2-3, the appearance of the strong stretching frequency located at 2091 cm^{-1} is indicative of the azide functional group. Unfortunately, there was no clear indication in the IR spectrum if residual bromide groups were present in **Poly-2** since the stretching frequency of a C-Br bond is typically found in the fingerprint region in the range from $\sim 300\text{-}500\text{ cm}^{-1}$ and there are several overlapping signals found in **Poly-1** and **Poly-2** in this region.⁴¹

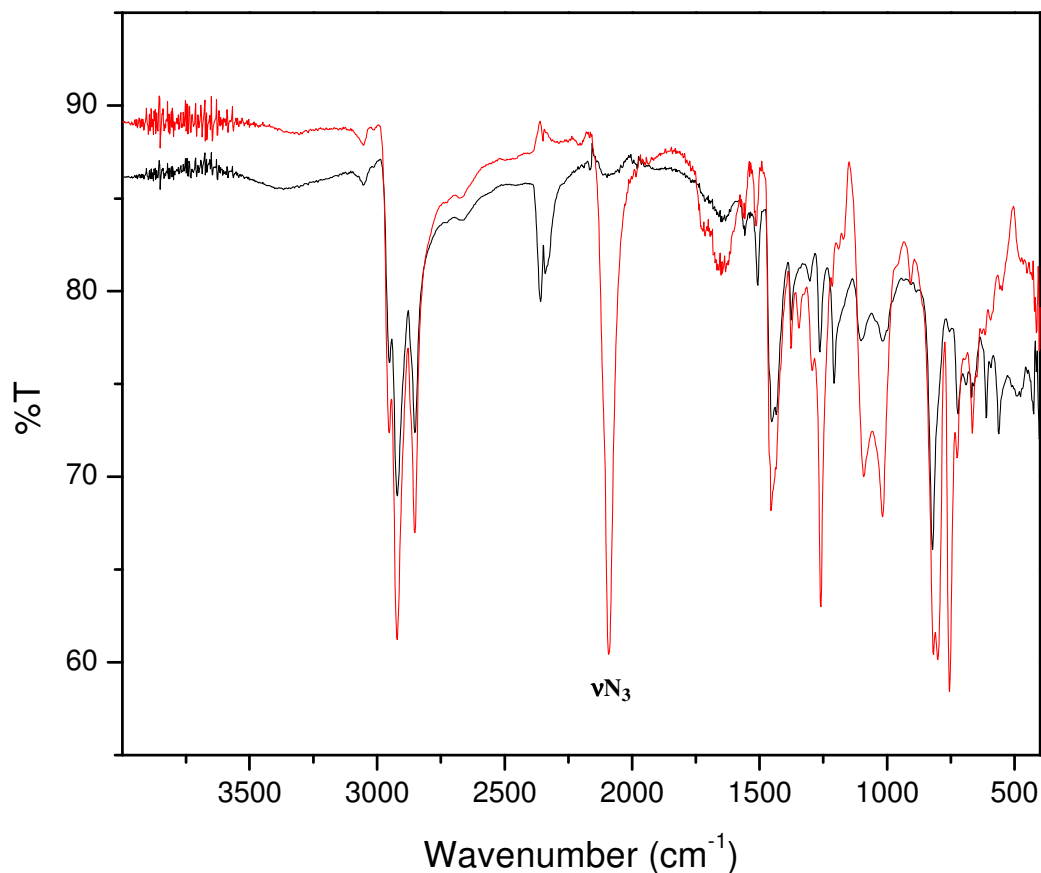


Figure 2-3. ATR-IR spectra of **Poly-1** (black) and **Poly-2** (red).

Table 2-1 summarizes the absorption and emission data of **Poly-1** and **Poly-2** obtained with UV-vis and fluorescence spectroscopy. These values are observed to be similar to that of HT rr-P3HT in both solution and solid state. In regio-random P3HT, containing 50% HT couplings, the solution absorbance maximum is at 436 nm,⁹ due to reduced conjugation along the polymer backbone caused by the steric induced twisting of the polymer backbone. The solid state absorption of **Poly-1** displays the expected red shift for samples of HT P3ATs due to self-orientation in the solid state.¹⁰ These optical studies further confirm the high degree of HT regioregularity along the backbones of both **Poly-1** and **Poly-2**.

Table 2-1. Absorption and emission data comparisons for **Poly-1** and **Poly-2**

	Poly-1	Poly-2	McCullough⁹ rr-P3HT	Rieke⁷ rr-P3HT	Random⁹ P3HT
Absorption ^a λ_{\max} (nm)	442	440	442	456	436
Emission ^a λ_{\max} (nm)	572	573	-	569	-
Absorption ^b λ_{\max} (nm)	519	-	504	-	480

^a CH₂Cl₂; ^b Thin films on glass slides cast from CHCl₃.

2.3.3 Monomer Click Reaction and Spectroscopy

Sharpless *et al.* showed that while Cu^I can be directly used in the Click reaction, preparation of the copper catalyst *in situ* by reduction of Cu^{II} salts is a better approach since Cu^{II} salts are typically less expensive and are often of higher purity than Cu^I salts.⁴² The Cu^I catalyzed reactions require a co-solvent, a molar equivalent of a nitrogen base, and lead to higher yields of undesired by-products. The catalyst chosen for the work discussed herein was CuSO₄·5H₂O which is reduced from Cu^{II} to Cu^I *in situ* using ascorbic acid.

Initial investigations of the Click reaction catalyzed by Cu^I were carried out using the azide thiophene **64** (Scheme 2-6). Compound **64** was dissolved in a mixture of *t*-BuOH:H₂O:CHCl₃ (2.5:2.5:1). To this solution was added one molar equivalent of methylpropiolate, 1 mol% CuSO₄·5H₂O and 10 mol% L-ascorbic acid. The solution was allowed to react overnight at reflux. The following day the sample was purified via column chromatography yielding the 1,4- and 1,5-substituted products **65** and **66** in a 6.5:1 ratio. In the ¹H NMR spectra (Figure 2-4) of **65** and **66**, the triazole protons of the

two isomers appear at δ 7.92 and δ 8.12, respectively, similar to analogous resonances in related compounds.^{42,43}

Scheme 2-6

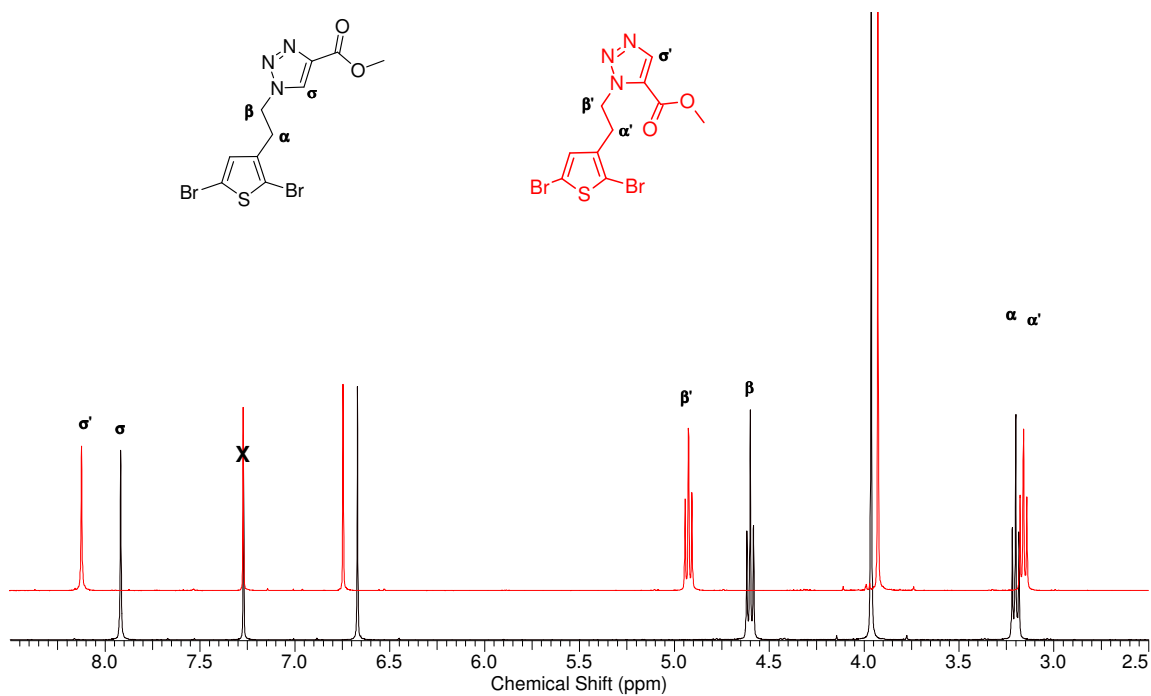
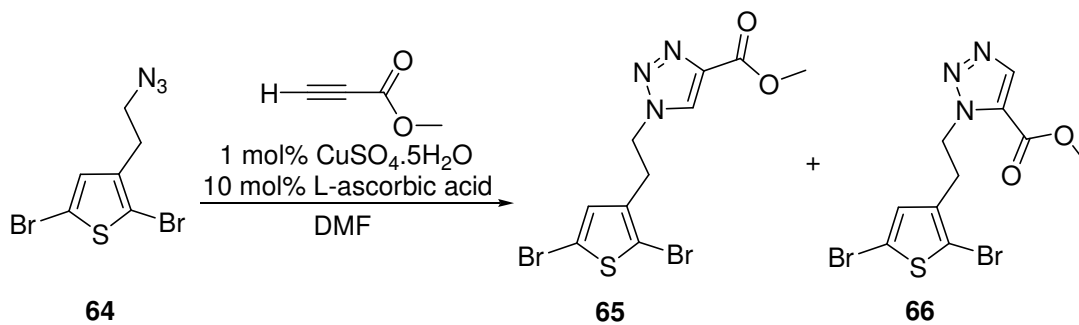


Figure 2-4. ^1H NMR spectra isomers **65** (black) and **66** (red). X = residual CHCl_3 in the deuterated solvent.

To distinguish between the two possible isomers, a ^1H NMR nuclear Overhauser effect (NOE) difference spectral analysis was carried out. With this analysis, one can determine through space ^1H - ^1H proximity within a molecule. A particular proton is irradiated and by means of the through space NOE, a proton close in space will display enhanced signal intensity.⁴⁴ When the triazole proton (δ 7.92) of compound **65** was irradiated, the resonance signal of the β methylene triplet at δ 4.60 geminal to the triazole ring increased in intensity (Figure 2-5). A slight increase in intensity of the ester $-\text{CH}_3$ group at δ 3.96 was also observed. In compound **66**, irradiation of the triazole proton at δ 8.12, led only to an increase in intensity for the $-\text{CH}_3$ group of the ester confirming that the major product is indeed the 1,4-substituted isomer.

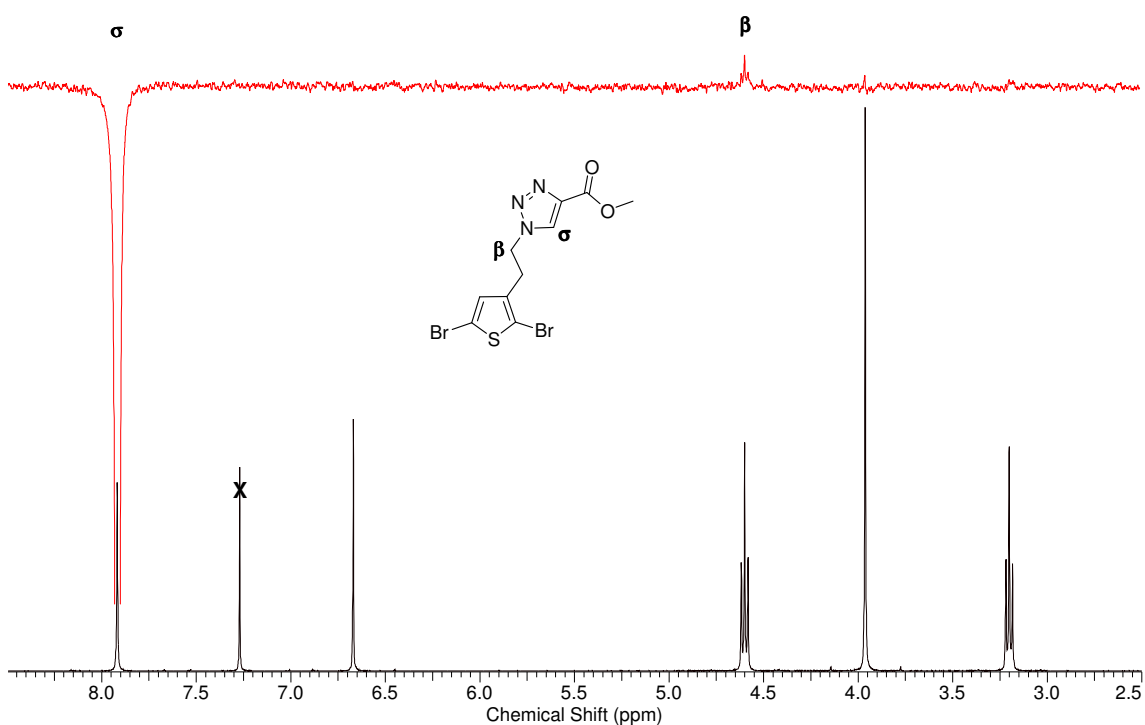
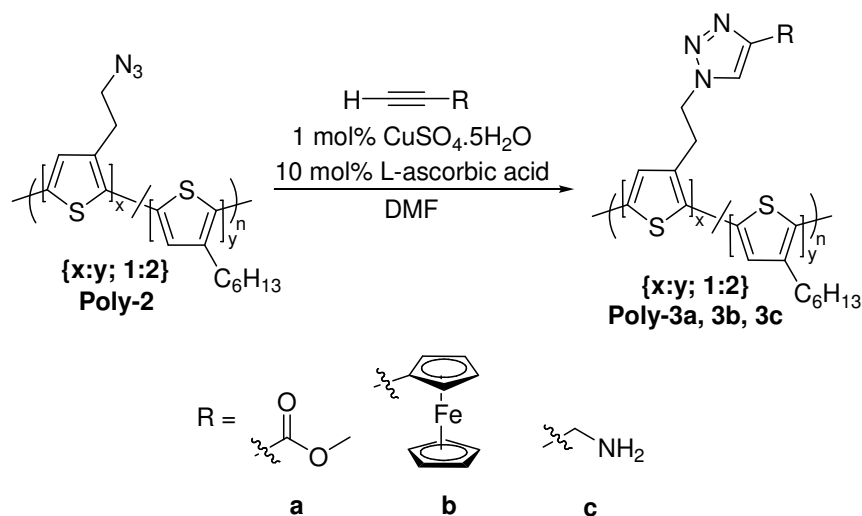


Figure 2-5. ^1H - ^1H NMR NOE difference spectrum (red) and ^1H NMR spectrum (black) of **65**. X = residual CHCl_3 in the deuterated solvent.

2.3.4 Polymer Click Reactions and Spectroscopy

We selected several different acetylenes to demonstrate functionalization of **Poly-2** via the Click reaction. Reaction of **Poly-2** with methylpropiolate, ethynylferrocene, or 3-aminopropyne gave **Poly-3a**, **-3b** and **-3c** respectively using reaction conditions similar to those established for the molecular Click reaction to generate thiophene **65** (Scheme 2-7).

Scheme 2-7



Poly-3c is insoluble in many common organic solvents such as CHCl_3 , CH_2Cl_2 , and THF and was characterized only by ATR-IR spectroscopy, which clearly shows the disappearance of the azide stretching band at 2091 cm^{-1} and the appearance of a broad signal at 3270 cm^{-1} , in the characteristic range of $-\text{NH}_2$ functional groups.⁴¹ It is possible that the insolubility is due to strong hydrogen bonding between amino groups on neighbouring polymer sidechains. **Poly-3a** and **-3b** were found to be soluble in common organic solvents such as CH_2Cl_2 and THF and were characterized by ^1H NMR and ATR-IR spectroscopy, as well as SEC. The absorption and emission spectra of both **Poly-3a**

and **-3b** did not show significant changes from those of **Poly-2**. To confirm the reaction of the azide moiety, the ^1H NMR spectrum of **Poly-3a** was compared to that of compound **64**. Figure 2-6 displays the new resonances attributed to reaction of the azide with methylpropiolate. In particular, the two sets of methylene protons (α' and β') shift downfield and the methyl ester protons appear at δ 3.92.

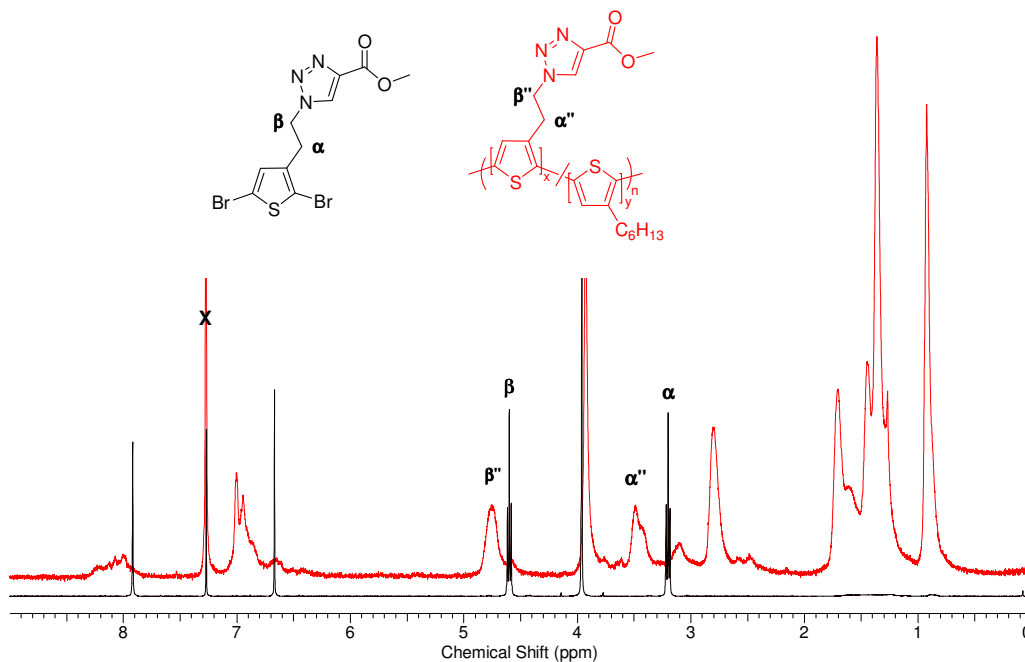


Figure 2-6. ^1H NMR spectra of **65** (black) and **Poly-3a** (red).

The relative purity of **Poly-3a** and **-3b** was confirmed by the lack of signals due to starting material in the ^1H NMR and ATR-IR spectra. In the ^1H NMR spectra, the signals due to the acetylene proton for the ester and ferrocenyl starting materials at δ 2.90 and δ 2.75 respectively were not observed. As well, the ATR-IR spectra of both **Poly-3a** and **-3b** were free of the characteristic acetylene stretching frequencies at ~ 3300 ($\nu_{\text{C-H}}$), and ~ 2150 ($\nu_{\text{C=C}}$) cm^{-1} . ATR-IR spectroscopy also confirmed that the reaction had gone to completion as the azide stretching frequency at 2091 cm^{-1} disappeared.

It is of interest to substitute PTs with groups such as metal complexes having redox and optical properties that can be coupled to the polymer. The metal may have the capacity to influence the properties of the π -conjugated polymer which can potentially give rise to new and enhanced properties.⁴⁵ The ferrocenyl substituted PT, **Poly-3b**, was prepared as an example, showing that the Click methodology is a useful route to metal functionalized PTs. Ferrocene functionalized PTs, prepared both via electrochemical and chemical coupling routes have been previously studied.^{46,47}

Cyclic voltammetry of **Poly-3b** was carried out in dry CH_2Cl_2 containing 0.1 M $[\text{n-Bu}_4\text{N}]\text{PF}_6$ as the supporting electrolyte. Scans were collected from +0.2 to +1.2 V vs. SCE on a Pt working electrode with a Pt-wire mesh counter electrode (Figure 2-7). The lower potential redox wave at $E_{\text{red}} = 0.59$ V is attributed to the ferrocenyl group based on CV studies of ethynylferrocene which shows a reversible redox wave at $E_{\text{red}} = 0.66$ V. The broad oxidation waves at higher potential are attributed to redox processes on the polymer backbone.⁴⁸

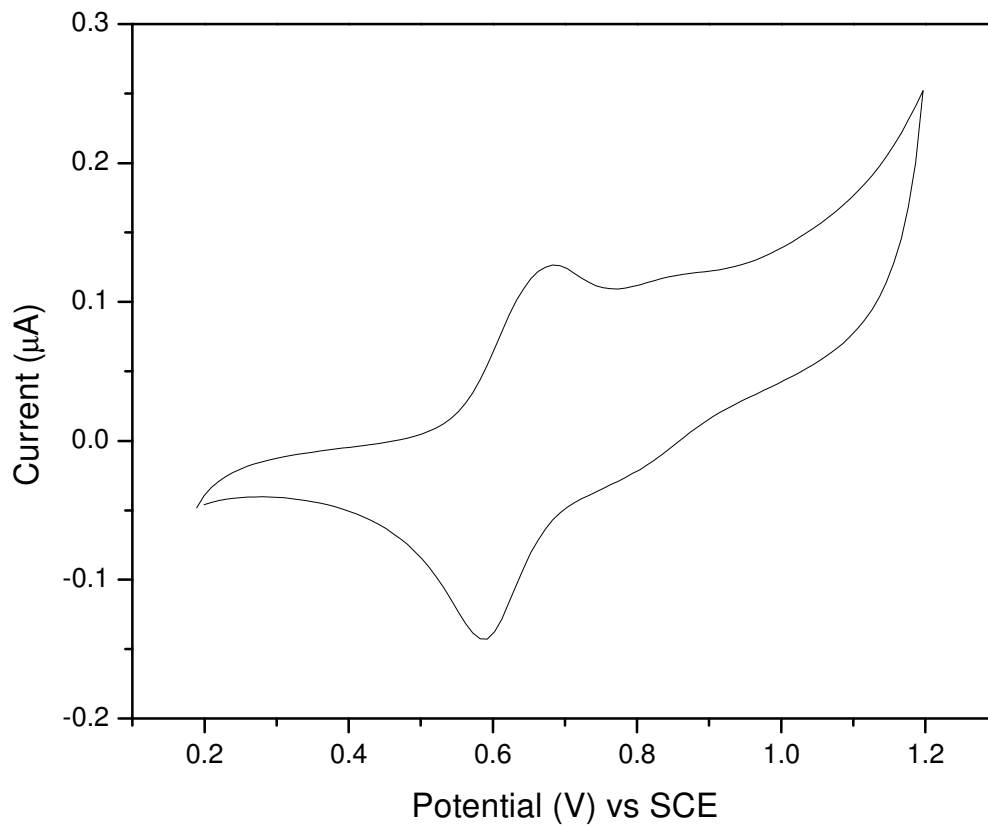


Figure 2-7. Cyclic voltammogram of **Poly-3b** on a Pt button electrode in dry CH_2Cl_2 containing 0.1 M $[\text{n-Bu}_4\text{N}]\text{PF}_6$. Scanned from +0.2 to +1.2 V vs. SCE, scan rate = 100 mVs^{-1} .

2.4 Conclusions

GRIM polymerization was successfully used to prepare a rr-PT which contained both solubilizing groups and latent functionality. The copolymer was determined to have an 85% HT content by ^1H NMR, and the extent of regioregularity was further validated by the significant red shift observed in the electronic absorption spectrum. It was demonstrated that latent functionality built into the original polymer facilitated synthetic manipulation of the side chains post-polymerization. Several functionalized PTs were prepared using the Sharpless Click reaction.

2.5 References

1. Assadi, A.; Svensson, C.; Willander, M.; Inganäs, O., *Appl. Phys. Lett.* **1988**, 53, (3), 195-197.
2. Bao, Z. N.; Lovinger, A. J., *Chem. Mater.* **1999**, 11, (9), 2607-2612.
3. Chang, J. F. et al., *Chem. Mater.* **2004**, 16, (23), 4772-4776.
4. Sirringhaus, H. et al., *Nature* **1999**, 401, (6754), 685-688.
5. Sirringhaus, H.; Tessler, N.; Friend, R. H., *Science* **1998**, 280, (5370), 1741-1744.
6. Chen, T. A.; Rieke, R. D., *Synth. Met.* **1993**, 60, (2), 175-177.
7. Chen, T. A.; Wu, X. M.; Rieke, R. D., *J. Am. Chem. Soc.* **1995**, 117, (1), 233-244.
8. McCullough, R. D.; Lowe, R. D., *J. Chem. Soc., Chem. Commun.* **1992**, (1), 70-72.
9. McCullough, R. D.; Lowe, R. D.; Jayaraman, M.; Anderson, D. L., *J. Org. Chem.* **1993**, 58, (4), 904-912.
10. McCullough, R. D. et al., *J. Am. Chem. Soc.* **1993**, 115, (11), 4910-4911.
11. McCullough, R. D. et al., *Synth. Met.* **1995**, 69, (1-3), 279-282.
12. Ewbank, P. C.; Stefan, M. C.; Sauve, G.; McCullough, R. D., Synthesis, Characterization and Properties of Regioregular Polythiophene-based Materials. In *Handbook of Thiophene-Based Materials: Applications in Organic Electronics and Photonics*, Perepichka, I. F., Perepichka, D. F., Eds. John Wiley & Sons: Chichester, 2009; Vol. 1, pp 157-217.
13. Chen, T. A.; Rieke, R. D., *J. Am. Chem. Soc.* **1992**, 114, (25), 10087-10088.
14. Iraqi, A.; Barker, G. W., *J. Mater. Chem.* **1998**, 8, (1), 25-29.
15. Guillerez, S.; Bidan, G., *Synth. Met.* **1998**, 93, (2), 123-126.

16. Loewe, R. S.; Khersonsky, S. M.; McCullough, R. D., *Adv. Mater.* **1999**, 11, (3), 250-253.
17. Loewe, R. S. et al., *Macromolecules* **2001**, 34, (13), 4324-4333.
18. Burroughes, J. H. et al., *Nature* **1990**, 347, (6293), 539-541.
19. Friend, R. H.; Greenham, N. C., Electroluminescence in Conjugated Polymers. In *Handbook of Conducting Polymers*, Skotheim, T. A., Elsenbaumer, R. L., Reynolds, J. R., Eds. Marcel Dekker: New York, 1986; pp 823-845.
20. Perepichka, I. F.; Perepichka, D. F.; Meng, H., Thiophene-based Materials for Electroluminescent Applications. In *Handbook of Thiophene-Based Materials: Applications in Organic Electronics and Photonics*, Perepichka, I. F., Perepichka, D. F., Eds. John Wiley & Sons: Chichester, 2009; Vol. 1, pp 695-756.
21. Facchetti, A., Electroactive Oligothiophenes and Polythiophenes for Organic Field Effect Transistors. In *Handbook of Thiophene-Based Materials: Applications in Organic Electronics and Photonics*, Perepichka, I. F., Perepichka, D. F., Eds. John Wiley & Sons: Chichester, 2009; Vol. 1, pp 595-646.
22. McCulloch, I.; Heeney, M., Thienothiophene Copolymers in Field Effect Transistors. In *Handbook of Thiophene-Based Materials: Applications in Organic Electronics and Photonics*, Perepichka, I. F., Perepichka, D. F., Eds. John Wiley & Sons: Chichester, 2009; Vol. 1, pp 647-672.
23. Dennler, G.; Scharber, M. C.; Brabec, C. J., *Adv. Mater.* **2009**, 21, (13), 1323-1338.
24. Kim, B. J.; Miyamoto, Y.; Ma, B. W.; Fréchet, J. M. J., *Adv. Funct. Mater.* **2009**, 19, (14), 2273-2281.

25. Xiao, S. Q.; Stuart, A. C.; Liu, S. B.; You, W., *ACS App. Mater. & Inter.* **2009**, 1, (7), 1613-1621.
26. Osaka, I.; McCullough, R. D., *Acc. Chem. Res.* **2008**, 41, (9), 1202-1214.
27. Kolb, H. C.; Finn, M. G.; Sharpless, K. B., *Angew. Chem. Int. Ed.* **2001**, 40, (11), 2004-2021.
28. Binder, W. H.; Kluger, C., *Curr. Org. Chem.* **2006**, 10, (14), 1791-1815.
29. Higuchi, H. et al., *Bull. Chem. Soc. Jpn.* **1995**, 68, (8), 2363-2377.
30. Aubertin, F.; Zhao, Y., *J. Polym. Sci., Part A: Polym. Chem.* **2004**, 42, (14), 3445-3455.
31. Hong, X. Y.; Tyson, J. C.; Middlecoff, J. S.; Collard, D. M., *Macromolecules* **1999**, 32, (13), 4232-4239.
32. Taranekar, P. et al., *J. Am. Chem. Soc.* **2007**, 129, 8958-8959.
33. Heffner, G. W.; Pearson, D. S., *Macromolecules* **1991**, 24, (23), 6295-6299.
34. Zhai, L. et al., *Macromolecules* **2003**, 36, (1), 61-64.
35. Murray, K. A.; Holmes, A. B.; Moratti, S. C.; Friend, R. H., *Synth. Met.* **1996**, 76, (1-3), 161-163.
36. Murray, K. A.; Holmes, A. B.; Moratti, S. C.; Rumbles, G., *J. Mater. Chem.* **1999**, 9, (9), 2109-2115.
37. Schuh, K.; Prucker, O.; Rühle, J., *Macromolecules* **2008**, 41, (23), 9284-9289.
38. Varma, I. K. et al., *J. Appl. Polym. Sci.* **2006**, 101, (1), 779-786.
39. Braun, D. et al., *Methods and Techniques for Synthesis, Characterization, Processing and Modification of Polymers*. In *Polymer Synthesis: Theory and*

- Practice: Fundamentals, Methods, Experiments*, 4 ed.; Berlin, A. G., Ed. Springer Berlin Heidelberg: New York, 2005; pp 55-172.
40. Iovu, M. C.; Sheina, E. E.; Gil, R. R.; McCullough, R. D., *Macromolecules* **2005**, 38, (21), 8649-8656.
 41. *Inorganic Spectroscopic Methods*. Brisdon, A. K., Ed. Oxford University Press: New York, 1998; p 20.
 42. Rostovtsev, V. V.; Green, L. G.; Fokin, V. V.; Sharpless, K. B., *Angew. Chem. Int. Ed.* **2002**, 41, (14), 2596-2599.
 43. Luxenhofer, R.; Jordan, R., *Macromolecules* **2006**, 39, (10), 3509-3516.
 44. Silverstein, R. M.; Webster, F. X., Nuclear Overhauser Effect Difference Spectrometry $^1\text{H}^1\text{H}$ Proximity Through Space. In *Spectrometric Identification of Organic Compounds*, 6 ed.; Swain, E., Ed. John Wiley & Sons, Inc.: New York, 1998; pp 189--191.
 45. Wolf, M. O., Synthesis and Properties of Oligo- and Polythiophenes Containing Transition Metals. In *Handbook of Thiophene-Based Materials: Applications in Organic Electronics and Photonics*, Perepichka, I. F., Perepichka, D. F., Eds. John Wiley & Sons: Chichester, 2009; Vol. 1, pp 293-314.
 46. Bu, H. B. et al., *Chem. Commun.* **2008**, (11), 1320-1322.
 47. Zotti, G. et al., *Synth. Met.* **1996**, 76, (1-3), 255-258.
 48. Roncali, J., *Chem. Rev.* **1992**, 92, (4), 711-738.

CHAPTER 3 Synthesis and Characterization of Dithienylethene Modified Oligo- and Polythiophenes*

3.1 Introduction

Polythiophenes (PTs) are an important class of CPs. They form some of the most environmentally and thermally stable materials for potential applications in: OLEDs,¹⁻³ sensors,^{4,5} batteries,^{6,7} OPVs,⁸⁻¹⁰ and transistors.^{11,12} The clear relationship between structure and function dictates that a directed synthesis will lead to a better defined structure and therefore more predictable properties. The GRIM polymerization is an ideal method because it affords high HT regioregularity within a polymer backbone,^{13,14} and contributes to improved chemical properties such as a smaller bandgap and higher conductivities.¹⁵⁻¹⁷

Introduction of additional functionality to the polymer backbone leads to further tuning and modification of the polymer properties compared to those of unsubstituted PT.¹⁸⁻²⁰ Modification of polymer properties via functional side groups that can have properties such as refractive index, conductivity, absorption or luminescence altered *in-situ* are appealing for applications in electronic and electrochemical devices.²¹ Of particular interest are a family of compounds that possess a hexatriene moiety that can be photochemically and reversibly transformed between two isomers; a phenomenon known as photochromism. Here, absorption of electromagnetic radiation of a specific wavelength induces a reversible chemical transformation between the two isomers **A** and

* A version of this chapter has been published. Finden, J.; Kunz, T. K.; Branda, N. R.; Wolf, M. O., Reversible Amplified Fluorescence Quenching of Dithienylethene Functionalized Polythiophene. *Adv. Mater.* **2008**, 20, (10), 1998-2002.

B, with each isomer having unique absorption spectra as well as distinct structural and chemical properties.²²

One of the most promising examples of the hexatriene backbones is found in 1,2-dithienylethenes (DTEs), a class of light-activated molecular switches. DTEs can be interchanged between two thermally stable isomers when irradiated with UV and visible light, inducing the ring-closing and ring-opening reactions respectively (Figure 3-1).^{21,23} In addition to thermal irreversibility, the ring-opening/ring-closing cycles are highly fatigue resistant, capable of more than 10,000 repetitions without losing photochromic performance.^{21,23} These properties are indispensable for application of DTE molecules in optoelectronic devices such as memories²⁴⁻²⁶ and switches.²⁷⁻³¹

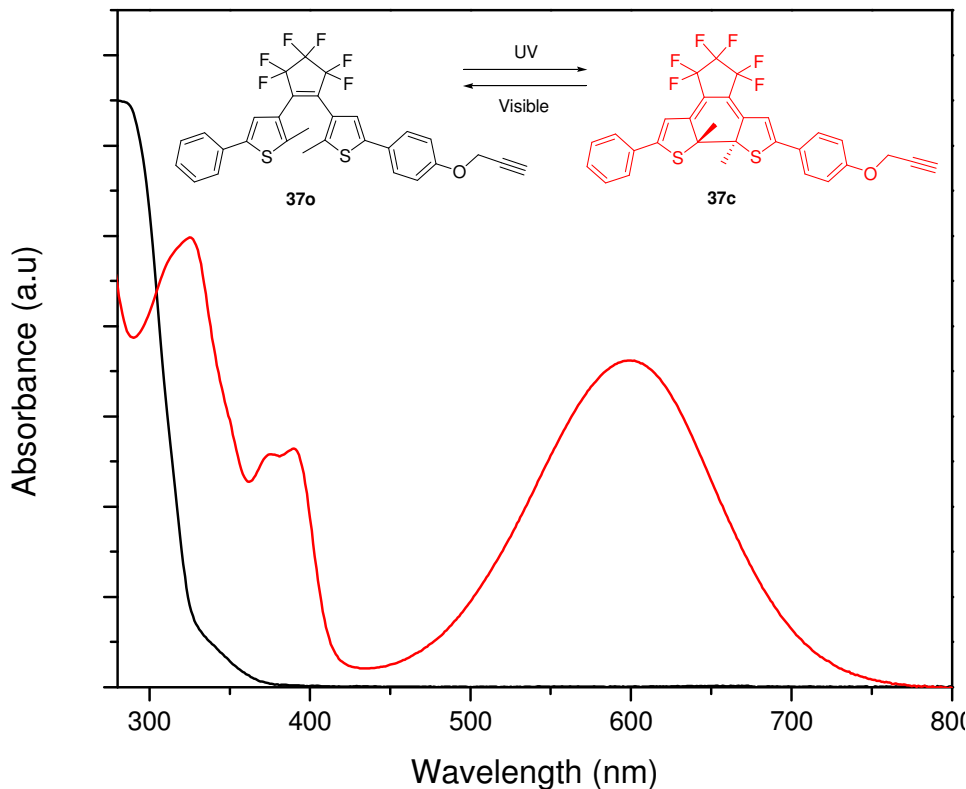


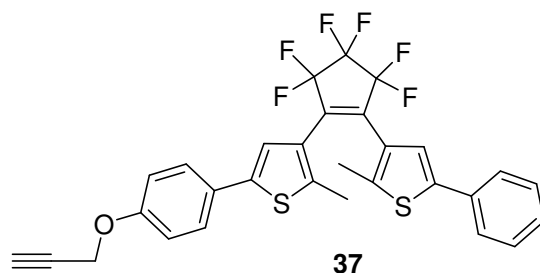
Figure 3-1. Typical absorption spectra of the ring-open (black) and ring-closed (red) isomers of substituted DTE.

In the following discussion, a rr-P3AT prepared via GRIM synthetic conditions is functionalized with acetylene modified DTE using the Click reaction. The coupling of the photo-induced cyclization of DTE to the enhanced electronic properties of a regioregular polymer may have potential for developing optically triggered organic materials. The syntheses of several DTE functionalized rr-P3AT analogs are reported. Typical spectroscopic and chromatographic characterizations of each analog are presented and structural differences are compared for their potential influence on the properties of the polymer backbone.

3.2 Experimental

3.2.1 General

All reagents and solvents including deuterated solvents for NMR analysis (Cambridge Isotope Laboratories) were used as received unless otherwise noted. Tetrahydrofuran (THF) was distilled from Na/benzophenone. Anhydrous N,N-dimethylformamide (DMF) was obtained from Aldrich (sure-seal). Column chromatography was performed using silica gel 60 (230-400 mesh) from Silicycle Inc. Compound **37** was prepared as described in literature³² by Dr. Jeremy Finden in Prof. Branda's group at Simon Fraser University.



¹H NMR and ¹³C NMR spectra were obtained on a Bruker AV-600, Varian Inova 500, Bruker AV-400 Inverse, Bruker AV-400 Direct, or Bruker AV-300 spectrometer. ¹⁹F NMR spectra were obtained on a Bruker AV-300 spectrometer. Chemical shifts (δ) are reported in parts per million (ppm), referenced to residual chloroform (CHCl₃). Coupling constants (J) are reported in Hertz (Hz). Integration of ¹H NMR spectra shows slight variations from batch to batch of similarly prepared GRIM polymers. Consistency between samples was maintained by preparing all subsequent samples from a single precursor polymer. Photostationary states (PSS) are reported as percent ring-closed isomer to ring-open as determined by integration of DTE resonance peaks in ¹H NMR

spectra. ATR-IR spectra were recorded on either a Thermo Scientific Nicolet 6700 FT-IR spectrometer as neat oils or powders. Molecular weight distribution curves of polymers were determined by size exclusion chromatography (SEC) was performed using a Waters SEC equipped with 3 μ g-Styrgel columns against polystyrene standards. Polymers were dissolved, filtered and eluted with THF at a flow rate of 1.0 mL/min and monitored with a UV-vis detector (Waters 2487). Data was acquired and analyzed using an IBM personal computer and custom-written software. All of the reactions and spectroscopic analyses involving the DTE species were performed in darkened rooms or nearly dark conditions to prevent unwanted ring-closing/opening events.

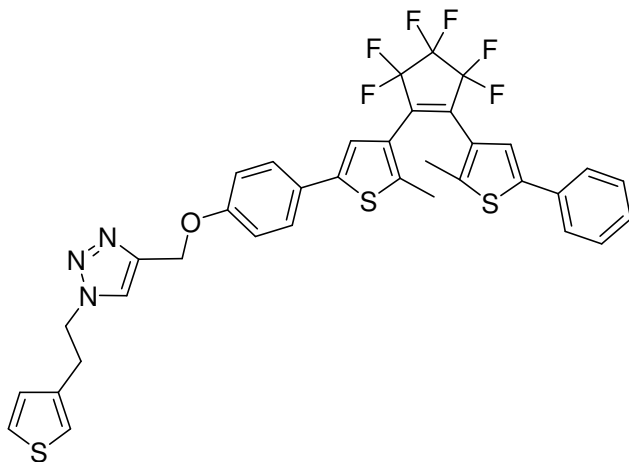
3.2.2 Procedures

Synthesis of 3-(2'-azidoethyl)thiophene (67)



This compound was prepared via modifications to the literature procedure.³³ To a vigorously stirred solution of 3-(2'-bromoethyl)thiophene (2.65 g, 13.9 mmol) in ethanol (50 mL), sodium azide (1.84 g, 28.3 mmol) was added and the resulting mixture was heated to and maintained at 85 °C overnight. The reaction was removed from heat, allowed to cool to room temperature, gravity filtered and concentrated under reduced pressure. The resulting oil was purified via column chromatography (silica, hexanes) to yield a colourless oil. Yield: 0.63 g (30%). ¹H NMR (300 MHz, CDCl₃, δ): 7.31 (m, 1H), 7.07 (m, 1H), 6.98 (dd, 1H), 3.52 (t, 2H), 2.95 (t, 2H).

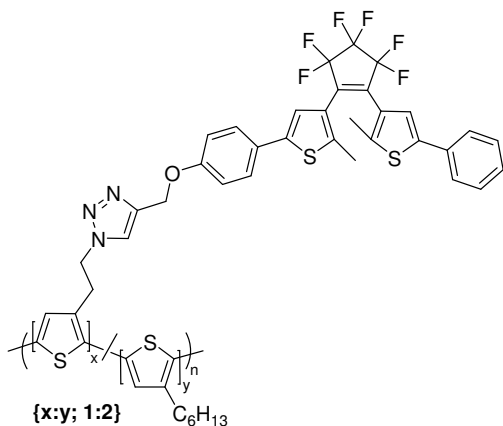
Synthesis of Compound **68**



A vigorously stirred solution of **67** (0.10 g, 0.65 mmol) and **DTE-37** (0.206 g, 0.359 mmol) in *t*-C₄H₉OH (15 mL) was treated with a solution of L-ascorbic acid (0.102 g, 0.065 mmol) and CuSO₄·5H₂O (2 mg, 0.006 mmol) in a minimal amount of water (2 mL). After stirring at room temperature for one hour, the organic fraction was extracted with chloroform (3 × 25 mL). The combined organic fractions were washed with distilled water (3 × 25 mL), dried over MgSO₄, filtered and evaporated under reduced pressure. Compound **68** was purified by column chromatography (silica, CH₂Cl₂/hexanes 3:1) and recrystallized from ethanol. Yield: 0.10 g (38%). mp = 158°C. ¹H NMR (400 MHz, CDCl₃, δ): 7.55 (d, *J* = 7.6 Hz, 2H), 7.47 (d, *J* = 8.5 Hz, 2H), 7.39 (m, 3H), 7.31 (m, 4H), 7.16 (s, 1H), 6.97 (d, *J* = 8.7 Hz, 2H), 6.88 (m, 1H), 6.83 (d, *J* = 4.9 Hz, 1H), 5.23 (s, 2H), 4.60 (t, *J* = 7.0 Hz, 2H), 3.26 (t, *J* = 7.0 Hz, 2H), 1.97 (s, 3H), 1.96 (s, 3H). ¹³C NMR (75.5 MHz, CDCl₃, δ): 158.0, 143.7, 142.2, 142.0, 141.3, 140.5, 137.0, 133.3, 129.0, 127.9, 127.6, 127.0, 126.7, 126.4, 125.8, 125.7, 125.6, 122.9, 122.4, 122.3, 121.4, 115.3, 62.1, 51.1, 31.1, 14.5, 14.4 (27 of 36 carbons found). HR-MS (ESI) calcd for C₃₆H₂₇N₃OF₆NaS₃ [M + Na]⁺: 750.1118, found 750.1129. ATR-IR (ν, cm⁻¹): 3040, 2928,

2872, 1606, 1557, 1538, 1510, 1506, 1464, 1339, 1269, 1241, 1214, 1185, 1138, 1112, 1052, 1035, 1011, 985, 899, 889, 857, 820, 803, 782, 750, 690, 669, 646, 555, 532, 505. UV-vis (C₆H₆) λ_{max} : (open) 293 nm (ϵ , L mol⁻¹ cm⁻¹: 3.3×10⁴); (closed) 276, 313, 590 nm (ϵ , L mol⁻¹ cm⁻¹: 1.4 × 10⁴). PSS: 95%.

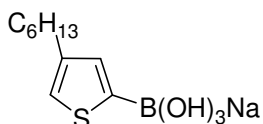
Synthesis of Poly-4



Poly-2³² (0.0296 g, 0.061 mmol) and **DTE-37** (0.0619 mg, 0.108 mmol) were dissolved in CHCl₃ (20 mL) resulting in an orange solution. L-ascorbic acid (2 mg, 0.01 mmol) and CuSO₄·5H₂O (1 mg, 0.004 mmol) were dissolved in a 1:1 mixture of H₂O and *t*-C₄H₉OH (10 mL) and added in one portion. The reaction mixture was heated to 90 °C to dissolve the polymer and the vigorously stirred solution was left overnight. The solution was cooled and the purple polymer was precipitated from methanol (600 mL) and isolated with vacuum filtration. **Poly-4** was then re-precipitated twice more to remove starting material and residual catalyst. Yield: 0.035 g (54%). ¹H NMR (300 MHz, CDCl₃, δ): 7.6–7.3 (m), 7.15 (s), 7.1–6.7 (m), 5.19 (br, s, -OCH₂C=), 4.67 (br, s, -CH₂CH₂N), 3.42 (br, s, -CH₂CH₂N), 2.79 (br, s, -CH₂CH₂(CH₂)₃CH₃), 1.93 (br, s, -CH₃), 1.70 (br, s, -CH₂CH₂(CH₂)₃CH₃), 1.5–1.1 (m, -CH₂CH₂(CH₂)₃CH₃), 0.91 (br, s, -CH₂CH₂(CH₂)₃CH₃).

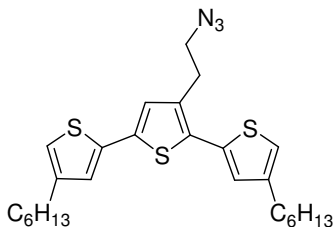
ATR-IR (ν , cm^{-1}): 2959, 2921, 2851, 1716, 1607, 1513, 1462, 1377, 1337, 1259, 1179, 1088, 1014, 886, 795, 688, 669. UV-vis (C_6H_6) λ_{max} : (open) 290, 444 nm; (closed) 321, 347, 367, 385, 444, 592 nm. Fluorescence (C_6H_6) λ_{max} : 574 nm. SEC: $\overline{M}_w = 16000 \text{ g mol}^{-1}$, $\overline{M}_n = 8800 \text{ g mol}^{-1}$, PDI = 1.9. PSS: 96%.

Synthesis of sodium 4-hexyl-2-thienylboronate (**69**)



Synthesized with modifications from literature procedures.^{34,35} *n*-BuLi (18.0 mL, 1.6 M in hexanes, 29 mmol) was added dropwise to a solution of diisopropylamine (2.8 mL, 20 mmol) in dry THF (10 mL) at 0 °C and stirred for half an hour under a N_2 atmosphere. A solution of 3-hexylthiophene (1.5 mL, 8.4 mmol) in dry THF (20 mL) was cooled to -78°C and to this an aliquot of the $\text{Li}[\text{N}(i\text{-Pr})_2]$ (14.3 mL, 10.0 mmol) solution was added dropwise and the resulting solution was stirred for one hour before allowing the mixture to warm to room temperature over several hours. The solution was then re-cooled to -78 °C, trimethylborate (2.0 mL, 18 mmol) was slowly added, and the resulting mixture was again allowed to warm to room temperature overnight. The solution was hydrolyzed with 1 M HCl (20 mL), extracted with diethyl ether (3 × 25 mL), and washed with distilled water. The organic fraction was dried (MgSO_4), filtered and sonicated (15 min) with solid NaOH. The resulting solid was filtered, re-acidified with 1 M HCl (20 mL), extracted with diethyl ether (3 × 25 mL) and precipitated with solid NaOH pellets to yield **69** as a white solid. Yield: 0.94 g (45%), ^1H NMR (300 MHz, D_2O , δ): 6.93 (s, 1H), 6.90 (s, 1H), 2.57 (t, 2H), 1.58 (m, 2H), 1.28 (m, 6H), 0.83 (s, 3H).

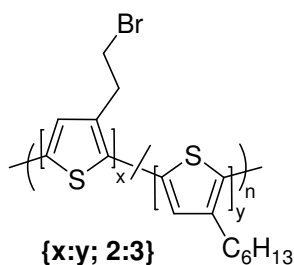
Synthesis of Compound **70**



2,5-dibromo-3-(2-azidoethyl)thiophene (**7**) (1.43 g, 4.60 mmol) was dissolved in dry, N₂ sparged THF (40 mL) with Pd(PPh₃)₄ (0.160 g, 0.138 mmol). A solution of **69** (2.37 g, 9.40 mmol) in saturated aqueous NaHCO₃ solution was added and the reaction mixture turned milky white in colour. The solution was brought to reflux for two hours, cooled and poured over a saturated solution of NH₄Cl. The organic compounds were extracted from the mixture with ethyl acetate (EtOAc) (3 × 25 mL), washed with distilled water, and dried (MgSO₄). The solvent was removed via rotary vacuum evaporation. The remaining oil was purified by column chromatography (silica, 10% EtOAc in hexanes, R_f = 0.60) to give pure **70** as a yellow oil. Yield: 1.2 g (54%). ¹H NMR (400 MHz, CDCl₃, δ): 7.02 (d, *J* = 1.4 Hz, 1H), 7.00 (s, 1H), 6.99 (d, *J* = 1.0 Hz, 1H), 6.93 (s, 1H), 6.82 (s, 1H), 3.54 (t, *J* = 7.3 Hz, 2H), 3.06 (t, *J* = 7.5 Hz, 2H), 2.61 (m, 4H), 1.65 (m, 4H), 1.35 (s, 12H), 0.92 (s, 6H). ¹³C NMR (100.5 MHz, CDCl₃, δ): 144.1, 143.8, 136.3, 136.0, 134.61, 134.57, 131.5, 127.5, 125.6, 125.7, 125.1, 120.3, 119.2, 51.2, 31.6, 30.43, 30.40, 30.3, 29.0, 28.9, 28.8, 22.6, 14.0 (23 of 26 carbons found). EI-MS (*m/z*): M⁺ 485. ATR-IR (ν, cm⁻¹): 3096, 3048, 2953, 2923, 2853, 2091(νN₃), 1547, 1529, 1459, 1416, 1377, 1346, 1295, 1247, 1212, 1140, 1113, 1040, 967, 907, 827, 728, 673, 640, 588, 563, 460. UV-vis (C₆H₆) λ_{max}: 350 nm (ε, L mol⁻¹ cm⁻¹: 2.0 × 10⁴). Fluorescence (C₆H₆) λ_{max}: 423, 440 nm. Anal. Calcd for C₂₆H₃₅N₃S₃ (%): C, 64.29; H, 7.26; N, 8.65. Found: C, 64.07; H, 7.33; N, 8.68.

121.37, 120.58, 119.47, 115.25, 62.08, 50.38, 31.64, 31.56, 30.46, 30.42, 30.33, 30.29, 30.16, 29.26, 28.98, 28.95, 22.63, 22.58, 14.51, 14.45, 14.08, 14.05 (48 of 56 carbons found). EI-MS (m/z): M^+ 1059. ATR-IR (ν , cm^{-1}): 2953, 2925, 2854, 1607, 1553, 1513, 1464, 1437, 1378, 1336, 1269, 1246, 1180, 1136, 1111, 1052, 986, 950, 887, 821, 754, 689, 632, 562, 533, 506, 437. UV-vis (C_6H_6) λ_{max} : (open) 298 nm (ϵ , $\text{L mol}^{-1} \text{cm}^{-1}$: 3.4×10^4), 350 nm (ϵ , $\text{L mol}^{-1} \text{cm}^{-1}$: 1.7×10^4); (closed) 350 nm (ϵ , $\text{L mol}^{-1} \text{cm}^{-1}$: 2.4×10^4), 596 nm (ϵ , $\text{L mol}^{-1} \text{cm}^{-1}$: 1.4×10^4). Fluorescence: $\lambda_{\text{max}} = 422, 440$ nm. PSS: 92%

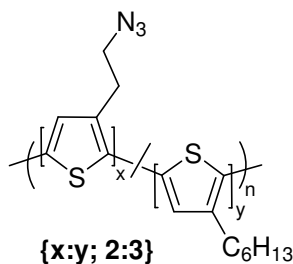
Synthesis of Poly-5



To a round bottom flask containing 100 mL of dry THF, 2,5-dibromo-3-(2'-bromoethyl)thiophene (2.66 g, 7.62 mmol) and 2,5-dibromo-3-hexylthiophene (2.51 g, 7.70 mmol) were added. Methyl magnesium bromide (1.4 M in THF/toluene) (11.0 mL, 15.4 mmol) was added and the solution was heated to reflux for 2 hours during which time the color changed from colorless to orange. The solution was then cooled slightly and 0.5 mol% of $\text{Ni}(\text{dppp})\text{Cl}_2$ was added in one portion. The color changed rapidly to dark red with yellow fluorescence and the solution was heated to reflux overnight. The reaction mixture was allowed to cool to room temperature and the dark purple polymer precipitated from vigorously stirred methanol. The solid was purified by sequential overnight Soxhlet extractions with methanol and hexanes. Yield: 0.13 g (5.9%). $^1\text{H NMR}$

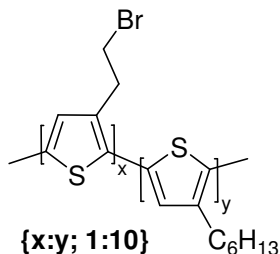
(300 MHz, CDCl₃, δ): 7.00 (br, s), 3.63 (br, s, -CH₂CH₂Br), 3.39 (br, s, -CH₂CH₂Br), 2.80 (br, s, -CH₂CH₂(CH₂)₃CH₃), 1.69 (br, s, -CH₂CH₂(CH₂)₃CH₃), 1.5-1.1 (m, -CH₂CH₂(CH₂)₃CH₃), 0.89 (br, s, -CH₂CH₂(CH₂)₃CH₃). ATR-IR (ν, cm⁻¹): 3054, 2956, 2922, 2852, 1557, 1506, 1449, 1376, 1303, 1260, 1208, 1087, 1015, 863, 796, 758, 723, 705, 662, 611, 593, 562, 483. UV-vis (C₆H₆) λ_{max}: 411 nm. Fluorescence (C₆H₆) λ_{max}: 565 nm. SEC: \overline{M}_w = 4400 g mol⁻¹, \overline{M}_n = 2100 g mol⁻¹, PDI = 2.8.

Synthesis of Poly-6



Following the same procedure used to synthesize **Poly-2**, **Poly-5** (0.064 g, 0.073 mmol) was dissolved in 2:1 CHCl₃:DMF (30 mL) and converted to **Poly-6** which was obtained as a dark purple solid. Yield: 0.033 g (56%). ¹H NMR (MHz, CDCl₃, δ): 7.00 (br, s), 3.60 (br, s, -CH₂CH₂N), 3.11 (br, s, -CH₂CH₂N), 2.79 (br, s, -CH₂CH₂(CH₂)₃CH₃), 1.71 (br, s, -CH₂CH₂(CH₂)₃CH₃), 1.5-1.1 (m, -CH₂CH₂(CH₂)₃CH₃), 0.91 (br, s, -CH₂CH₂(CH₂)₃CH₃). ATR-IR (ν, cm⁻¹): 2960, 2920, 2851, 2094 (νN₃), 1655, 1521, 1437, 1415, 1376, 1346, 1258, 1168, 1082, 1013, 863, 793, 697, 661, 589, 546, 485. UV-vis (C₆H₆) λ_{max}: 411 nm. Fluorescence (C₆H₆) λ_{max}: 564 nm. SEC: \overline{M}_w = 4700 g mol⁻¹, \overline{M}_n = 2600 g mol⁻¹, PDI = 2.1.

Synthesis of **Poly-9**



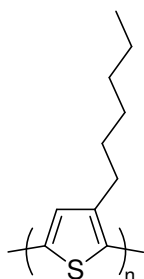
A round bottom flask was charged with 2,5-dibromo-3-hexylthiophene (**60**) (1.55 g, 4.76 mmol) in dry THF (40 mL) and cooled to $-78\text{ }^{\circ}\text{C}$ under a N_2 atmosphere. To this solution, methylmagnesium bromide (3.4 mL, 1.4 M in hexanes, 4.8 mmol) was added dropwise and then allowed to warm to room temperature before bringing the solution to reflux for 1.5 hours. The solution was cooled to allow addition of $\text{Ni}(\text{dppp})\text{Cl}_2$ (0.154 g, 0.286 mmol), immediately turning the solution red in colour. The resulting mixture was brought to reflux where yellow fluorescence was observed within 30 minutes via excitation with a hand held UV lamp. After three hours, the solution was cooled to room temperature, and a solution of **73** was added dropwise via syringe to the mixture.

Intermediate **73** was prepared as follows. A round bottom flask was charged with 2,5-dibromo-3-(2'-bromoethyl)thiophene (**5**) (0.166 g, 0.476 mmol) in dry THF (10 mL) and cooled to $-78\text{ }^{\circ}\text{C}$ under a N_2 atmosphere. To this solution, methylmagnesium bromide (0.34 mL, 1.4 M in hexanes, 0.48 mmol) was added dropwise and then allowed to warm to room temperature before bringing the solution to reflux for two hours.

Prior to addition of **73**, a small aliquot of P3HT (**Poly-8**) was removed via syringe and precipitated from vigorously stirred methanol. The polymerization reaction was continued overnight, after which time the dark red solution was removed from heat and precipitated from vigorously stirred methanol. The resulting copolymer, **Poly-9**, was

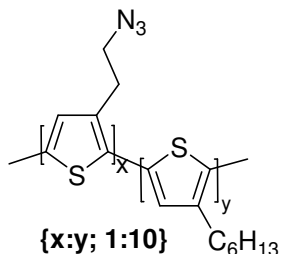
worked up via sequential Soxhlet extractions (16 h CH₃OH, 16 h hexanes, 4 h CHCl₃). Yield: 0.11 g (12%). ¹H NMR (400 MHz, CDCl₃, δ): 6.99 (br, s), 3.57 (br, s, -CH₂CH₂Br), 3.48 (br, s, -CH₂CH₂Br), 2.81 (br, s, -CH₂CH₂(CH₂)₃CH₃), 1.71 (br, s, -CH₂CH₂(CH₂)₃CH₃), 1.36 (br, s, -CH₂CH₂(CH₂)₃CH₃) 0.92 (br, s, -CH₂CH₂(CH₂)₃CH₃). ATR-IR (ν, cm⁻¹): 3054, 2953, 2921, 2852, 1633, 1563, 1510, 1455, 1376, 1263, 1187, 1171, 1105, 962, 887, 819, 577, 722, 667, 613, 592, 564, 536. UV-vis (C₆H₆) λ_{max}: 427 nm. Fluorescence (C₆H₆) λ_{max}: 567 nm. SEC: $\overline{M}_w = 15000 \text{ g mol}^{-1}$, $\overline{M}_n = 6900 \text{ g mol}^{-1}$, PDI = 2.0

Poly-8:



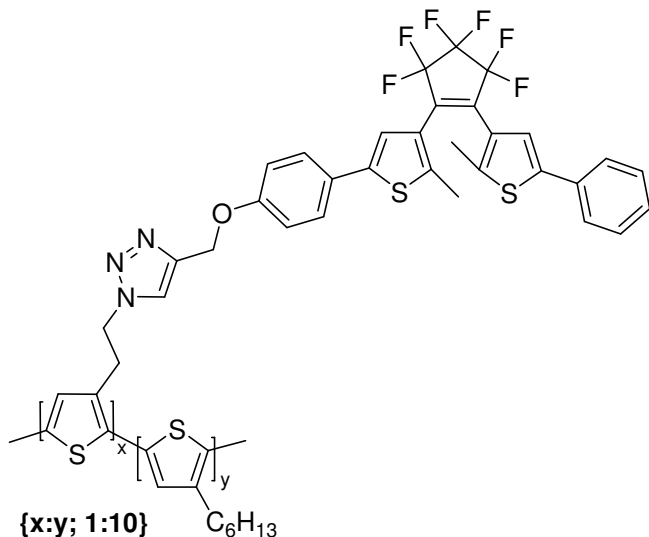
¹H NMR (400 MHz, CDCl₃, δ) 6.99 (br, s), 2.81 (br, s, -CH₂CH₂(CH₂)₃CH₃), 1.71 (br, s, -CH₂CH₂(CH₂)₃CH₃), 1.36 (br, s, -CH₂CH₂(CH₂)₃CH₃) 0.92 (br, s, -CH₂CH₂(CH₂)₃CH₃). ATR-IR (ν, cm⁻¹): 3054, 2954, 2919, 2850, 1633, 1563, 1510, 1454, 1376, 1260, 1094, 1017, 818, 800, 724, 662, 614, 597, 480. UV-vis (C₆H₆) λ_{max}: 427 nm. Fluorescence (C₆H₆) λ_{max}: 568 nm. SEC: $\overline{M}_w = 7300 \text{ g mol}^{-1}$, $\overline{M}_n = 5600 \text{ g mol}^{-1}$, PDI = 1.4

Synthesis of **Poly-10**



Following the same procedure used to synthesize **Poly-2**, **Poly-9** (0.082 g, 0.044 mmol) was converted to **Poly-10** and obtained as a dark purple solid. Yield: 0.055 g (68%). ¹H NMR (400 MHz, CDCl₃, δ) 6.99 (br, s), 3.53 (br, s, -CH₂CH₂N), 3.12 (br, s, -CH₂CH₂N), 2.82 (br, s, CH₂CH₂(CH₂)₃CH₃), 1.72 (br, s, -CH₂CH₂(CH₂)₃CH₃), 1.45-1.36 (br, s, -CH₂CH₂(CH₂)₃CH₃), 0.92 (br, s, -CH₂CH₂(CH₂)₃CH₃). ATR-IR (ν, cm⁻¹): 2955, 2921, 2852, 2097 (νN₃), 1728, 1514, 1455, 1376, 1260, 1090, 1017, 863, 798, 723, 695, 482. UV-vis (C₆H₆) λ_{max}: 428 nm. Fluorescence (C₆H₆) λ_{max}: 568 nm. SEC: \overline{M}_w = 5400 g mol⁻¹, \overline{M}_n = 4700 g mol⁻¹, PDI = 1.2

Synthesis of Poly-11



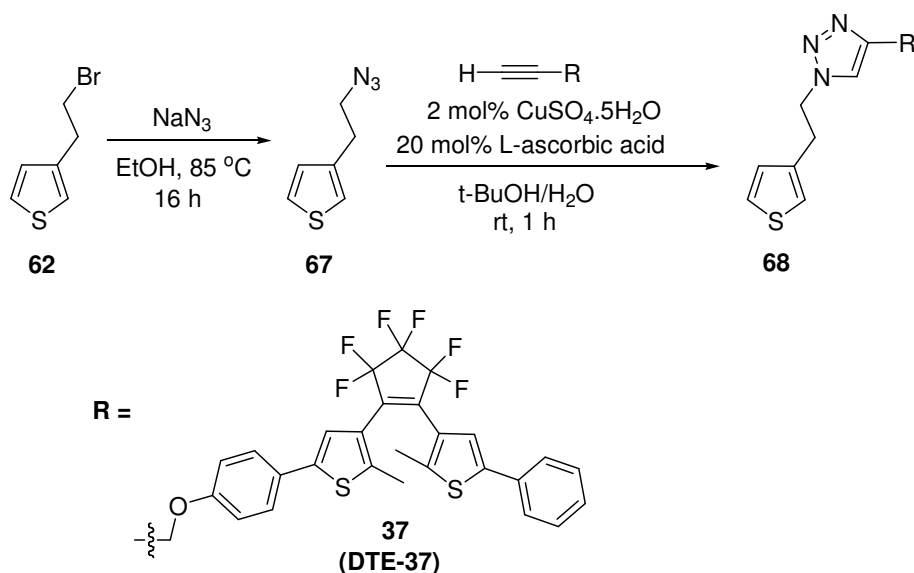
Following the same procedure used to synthesize **Poly-4**, **Poly-10** (0.029 g, 0.016 mmol) was converted to **Poly-11** and obtained as a dark purple solid. Yield: 0.020 g (51%). ¹H NMR (300 MHz, CDCl₃, δ): 7.51 (br), 6.99 (br, s), 5.14 (br, -OCH₂C=), 4.54 (br, -CH₂CH₂N) 3.49 (br, -CH₂CH₂N), 2.81 (br, s, -CH₂CH₂(CH₂)₃CH₃), 1.92 (br, -CH₃), 1.71 – 1.1 (br, -CH₂CH₂(CH₂)₃CH₃), 0.91 (br, s, -CH₂CH₂(CH₂)₃CH₃). ¹⁹F NMR (282 MHz, CDCl₃, δ): -110.3, -132.2. ATR-IR (ν, cm⁻¹): 2959, 2923, 2852, 1513, 1455, 1376, 1259, 1082, 1015, 863, 795, 724, 689, 468. UV-vis (C₆H₆) λ_{max}: (open) 430 nm; (closed) 430, 600 nm. Fluorescence (C₆H₆) λ_{max}: 567 nm. SEC: $\bar{M}_w = 6000 \text{ g mol}^{-1}$, $\bar{M}_n = 4900 \text{ g mol}^{-1}$, PDI = 1.3

3.3 Results and Discussion

3.3.1 Synthesis

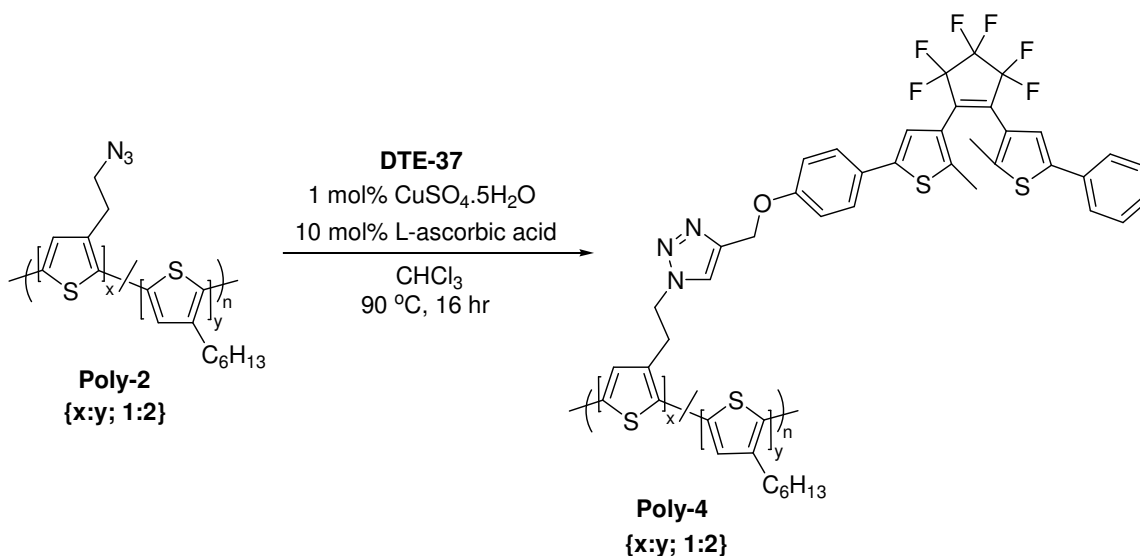
Initial investigations of the Click reaction with **DTE-37** were carried out with a model compound (**68**) which was prepared to ensure that the reaction conditions were not incompatible with the DTE moiety. The model for a DTE functionalized random copolymer was synthesized via a Huisgen 1,3-dipolar cycloaddition Click reaction, from **DTE-37** and 3-(2'-azidoethyl)thiophene (**67**) as shown in Scheme 3-1. The progress of the reaction between compound **67** and **DTE-37** was monitored by thin layer chromatography (TLC), which showed that the reaction had reached completion within an hour while stirring at room temperature. The pure product, **68**, was isolated by column chromatography, and further recrystallized from ethanol to yield a pale blue solid.

Scheme 3-1



The DTE modified PT **Poly-4** was prepared using the same methodology as described for compound **68** (Scheme 3-2). The azide functionalized PT **Poly-2** was dissolved in DMF containing an excess of **DTE-37**, based on the 2:1 ratio of hexyl to azide side chains within the polymer backbone determined from ^1H NMR. The dark purple **Poly-4** was precipitated directly into methanol and isolated by vacuum filtration. **Poly-4** was purified by dissolving it in a minimal amount of CHCl_3 and re-precipitation into methanol to remove catalyst and starting material.

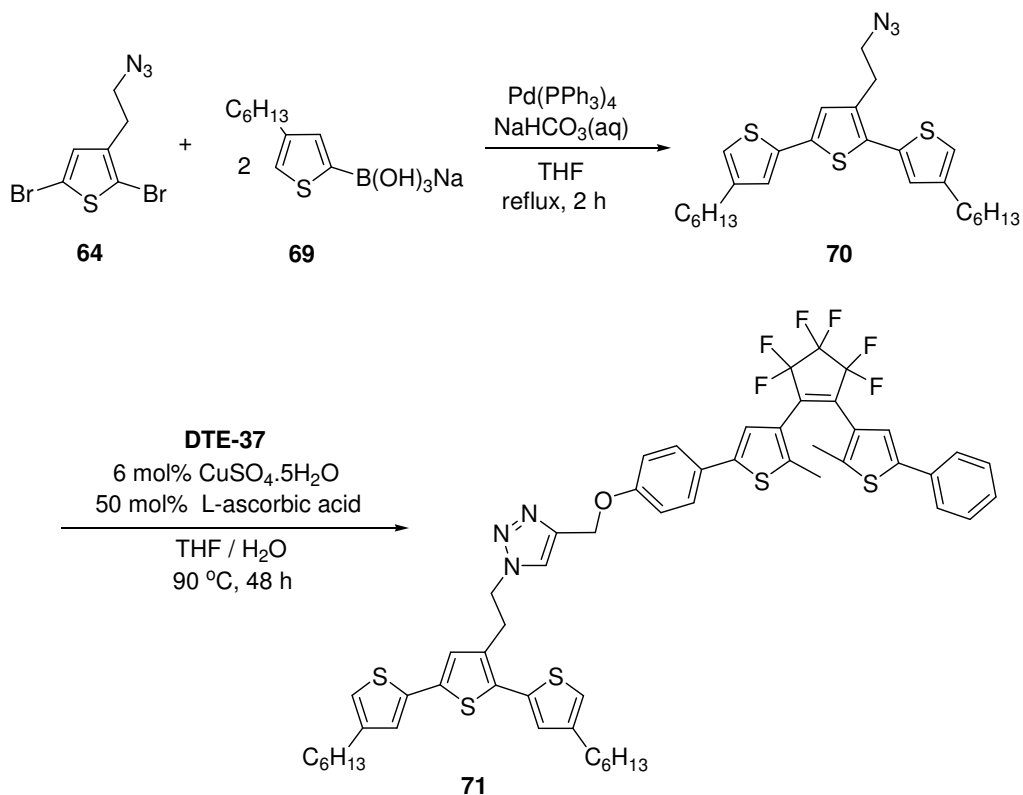
Scheme 3-2



It was of interest to prepare several analogs of **Poly-4** in order to investigate the effect of the conjugation length along the conjugated backbone. The well-defined structure of α -conjugated oligothiophenes can provide valuable information about the structure-property relationships, which are more difficult to deduce from the corresponding polydisperse polymer samples. Studies have shown that oligomers beyond six to seven repeat units in length begin to display electrical, optical and physical

properties similar to an extended CP.³⁶⁻³⁸ For example, the π - π^* optical transition of poly(3-hexylthiophene) has been observed in the region of 430-440 nm, comparable to a heptathiophene (440 nm) derivative.³⁹ The similarity is related to the saturation of the effective conjugation length. In order to study a conjugated backbone of defined length with distinct properties, a terthiophene mimic of **Poly-4** was prepared in two steps (Scheme 3-3). The azide **70** was prepared via Suzuki cross-coupling between compound **64** and two equivalents of sodium 4-hexyl-2-thienylboronate (**69**). Compound **64** was chosen as the central thiophene unit to incorporate the latent side chain functionality consistent with the structure of the backbone of **Poly-4**.

Scheme 3-3



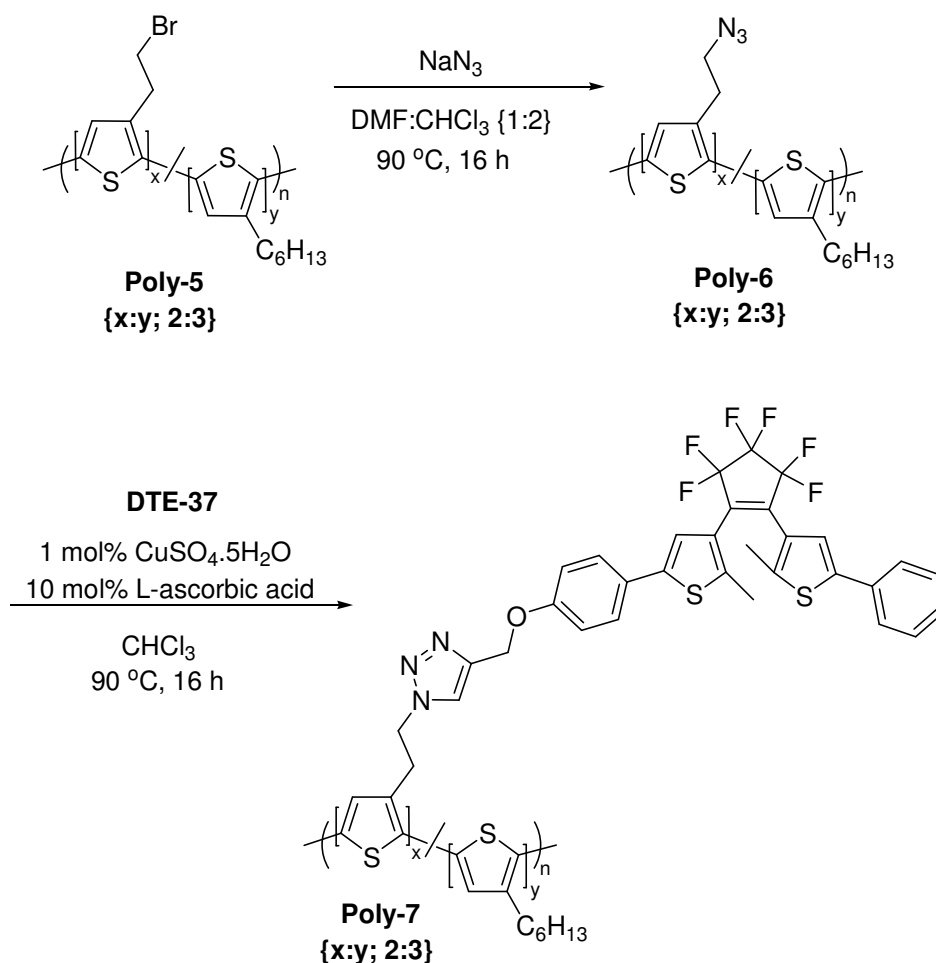
Compound **70** is not regioregular; it contains both a HT and a TT coupling due to the asymmetry of the central thiophene unit. There are, however, no HH couplings that could cause steric disruptions between the alkyl chains and lead to undesirable twisting of the backbone.

Click reactions between **70** and **DTE-37** were initially performed using the same conditions described for the aforementioned model Click species, **68**. Analysis by TLC of the crude mixture, after overnight reaction at reflux, showed large amounts of starting material and almost negligible amounts of product. Several trials were performed until favourable reaction conditions were determined. As shown in

Scheme **3-3**, it was found that **70** and **DTE-37** required a much higher amount of the $\text{CuSO}_4 \cdot 5\text{H}_2\text{O}$ catalyst and L-ascorbic acid reducing agent, for unknown reasons. Using these conditions, pure **71** was obtained as a light green solid isolated by column chromatography.

In addition to the oligomer analog **71**, two polymeric variants of **Poly-4** were prepared. The first variation, **Poly-7**, is most closely related in backbone structure to that of **Poly-4** and varies only slightly in ratio between the two monomers but is significantly shorter in average chain length. The bromide precursor to **Poly-7**, **Poly-5**, was prepared under similar conditions to **Poly-1**, in order to obtain a comparable regiorandom backbone. To obtain a polymer with a shorter average chain length, **Poly-5** was isolated from the hexanes fraction of the Soxhlet extraction during purification of the reaction mixture, and was reacted with NaN_3 to yield **Poly-6**. Following the same synthetic route established for **Poly-4**, **Poly-6** was converted to DTE containing **Poly-7** (Scheme 3-4).

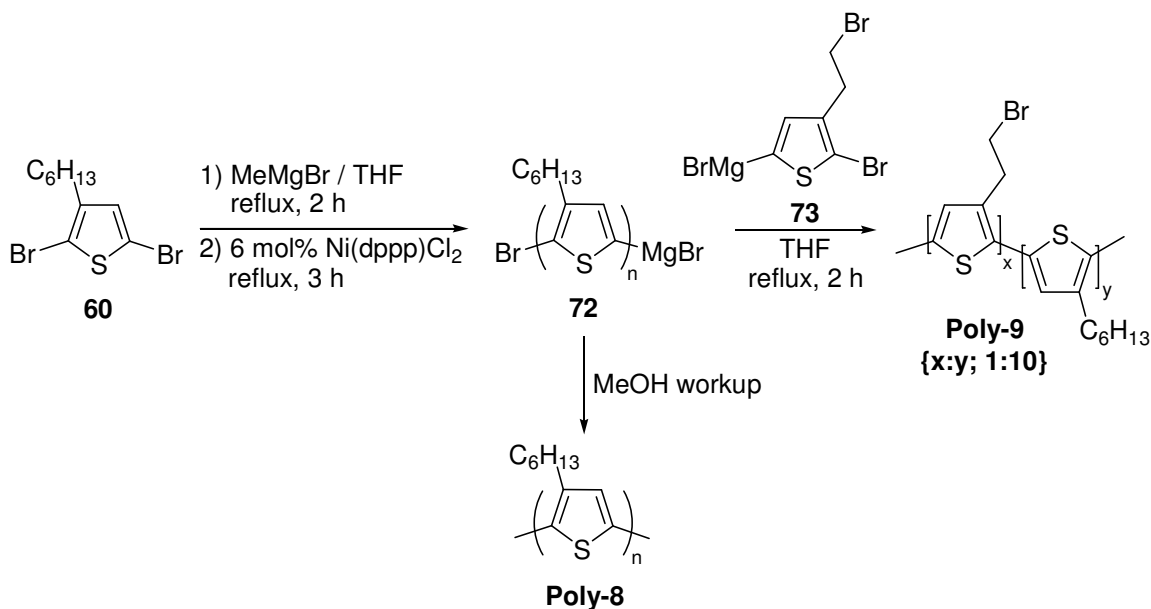
Scheme 3-4



Secondly, the HT rr-block copolymer, **Poly-9** was synthesized (Scheme 3-5). Studies have shown that GRIM polymerization proceeds in a quasi-living fashion via a chain growth mechanism.⁴⁰⁻⁴³ This allows for block copolymers to be prepared by the sequential addition of activated monomers. It has been shown that $Ni(dppp)Cl_2$ behaves as an initiator for polymerization rather than as a catalyst. Thus the concentration of added $Ni(dppp)Cl_2$ can be directly related to the number of initiated chains, and therefore can be used to predict the approximate molecular weight of the polymer.

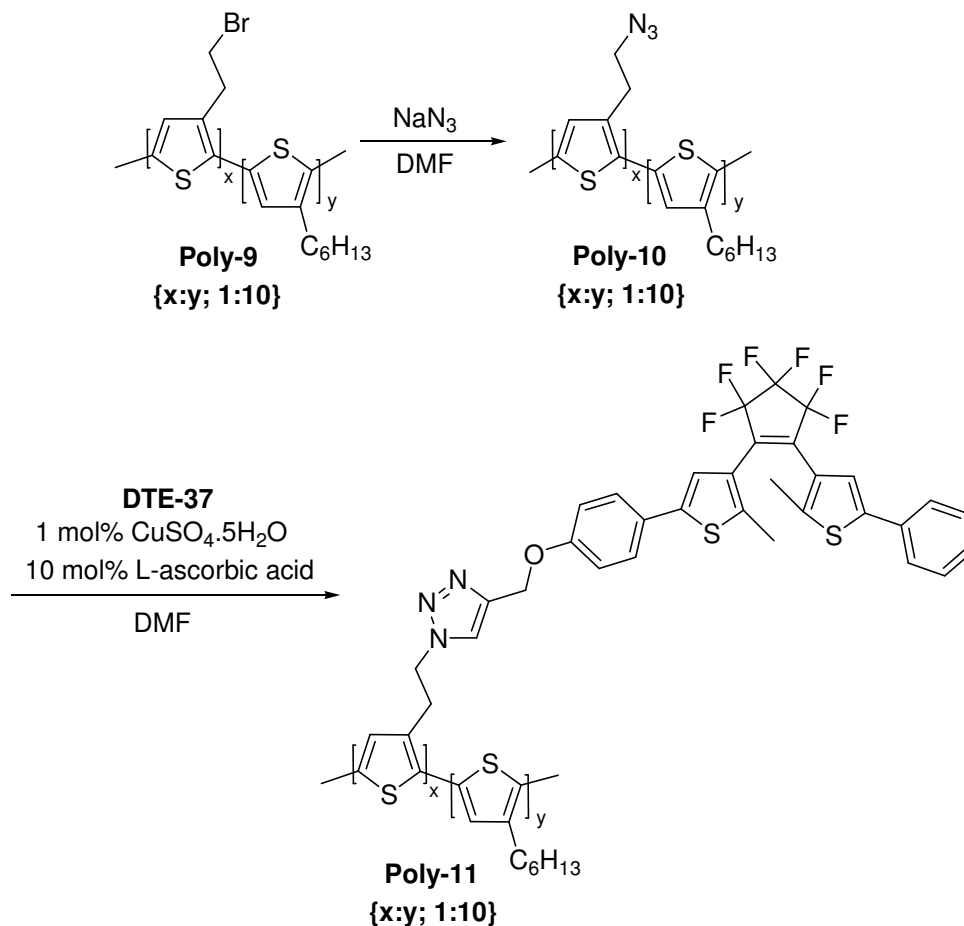
Poly-9 was synthesized first with the generation of a pure P3HT block (**Poly-8**) using GRIM polymerization conditions (Scheme 3-5). Ni(dppp)Cl₂ (6 mol%) was added in order to generate a polymer that would be shorter, on average, in length than **Poly-4**. The second block was formed with the addition of the activated monomer, 2-bromo-5-bromomagnesio-3-(2'-bromoethyl)thiophene (**73**) to allow further elaboration of the polymer to the DTE analog. Prior to the addition of **73**, an aliquot of **Poly-8** was removed and precipitated twice from methanol. Obtaining **Poly-8** allowed for characterization of the initial block structure and was used to help confirm that the backbone was indeed composed of two different blocks.

Scheme 3-5



Poly-9 was first converted to an azide functionalized polymer (**Poly-10**) and then to the DTE functionalized species (**Poly-11**) following similar procedures used for each of the previously modified polymers (Scheme 3-6).

Scheme 3-6



3.3.2 NMR spectroscopy

The ¹H NMR spectrum (Figure 3-2) of compound **68** contained several signals assigned to the DTE moiety at δ 1.69, 1.70, and 4.98. These correspond to the two methyl groups (ϕ) located on the thiophene rings of the DTE, and the methylene spacer (χ) between the triazole ring and the ether tether of the DTE respectively. Two triplets, located at δ 2.57 and 3.75 are due to the α and β methylene protons of the ethylene

moiety adjacent to the thiophene ring. The aromatic region shows signals consistent with both the DTE group and thiophene ring.

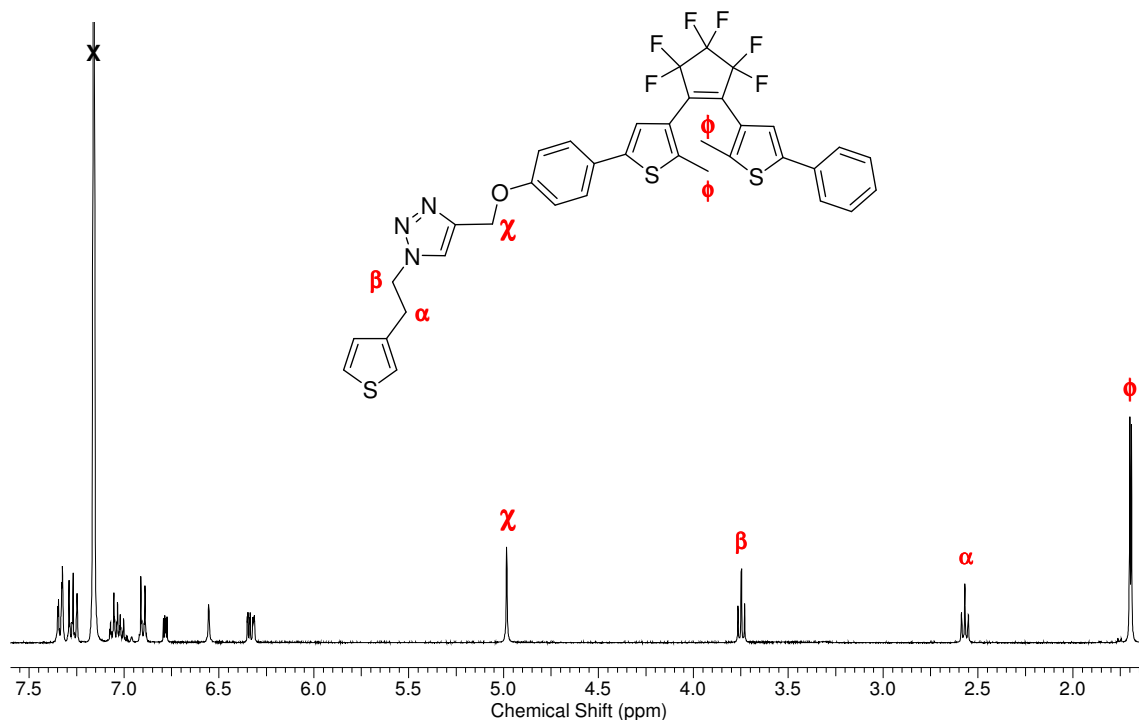


Figure 3-2. ^1H NMR spectrum **68** dissolved in C_6D_6 (400 MHz). X = residual C_6H_6 in the deuterated solvent.

^1H NMR spectroscopy was also used to monitor the extent of the ring-closing reaction as a function of irradiation time (Figure 3-3). The two resonances attributed to the methyl groups (ϕ) on the DTE core are observed at δ 1.70 and 1.69 in **68o**. Upon irradiation of a C_6D_6 solution of **68** with 302 nm light, the singlets at δ 1.70 and 1.69 disappear and new singlets appear at δ 2.14 and 2.13 corresponding to ring-closed isomer (**68c**). When the ratio of **68o** and **68c** no longer changes the reaction is deemed to have reached the photostationary state (PSS). Here the PSS is comprised of 95% the ring-closed isomer. The PSS is defined as the point where equilibrium is reached between the competing ring-opening and ring-closing reactions. During the photo-induced ring-

closing reaction there is also a notable shift in the DTE methylene signal (χ) from δ 4.98 to 4.91. Irradiation of the ring-closed isomer with light greater than 530 nm resulted in the complete regeneration of the ring-open form without any indication of side products in the NMR spectrum.

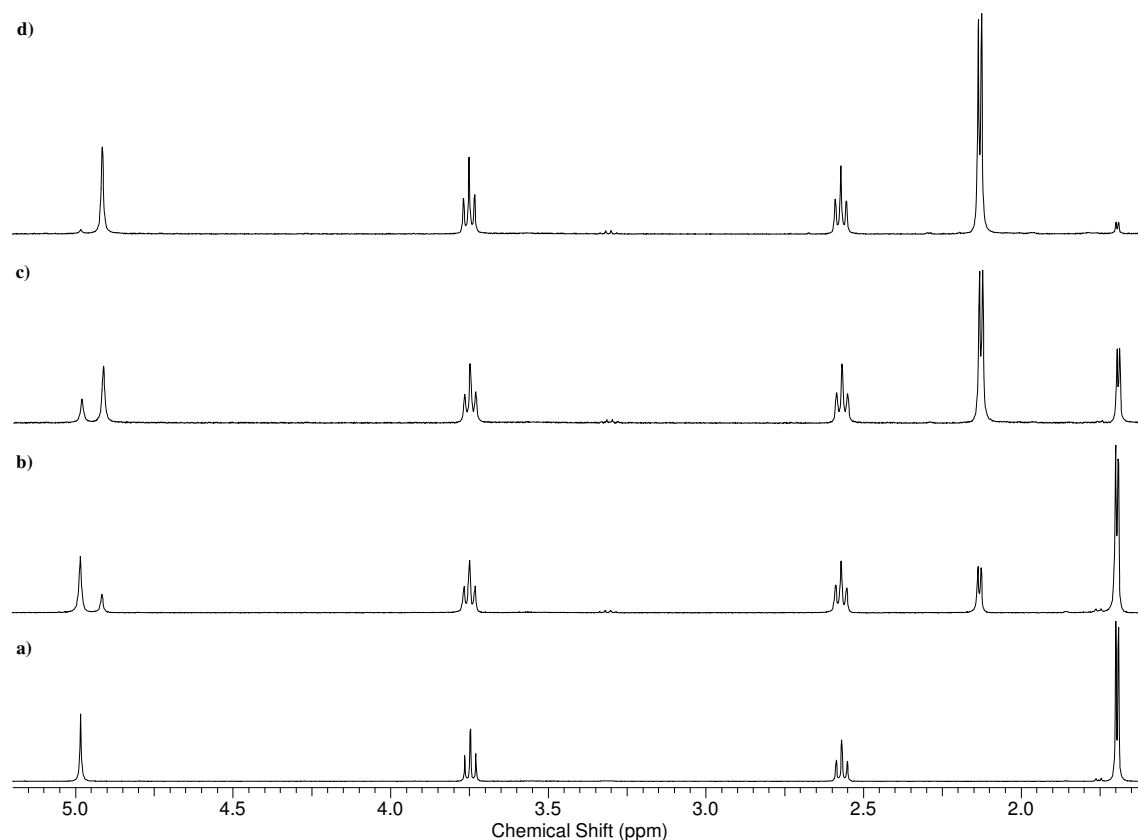


Figure 3-3. ^1H NMR spectra of a C_6D_6 solution of **68o** as a function of irradiation time (a) 0 min, (b) 10 min, (c) 90 min, (d) 145 min (400 MHz). Irradiation with UV-lamp at 302 nm.

In the ^1H NMR spectrum of **Poly-4**, the absence of the terminal acetylene resonance at δ 2.54 confirmed that none of the DTE starting material was present in the product. Further evidence that the Click reaction proceeded are peaks in the ^1H NMR spectrum that are consistent with those observed for the model compound **68**. Two

diagnostic signals are located at δ 5.19 and 1.93 corresponding to the methylene spacer (χ) and the two methyl groups (ϕ) of the pendant DTE group (Figure 3-4). The characteristic broadening of these signals also indicates that the DTE is covalently bound to the polymer. The α and β methylene signals located at δ 4.67 and 3.43 have both shifted from lower frequency in agreement with the shift observed for the corresponding protons in the ^1H NMR spectrum of **68**. Integration of the aromatic region from δ 7.51 to 6.93 accounts for all of the expected thienyl and phenyl protons of the thiophene backbone and DTE pendant group. Several weak signals are found in the region from δ 2.0 to 5.0 which are attributed to HH/TT mis-couplings in the polymer backbone. The resonance located at δ 3.09 is attributed to residual $-\text{CH}_2\text{CH}_2\text{Br}$ groups from incomplete conversion of **Poly-1** to **Poly-2**.³²

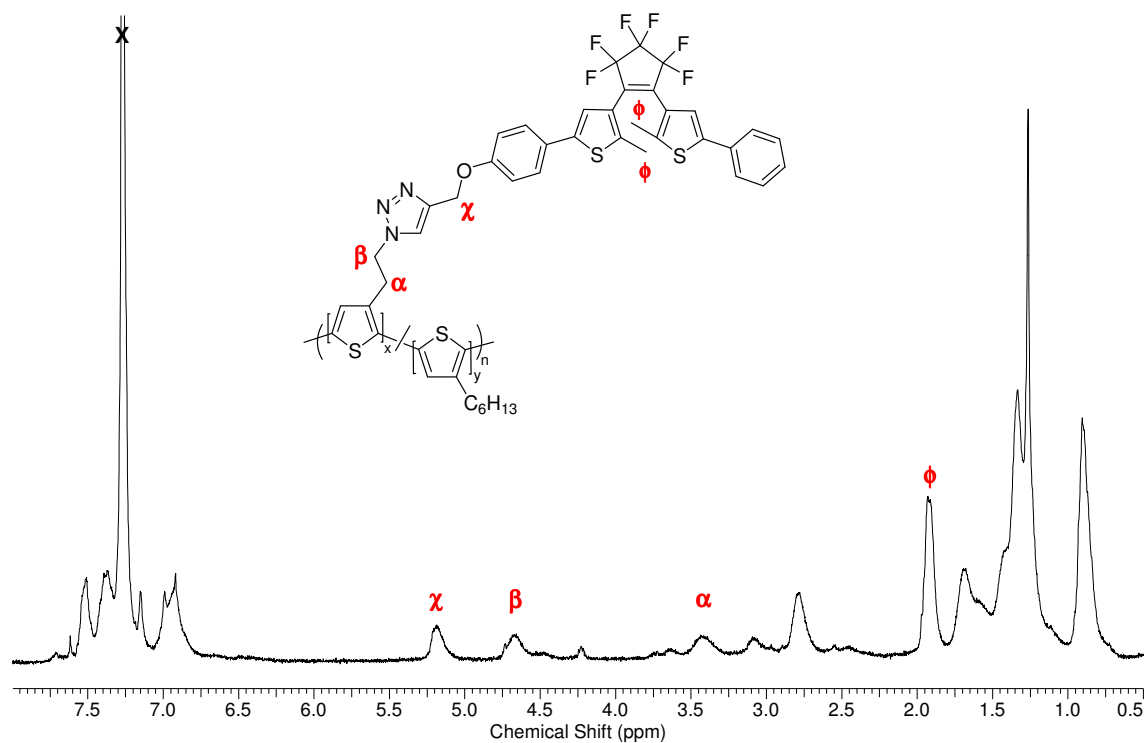


Figure 3-4. ^1H NMR spectrum of **Poly-4** dissolved in C_6D_6 (300 MHz). X = residual CHCl_3 present in the deuterated solvent.

The ^1H NMR spectrum of **70** exhibits resonances between δ 7.02 to 6.82, with five distinctive signals; the two terminal thiophene rings each have two aryl protons, resulting in four doublets, while the internal thiophene ring has only one aryl proton resulting in a singlet. In the alkyl region of the ^1H NMR spectrum, two triplets due to the α and β methylene protons of the internal ethylene group are observed at δ 3.54 and 3.06 respectively. Four distinct resonance signals are observed for the two hexyl chains of the terminal thiophenes.

Conversion of **70** to the DTE functionalized terthiophene **71** was verified via the ^1H NMR spectrum of **71**. The peaks at δ 5.21, 1.98, and 1.96 are the signals for the

methylene spacer (χ) and two methyl (ϕ) groups of the DTE group, respectively. As with **68**, the β methylene protons shift significantly downfield from δ 3.54 to 4.62 upon formation of the triazole ring.

^1H NMR confirmed the structure of **Poly-5**, **-6** and **-7** with spectra similar to that of the corresponding analogs **Poly-1**, **-2** and **-4**. However, there were several significant structural differences indicated from the NMR spectra, between the backbone of **Poly-5** to that of **Poly-1**. Integration of the signals at δ 2.80 and 3.63 in the ^1H NMR spectrum of **Poly-5**, reveals a ratio of 3:2 for hexyl:bromoethyl side chains distributed along the polymer backbone. Furthermore, it was determined that the regioregularity of **Poly-5** was lower than for **Poly-1** with $\sim 70\%$ HT couplings for **Poly-5** compared to 85% for **Poly-1**. This is contrary to the expected trend in regioregularity for GRIM polymerization. When the growing polymer chain experiences a HH or TT coupling this may reduce the activity of the growing chain end such that the steric bulk from the alkyl chain may inhibit further monomer addition. Thus, chains of higher regularity will preferentially react with the activated monomer to result in longer chains. The regioirregular chains are sterically compromised, resulting in shorter chains that end up being removed in the hexanes cycle of the Soxhlet extraction, from which **Poly-5** was obtained.

To verify the block structure of the resulting polymer, ^1H NMR spectroscopic investigations of **Poly-8** (essentially of the form rr-P3HT), were compared to the final block copolymer **Poly-9**. As seen in Figure 3-5, **Poly-8** displays the expected resonance signals for a P3HT homopolymer.^{16,44} The broad singlets at δ 2.81, 1.71, 1.36 and 0.92 are due to the hexyl side chains, while the singlet at δ 6.99 is the resonance signal from the thienyl protons. Integration of the signals at δ 2.81 and 2.52 indicate that the polymer

backbone contains 82% HT couplings. In the ^1H NMR spectrum of **Poly-9**, new signals are observed in the alkyl region from δ 3.0 to 3.6. The concentration of the activated monomer **73** was only 10 mol% that of 3-hexylthiophene, thus these new peaks are weak. Upon closer inspection of the spectrum, two signals were resolved at $\sim \delta$ 3.6 and 3.5, at similar chemical shifts to the signals of the α and β methylene protons on the ethyl chain of **Poly-1**.

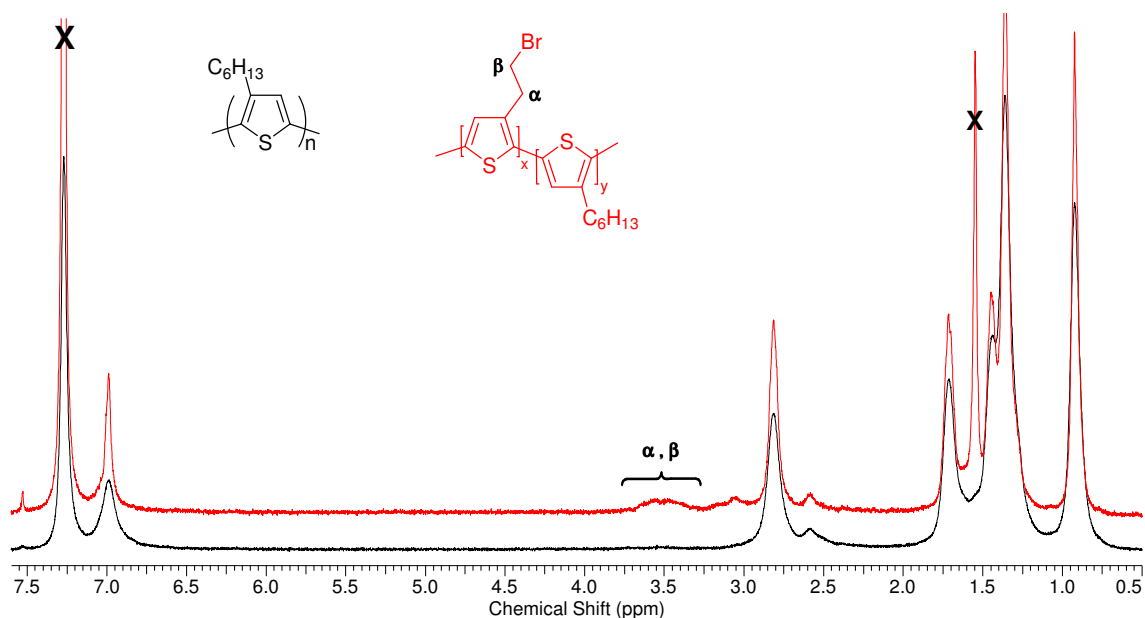


Figure 3-5. ^1H NMR spectra for **Poly-8** (black) and **Poly-9** (red) dissolved in CDCl_3 (400 MHz). X = residual CHCl_3 and water in the deuterated solvent.

The ^1H NMR spectrum of **Poly-10** also shows extremely weak signals in the methylene region from δ 3.0 to 3.6. This region can be magnified to show two signals that appear at the same relative chemical shift as those observed for the methylene protons of the ethyl chain in **Poly-2** when the bromide is converted to an azide group.

Upon reaction of **Poly-10** with **DTE-37**, the new signals in the ^1H NMR spectrum were very weak (Figure 3-6). At high magnification very weak signals at δ 5.14, 4.54 and

3.49 as well as tiny shoulder resonance signals at δ 7.51 and 1.91 were observed. In comparison to **Poly-4**, these match signals for the methylene protons at δ 5.19, 4.67, and 3.43, and phenyl and DTE-based methyl protons at δ 7.51 and 1.93, respectively.

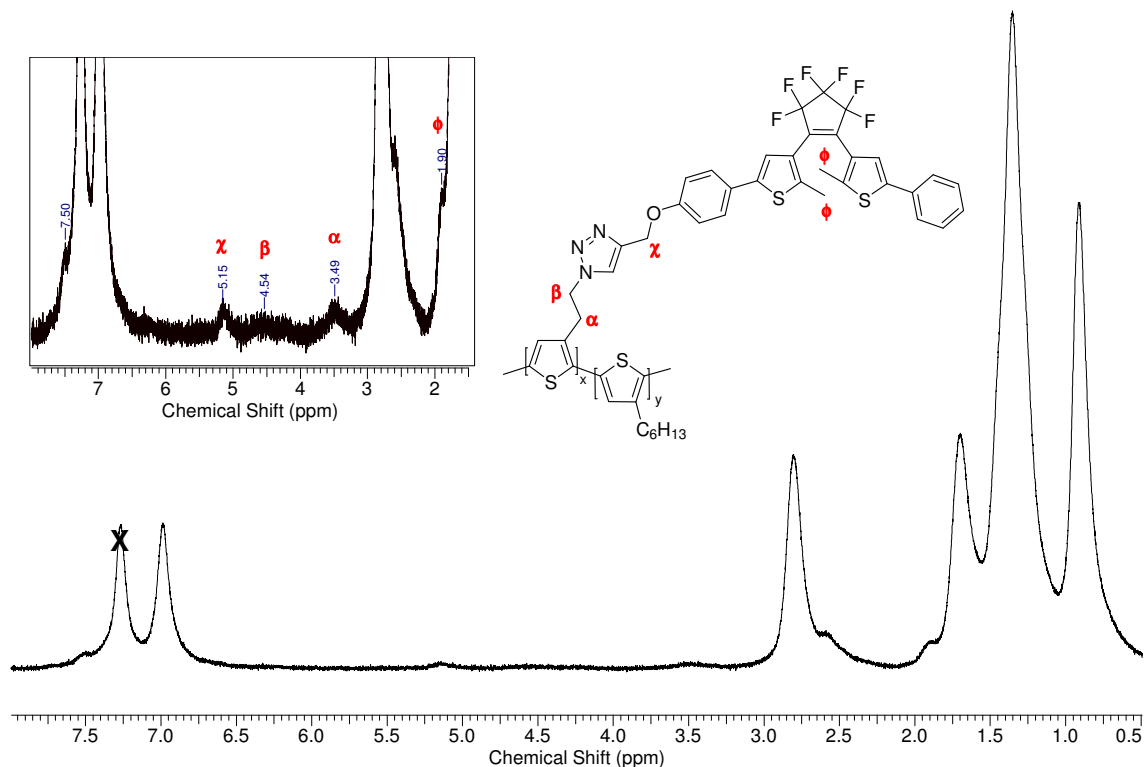


Figure 3-6. ^1H NMR spectrum of **Poly-11** dissolved in CDCl_3 (300 MHz). Inset shows the magnified baseline. X = residual CHCl_3 in the deuterated solvent.

A ^{19}F NMR spectrum of **Poly-11** was also obtained to help confirm the presence of pendant fluorinated DTE. Two signals corresponding to **DTE-37** were observed at δ -110.3 and -132.2.

3.3.3 Size Exclusion Chromatography

SEC analyses were performed on each of the polymer species and the data is presented in Table 3-1. The first polymer prepared, **Poly-4**, was determined to have an average molecular weight of 16000 g mol⁻¹ (vs. polystyrene in THF). From this value, the average number of thiophene rings in a chain could be calculated using the molecular weight of the average repeat unit. In the case of **Poly-4**, the average repeat unit consisted of three thiophene rings (1 DTE:2 hexyl; determined from ¹H NMR) and the average polymer chain was calculated to contain 45 thiophene rings (15 repeat units).

Table 3-1. SEC comparative data for polymer series.

Compound	\overline{M}_w (g mol ⁻¹)	\overline{M}_n (g mol ⁻¹)	PDI	Calculated # of Thiophene Units (monomers ^a)
Poly-4	16000	8800	1.9	45(15)
Poly-5	4400	2100	2.8	25(5)
Poly-6	4700	2600	2.1	30(6)
Poly-7	6300	4300	1.6	15(3)
Poly-8	7300	5600	1.4	43
Poly-9	15000	6900	2.0	88(8)
Poly-10	5400	4700	1.2	33(3)
Poly-11	6000	4900	1.3	33(3)

^a Monomer: refers to the repeat unit determined from ¹H NMR spectroscopy.

It was determined that the average molecular weights of **Poly-5**, **-6**, and **-7** were approximately 3 times lower than that of **Poly-4**, with values in the range of ~ 5000 g mol⁻¹ versus 16000 g mol⁻¹. This was to be expected since **Poly-5** had been isolated from the hexanes fraction of the Soxhlet extraction. The relatively high polydispersity of this

polymer series (**Poly-5**, **-6**, and **-7**) was unexpected such that fractionation should lead to a sample with more uniform molecular weights.

Poly-8 was found to have an average molecular weight of 7300 g mol^{-1} (vs. polystyrene). Upon addition of the second monomer an increase in molecular weight was expected. The value obtained for **Poly-9** was found to be approximately double that of the original hexyl block with an average molecular weight of 15000 g mol^{-1} . This value does not agree with the results obtained from the ^1H NMR spectrum. As well, the extremely low concentration of the second monomer made the dramatic increase in molecular weight inexplicable and deemed the results inconclusive. However, the SEC analyses of **Poly-10** and **Poly-11** yielded results more consistent with those of **Poly-8**, the synthetic procedures, and results from the ^1H NMR spectra.

It has been reported that extensive aggregation can occur in rr-P3AT that can lead to lead to significant errors in SEC.⁴⁵ It has also been determined that molecular weights of PT can be overestimated by a factor of 10 when using polystyrene standards.⁴⁶ The structure of the polymer backbone affects the behaviour of the polymers in solution, resulting in different amounts of coiling, spinning, and interaction of the polymer with the separation gel along the length of the column. Values of \overline{M}_w have been reported at $130,000 \text{ g mol}^{-1}$ after five repetitive analyses, until finally a value of $25,000 \text{ g mol}^{-1}$ was obtained.⁴⁷ Therefore, the inconsistencies discussed above are rationalized as SEC experimental errors.

3.4 Conclusions

Several analogs of a DTE functionalized rr-PT were prepared. Variation of the GRIM polymerization methodology was successfully carried out to obtain both random and block copolymers while maintaining relatively high regioregularity; a minimum value of 70% HT couplings was obtained. A regioregular terthiophene was also prepared, via a modified Suzuki coupling reaction, to obtain an analog with a discrete conjugation path length. The Click reaction provided a clean and efficient method for modification of each of the PT analogs resulting in DTE modified species, each displaying characteristic ^1H NMR spectra. The average polymer length and number of repeat units were determined from SEC data and the relative ratios of monomer species determined from ^1H NMR spectroscopy.

3.5 **References**

1. Friend, R. H.; Greenham, N. C., Electroluminescence in Conjugated Polymers. In *Handbook of Conducting Polymers*, Skotheim, T. A., Elsenbaumer, R. L., Reynolds, J. R., Eds. Marcel Dekker: New York, 1986; pp 823-845.
2. Burroughes, J. H. et al., *Nature* **1990**, 347, (6293), 539-541.
3. Perepichka, I. F.; Perepichka, D. F.; Meng, H., Thiophene-based Materials for Electroluminescent Applications. In *Handbook of Thiophene-Based Materials: Applications in Organic Electronics and Photonics*, Perepichka, I. F., Perepichka, D. F., Eds. John Wiley & Sons: Chichester, 2009; Vol. 1, pp 695-756.
4. Ho, H.-A.; Leclerc, M., Chemical and Biological Sensors Based on Polythiophene. In *Handbook of Thiophene-Based Materials: Applications in Organic Electronics and Photonics*, Perepichka, I. F., Perepichka, D. F., Eds. John Wiley & Sons: Chichester, 2009; Vol. 1, pp 813-832.
5. Thomas, S. W.; Joly, G. D.; Swager, T. M., *Chem. Rev.* **2007**, 107, (4), 1339-1386.
6. Suga, T.; Konishi, H.; Nishide, H., *Chem. Commun.* **2007**, (17), 1730-1732.
7. Suga, T. et al., *Adv. Mater.* **2009**, 21, (16), 1627-1630.
8. Dennler, G.; Scharber, M. C.; Brabec, C. J., *Adv. Mater.* **2009**, 21, (13), 1323-1338.
9. Xiao, S. Q.; Stuart, A. C.; Liu, S. B.; You, W., *ACS App. Mater. & Inter.* **2009**, 1, (7), 1613-1621.
10. Kim, B. J.; Miyamoto, Y.; Ma, B. W.; Fréchet, J. M. J., *Adv. Funct. Mater.* **2009**, 19, (14), 2273-2281.

11. Facchetti, A., Electroactive Oligothiophenes and Polythiophenes for Organic Field Effect Transistors. In *Handbook of Thiophene-Based Materials: Applications in Organic Electronics and Photonics*, Perepichka, I. F., Perepichka, D. F., Eds. John Wiley & Sons: Chichester, 2009; Vol. 1, pp 595-646.
12. McCulloch, I.; Heeney, M., Thienothiophene Copolymers in Field Effect Transistors. In *Handbook of Thiophene-Based Materials: Applications in Organic Electronics and Photonics*, Perepichka, I. F., Perepichka, D. F., Eds. John Wiley & Sons: Chichester, 2009; Vol. 1, pp 647-672.
13. Loewe, R. S.; Khersonsky, S. M.; McCullough, R. D., *Adv. Mater.* **1999**, 11, (3), 250-253.
14. Loewe, R. S. et al., *Macromolecules* **2001**, 34, (13), 4324-4333.
15. McCullough, R. D. et al., *Synth. Met.* **1995**, 69, (1-3), 279-282.
16. McCullough, R. D.; Lowe, R. D., *J. Chem. Soc., Chem. Commun.* **1992**, (1), 70-72.
17. Chen, T. A.; Rieke, R. D., *Synth. Met.* **1993**, 60, (2), 175-177.
18. Roncali, J., *Chem. Rev.* **1997**, 97, (1), 173-205.
19. Somanathan, N.; Radhakrishnan, S., *Int. J. Mod. Phys. B* **2005**, 19, (32), 4645-4676.
20. Chan, H. S. O.; Ng, S. C., *Prog. Polym. Sci.* **1998**, 23, (7), 1167-1231.
21. Irie, M., Photoswitchable Molecular Systems Based On Diarylethenes. In *Molecular Switches*, Feringa, B. L., Ed. Wiley-VCH GmbH: Weinheim, 2001; pp 37-61.
22. Bouas-Laurent, H.; Dürr, H., *Pure Appl. Chem.* **2001**, 73, (4), 639-665.

23. Irie, M., *Chem. Rev.* **2000**, 100, (5), 1685-1716.
24. Myles, A. J.; Branda, N. R., *Adv. Funct. Mater.* **2002**, 12, (3), 167-173.
25. Myles, A. J.; Wigglesworth, T. J.; Branda, N. R., *Adv. Mater.* **2003**, 15, (9), 745-748.
26. Wigglesworth, T. J.; Branda, N. R., *Chem. Mater.* **2005**, 17, 5473-5480.
27. Bertarelli, C. et al., *Adv. Funct. Mater.* **2004**, 14, (4), 357-363.
28. Biteau, J. et al., *Chem. Mater.* **1998**, 10, (7), 1945-1950.
29. Kronemeijer, A. J. et al., *Adv. Mater.* **2008**, 20, (8), 1467-1473.
30. Sun, L.; Wang, S.; Tian, H., *Chem. Lett.* **2007**, 36, (2), 250-251.
31. Tian, H.; Wang, S., *Chem. Commun.* **2007**, (8), 781-792.
32. Finden, J.; Kunz, T. K.; Branda, N. R.; Wolf, M. O., *Adv. Mater.* **2008**, 20, (10), 1998-2002.
33. Rogers, S. A.; Melander, C., *Angew. Chem. Int. Ed.* **2008**, 47, (28), 5229-5231.
34. Pei, J. et al., *J. Org. Chem.* **2002**, 67, (14), 4924-4936.
35. Kirschbaum, T.; Briehn, C. A.; Bäuerle, P., *J. Chem. Soc., Perkin Trans. 1* **2000**, 8, 1211-1216.
36. Donat-Bouillud, A. et al., *Chem. Mater.* **1997**, 9, (12), 2815-2821.
37. Sato, M. A.; Hiroi, M., *Polymer* **1996**, 37, (9), 1685-1689.
38. Tenhoeve, W.; Wynberg, H.; Havinga, E. E.; Meijer, E. W., *J. Am. Chem. Soc.* **1991**, 113, (15), 5887-5889.
39. Ten Hoeve, W.; Wynberg, H.; Havinga, E. E.; Meijer, E. W., *J. Am. Chem. Soc.* **1991**, 113, (15), 5887-5889.
40. Sheina, E. E. et al., *Macromolecules* **2004**, 37, (10), 3526-3528.

41. Miyakoshi, R.; Yokoyama, A.; Yokozawa, T., *J. Am. Chem. Soc.* **2005**, 127, (49), 17542-17547.
42. Iovu, M. C.; Sheina, E. E.; Gil, R. R.; McCullough, R. D., *Macromolecules* **2005**, 38, (21), 8649-8656.
43. Hiorns, R. C.; Khoukh, A.; Gourdet, B.; Dagrón-Lartigau, C., *Polym. Int.* **2006**, 55, (6), 608-620.
44. Chen, T. A.; Rieke, R. D., *J. Am. Chem. Soc.* **1992**, 114, (25), 10087-10088.
45. Yue, S.; Berry, G. C.; McCullough, R. D., *Macromolecules* **1996**, 29, (3), 933-939.
46. Havinga, E. E.; Vanhórsen, L. W., *Makromol. Chem., Macromol. Symp.* **1989**, 24, 67-76.
47. McCullough, R. D., *Adv. Mater.* **1998**, 10, (2), 93-116.

CHAPTER 4 Reversible Amplified Fluorescence Quenching of Dithienylethene Functionalized Polythiophene*

4.1 Introduction

The ability to convert a chemical event into measurable electrical or optical output signal is one of the main thrusts for the investigation of CPs.¹ For instance, amplified fluorescent polymers (AFPs) exhibit enhanced fluorescence in response to the interactions between the CP and analytes of interest such as ions,²⁻⁷ proteins,^{8,9} and DNA.¹⁰⁻¹² In these systems, the CP acts as a highly efficient transport medium (via electronic excited state quasiparticles, otherwise known as excitons) that facilitates an observed increase in sensitivity or *amplification* in fluorescence. The mobile excitons quickly diffuse throughout the polymer chain via mechanisms that involve both through space dipolar couplings and the strong mixing of electronic states.¹³⁻¹⁶ This phenomenon of delocalization implies that any perturbation of the electronic structure at a single point along the backbone of a CP, can be translated along the entirety of a CP chain thereby amplifying the effect of some stimulus.

This effect was demonstrated by Swager *et al.* using an alternating copolymer which contained poly(*p*-phenylene ethynylene) (PPE) and bis(*p*-phenylene)-34-crown-10 (BPP) repeat units. The BPP behaves as an excellent receptors for paraquat, a well known electron-transfer quenching agent.^{1,17-19} They showed that addition of paraquat to a solution of conjugated PPE-co-BPP gave rise to a 47-66 fold enhancement in fluorescent quenching relative to a molecular model containing a single receptor unit. As illustrated

* A version of this chapter has been published. Finden, J.; Kunz, T. K.; Branda, N. R.; Wolf, M. O., Reversible Amplified Fluorescence Quenching of Dithienylethene Functionalized Polythiophene. *Adv. Mater.* **2008**, 20, (10), 1998-2002.

in Figure 4-1, a solution that contains only single receptor units will only be quenched in a stoichiometric ratio with respect to added quencher. In a solution of polymers containing multiple receptor units along the polymer chain, the fast migration of excitons along the backbone translates into 100% of the fluorescence being quenched upon addition of one stoichiometric equivalent of quencher with respect to each polymer chain.

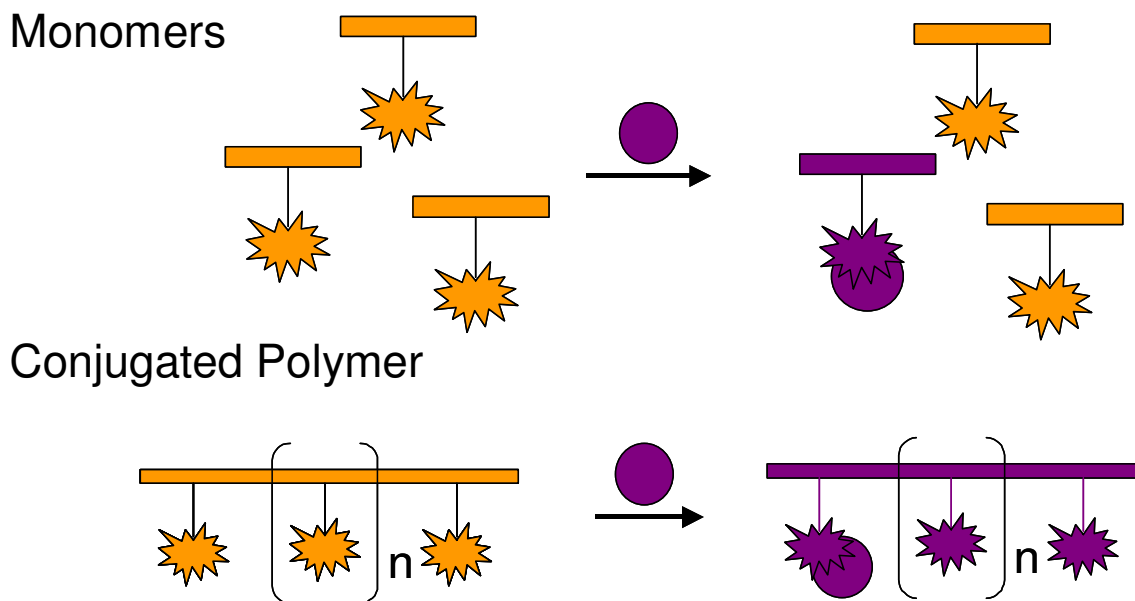


Figure 4-1. Demonstration of amplified fluorescence quenching along a polymer backbone through binding of a quencher (●) to a receptor (★).

In the system studied by Swager *et al.*, fluorescence quenching was found to be dependant on the binding of an active analyte upon which the excited state was immediately quenched. For applications towards sensory systems for the detection of explosives,²⁰⁻²⁴ this high level of sensitivity is appropriate. However, if the binding is highly favourable (i.e. the binding constant is high), then loss of analyte from the binding site is unlikely. This may have drawbacks towards using such a system for repetitive analyses. Hence, it is of interest to develop systems that not only provides a fully

reversible quenching process, but also could be modulated between on/off states very quickly and without any physical manipulation of the system.

Compounds that are responsive to external stimuli such as heat or light, rather than a chemical binding event are appealing for materials applications. The thermal irreversibility, and fatigue resistance of DTEs make them particularly interesting as molecular switches, functioning with true on/off capabilities. The DTE moiety has already shown promising results for applications in OLEDs,²⁵ OPVs,²⁶ and memory media.²⁷

In this chapter, modification of a PT backbone with the DTE moiety was carried out in order to investigate the influence of the photo-induced isomerisation on the optical and electronic properties of the CP backbone. Absorption and emission studies have been used to monitor the ring-opening/closing reaction, and are discussed with respect to amplification along the CP backbone.

4.2 ***Experimental***

4.2.1 **General**

Solution electronic absorption spectra were obtained on a Varian Cary 5000 or Varian Cary 300 Bio UV-vis spectrophotometer in reagent grade C_6H_6 and HPLC grade CH_2Cl_2 . Fluorescence measurements were made on a PTI QM-2000-4 scanning spectrofluorometer in the same solvent used for the corresponding UV-vis measurements. Absolute fluorescence quantum yield measurements were recorded on a PTI QM-2006-4 cw spectrofluorometer equipped with a CGM9-2-2006 integrating sphere and operated with the Felix32 software package. All samples for fluorescence measurements were excited with 470 nm irradiation. In order to improve the emission S/N ratio, an even-pass filter was placed in the light path when detecting only the excitation wavelength range, which is required to measure the number of light quanta absorbed by the sample by subtraction of sample from blank light intensity. The use of the filter ensured that similar light intensities were detected by the instrument for both excitation and emission scans so that an identical instrument configuration was maintained for both. The decrease in light intensity for the excitation scan was subsequently corrected for in the final quantum yield calculation.

4.3 *Results and Discussion*

4.3.1 **Absorption and Emission Studies**

In order for the DTE to behave as a molecular switch, it was necessary for the DTE to electronically interact with the CP in only one of the two isomeric forms. The particular DTE derivative incorporated into **Poly-4** was chosen based on two main criteria. First, the absorption band of the PT backbone had to lie in a spectral region where both DTE isomers (open and closed) were transparent. This allowed the polymer to be independently photoexcited without causing ring-opening or closing. Secondly, emission from the polymer had to overlap with the absorption band of only one of the DTE isomers (either open or closed) to provide only one pathway through which the two species could interact electronically.

Absorbance studies of model compound **68** (Figure 4-2) were compared to those reported previously for **DTE-37**.²⁸ The absorption maxima (λ_{max}) for the open isomer (294 nm) and the closed form (592 nm), are shifted only very slightly from those of **DTE-37**. This demonstrates that formation of the triazole ring does not significantly affect the electronic structure of either isomer of **DTE-37**. The data in Figure 4-2 clearly demonstrates that the absorption and emission spectra of **Poly-2** ($\lambda_{\text{max}} = 440$ and 575 nm respectively), fulfill the criteria given above. Namely, the emission of **Poly-2** overlaps only with the absorbance of the ring-closed isomer of DTE, and the main polymer absorption clearly lies between the open and closed absorption bands of the DTE moiety.

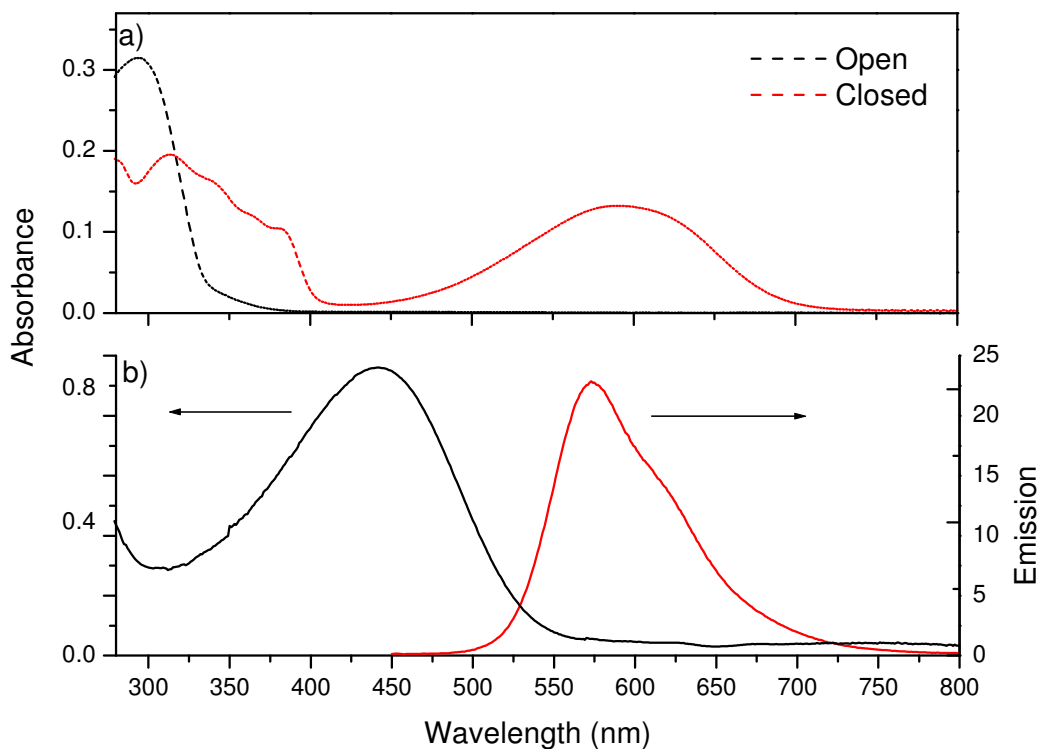


Figure 4-2. (a) Absorption spectra of **68o** (black dashed) and **68c** (red dashed) and (b) absorption (black) and emission (red) spectra of **Poly-2**.

The photo-induced ring-closing reaction of **Poly-4** is easily monitored by UV-vis absorption spectroscopy (Figure 4-3). Irradiation of a benzene solution of **Poly-4o** with 310 nm light results in an immediate decrease in the intensity of the absorption band at 290 nm and the appearance of a new absorption band at 595 nm. These spectral changes correspond to the disappearance of the ring-open isomer and the concurrent appearance of the ring-closed isomer. This ring-closing reaction can also be visually observed as the colour of the solution changes from orange to green. There is no change observed in the PT absorption band at 440 nm, showing it is unaffected by irradiation at this wavelength.

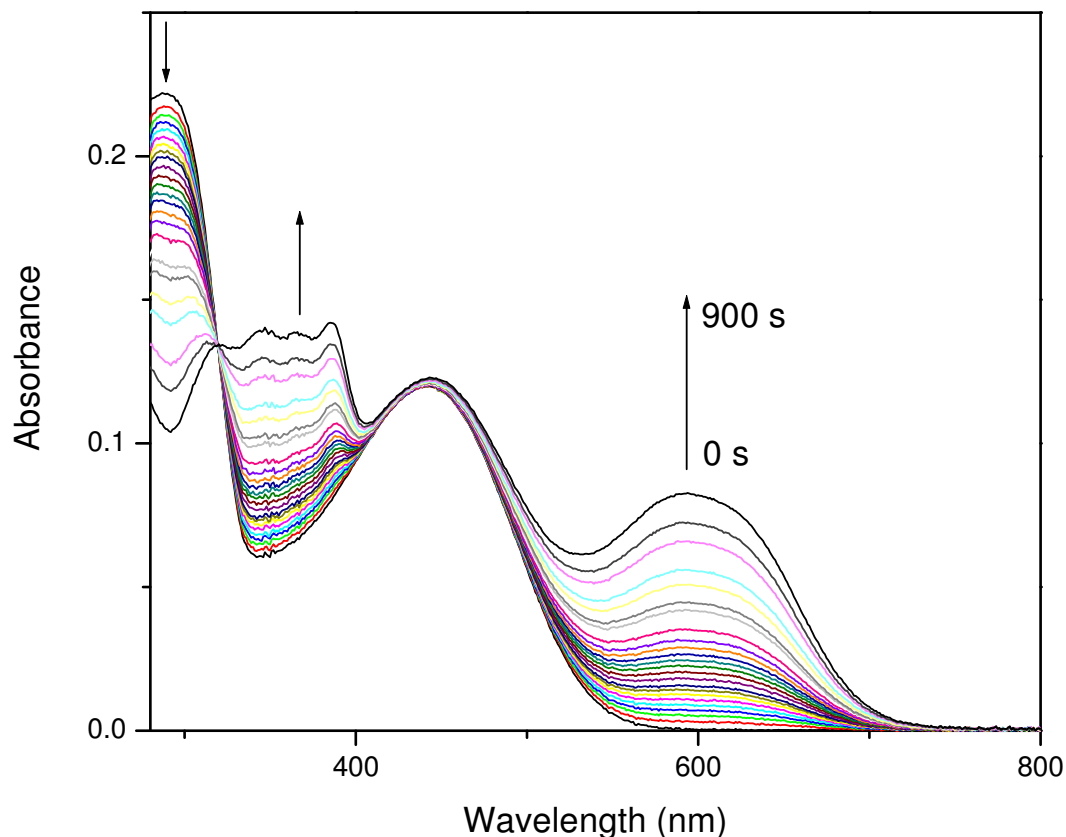


Figure 4-3. UV-vis absorption spectra of a C_6H_6 solution of **Poly-4**, with irradiation at 310 nm.

There is significant spectral overlap between the absorbance of the ring-closed isomer **68c** and the emission of the PT backbone. This implies that intramolecular quenching of the PT excited state via energy transfer should be efficient in **Poly-4c**, resulting in a decrease in emission relative to the ring-open form, **Poly-4o**. The change in emission that accompanies the photo-induced ring-closing reaction of **Poly-4o** is shown in Figure 4-4. The conversion of the ring-open isomer **Poly-4o** to its ring-closed counterpart (**Poly-4c**) results in efficient fluorescence quenching and virtually no emission is observed when the PSS is reached. Additionally, continuous irradiation of **Poly-4** with 440 ± 5 nm light over a period of one hour caused no change in the

absorption spectrum, confirming that the polymer fluorescence and the ring-closing events can be accessed individually.²⁹

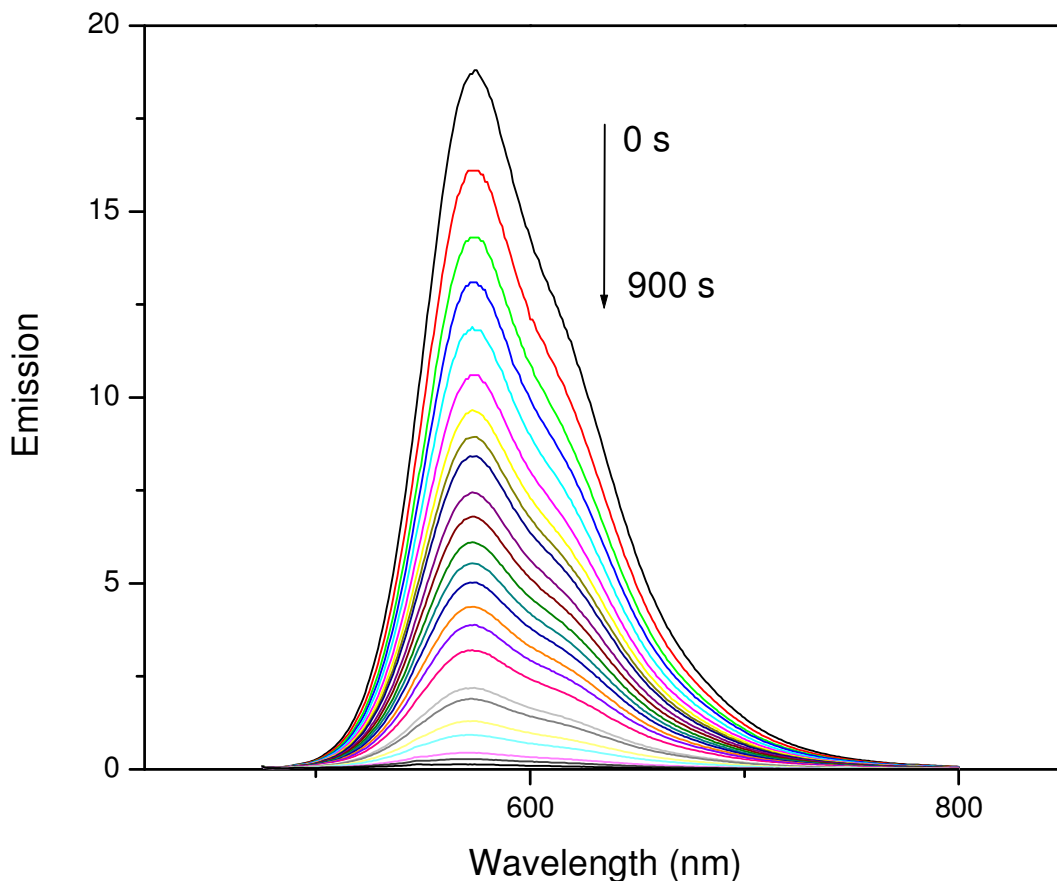


Figure 4-4. Emission spectra of a C₆H₆ solution of **Poly-4**, with irradiation at 310 nm.

An overview of the maximum absorption and emission wavelengths for each analog of **Poly-4** is presented in Table 4-1. In general, the data display similar values for the absorption and emission maxima within a polymer series. This demonstrates that changing functional groups (i.e. from bromide, to azide, and finally to DTE) does not inherently affect the conjugated backbone. It is also observed that in general the maximum absorption shifts to longer wavelengths as the average polymer chain length

increases. This corresponds to the SEC data presented in Chapter 3 and corroborates the extension of conjugation along the polymer backbone.

Table 4-1. UV-vis absorption and emission data from different polymer species

Compound	Absorption λ_{\max} (nm)	Absorption ^a λ_{\max} (nm)	Emission ^b λ_{\max} (nm)	\overline{M}_w (g mol ⁻¹)
68	293	276, 313, 590	-	-
70	350	-	423, 440	-
71	298, 350	350, 596	422, 440	-
Poly-2	440	-	573	12000
Poly-4	290, 444	444, 592	574	16000
Poly-5	411	-	565	4400
Poly-6	411	-	564	4700
Poly-7	289, 421	421, 595	564	6300
Poly-8	427	-	568	7300
Poly-9	427	-	567	15000*
Poly-10	428	-	568	5400
Poly-11	430	430, 600	568	6000

For derivatives containing DTE: ^a Ring closed; ^b Measured in the Ring Open State.

* The discrepancy of this value is discussed in Chapter 3.

Both the absorbance and emission spectra of **70** are significantly blue shifted from that of **Poly-2**. When the absorbance spectra of the two DTE isomers (**68**) were compared to the absorbance and emission data for compound **70** (Figure 4-5), the spectra display poor overlap of the emission of **70** with the absorbance of the ring-closed isomer (**68c**), relative to the overlap in **Poly-2**. As well, the absorbance band of **70** does not lie between the absorbance band of the ring-open and closed forms but has significant overlap with the absorbance of **68c** at higher energy.

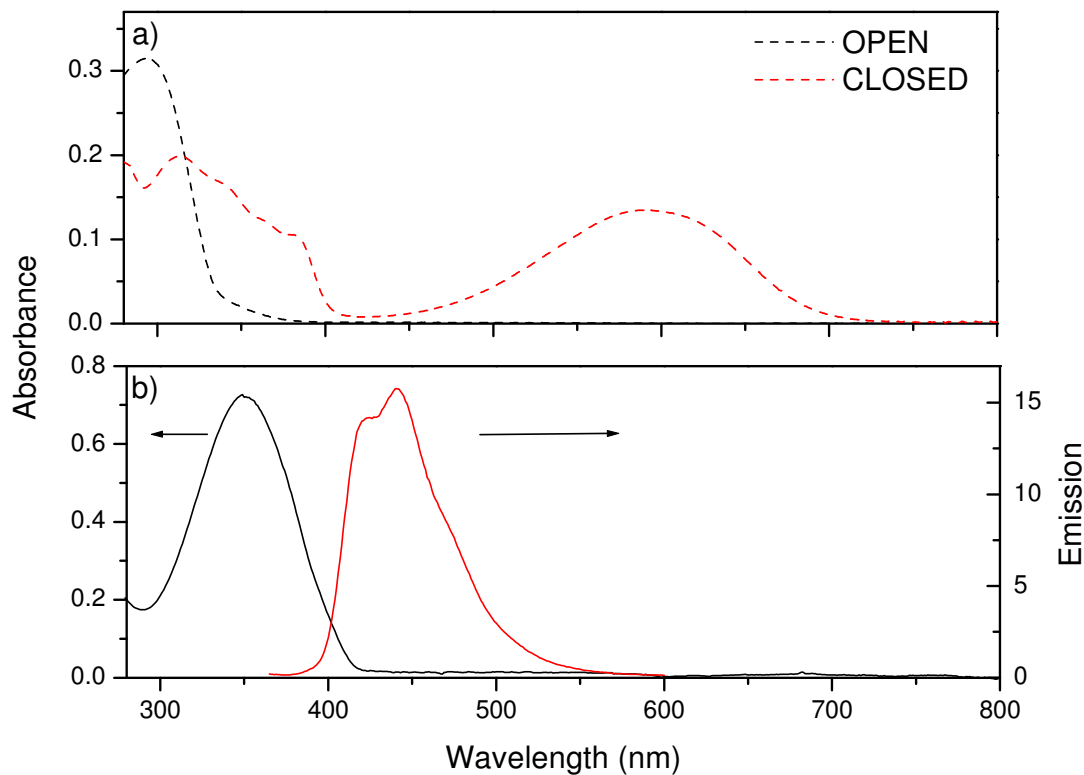


Figure 4-5. (a) Absorbance spectra of **68o** (black dashed) and **68c** (red dashed) and (b) absorbance (black) and emission (red) of **70**.

A decrease in the emission from **71** at 440 nm is still expected as the concentration of **71c** increases with irradiation. In fact, irradiation of a benzene solution of **71o** with 302 nm light results in an immediate decrease in the absorbance band at 298 nm, an increase in the absorbance band at ~ 600 nm, and a decrease of the emission at ~ 440 nm (Figure 4-6).

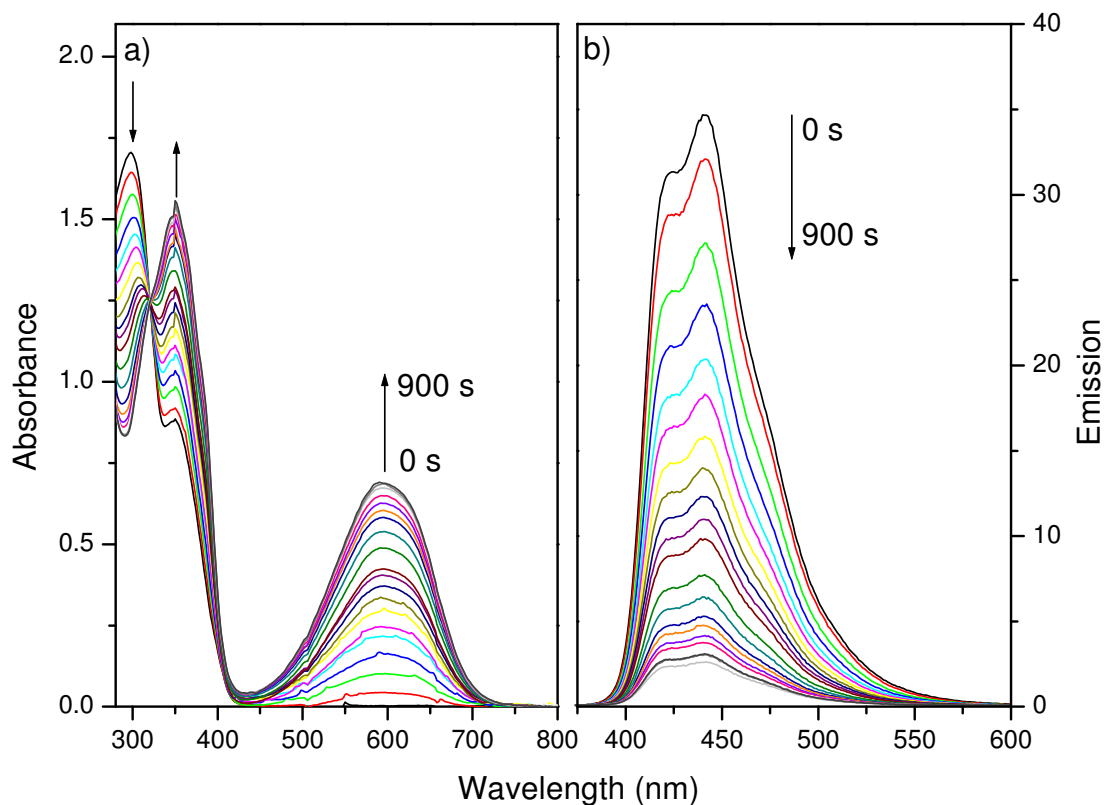


Figure 4-6. (a) UV-vis absorption and (b) emission spectra of the photo-induced ring closing reaction of a C_6H_6 solution of **71** upon irradiation with a 302 nm lamp.

In the absorption spectrum of **71o**, a shoulder is observed at 350 nm corresponding to the absorbance for **70**, and is attributed to the terthiophene group. Upon irradiation of **71o**, this absorption band appears to increase. Irradiation with light greater in wavelength than 530 nm results in the ring-opening reaction, returning **71c** to **71o** with complete regeneration of the original absorbance at 350 nm. An isobestic point appears at 320 nm, indicating that the irradiation results only in conversion of **71o** to **71c**, and not to formation of unwanted side products. The lack of formation of a significant amount of side products is also demonstrated in the cycling experiment depicted in Figure 4-7. The maximum absorptions at 295 and 595 nm, as well as the maximum emission intensity at 440 nm were monitored over 10 ring-opening/closing cycles. There is little change in the

intensity of the absorption maximum between successive irradiations confirming that the photo-induced isomerisation is not leading to a degradation of the sample.

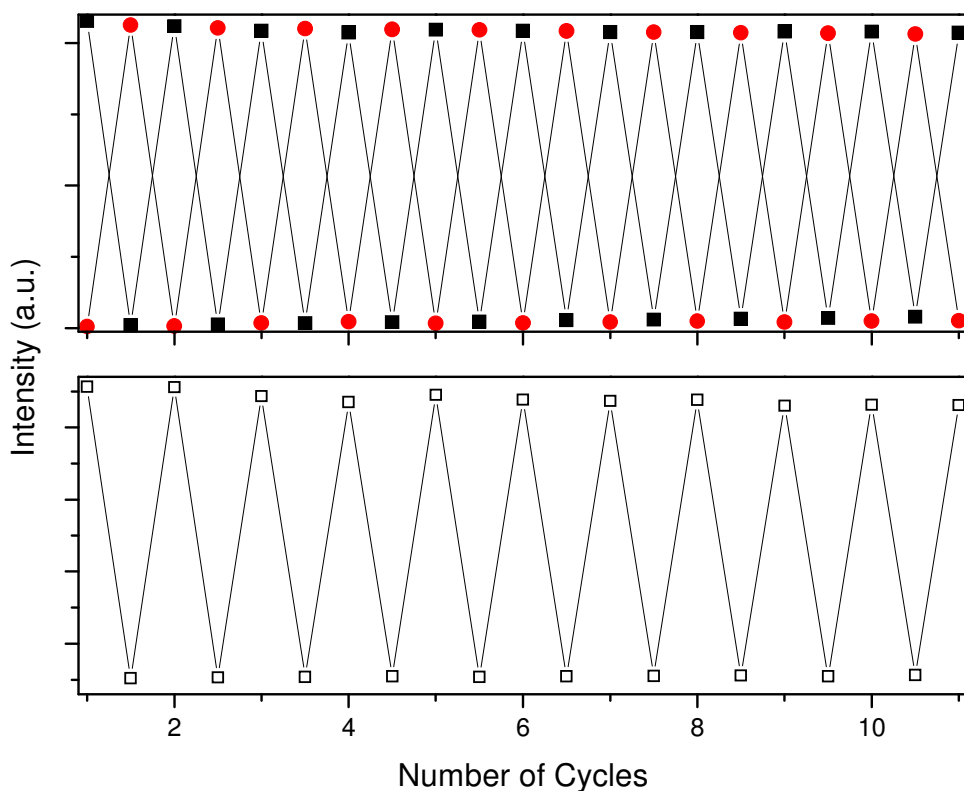


Figure 4-7. Monitoring the change in absorbance and emission intensity of **71** over 11 ring-opening and ring-closing cycles. Absorbance monitored at 298 nm (■), and 595 nm (●). Emission monitored at 440 nm (□).

Absorption and emission studies as a function of irradiation time were also carried out on benzene solutions of **Poly-7** and **Poly-11**. The ring-closing reactions in both of these polymers were induced by irradiation at 302 nm. In the absorption spectrum of **Poly-7o** (Figure 4-8a), there are a few significant differences observed in comparison to **Poly-4o**. The most significant difference is the large hypsochromic shift in the absorption due to the polymer backbone ($\lambda_{\text{max}} = 421$ nm for **Poly-7** compared $\lambda_{\text{max}} = 440$ nm for **Poly-4**). As discussed in Chapter 2, the extent of backbone conjugation is related to the

energy of the π - π^* transition in the absorption spectrum. Here, λ_{max} is closer to that observed for regio-irregular P3HT derivatives (50% HT couplings), reported to have $\lambda_{\text{max}} = 428 \text{ nm}$.³⁰ While these data are indicative of a loss of regioregularity along the polymer backbone in **Poly-7**, a blueshift relative to **Poly-4** is also expected due to reduction in the average polymer chain length. In fact, the ^1H NMR spectrum of **Poly-7** indicates a somewhat lower degree of regioregularity ($\sim 70\%$ HT for **Poly-7** versus 85% HT couplings within **Poly-4**). However, this does not appear to dramatically affect the extent of fluorescence quenching along the polymer backbone such that the polymer fluorescence is still observed to be quenched to 95% of its original intensity.

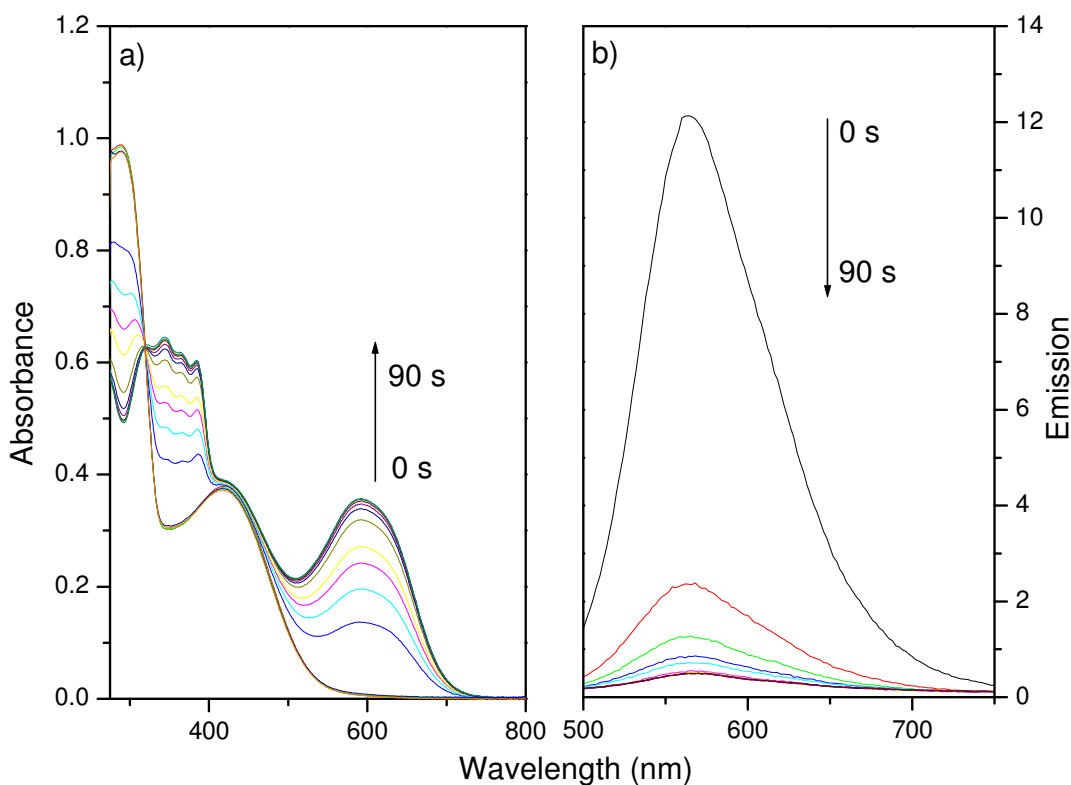


Figure 4-8. (a) UV-vis absorption and (b) emission spectra of the photo-induced ring closing reaction of a C_6H_6 solution of **Poly-7** upon irradiation with a 302 nm lamp.

In addition, the ratio of the absorbance at λ_{\max} of the ring-closed isomer (600 nm) to that of the polymer backbone (at 421 nm) changes from 69% in **Poly-4** to 93% in **Poly-7**. This indicates a higher amount of DTE is present in **Poly-7**, confirmed by the 3:2 ratio of hexyl:DTE groups (from ^1H NMR spectroscopy).

In the emission studies of **Poly-7o** (Figure 4-8b), there is a large decrease of emission intensity directly corresponding to the increase in absorption of the ring-closed **Poly-7c**. As expected, there is a substantial amount of overlap between the absorbance of the ring-closed form **Poly-7c** and the emission of **Poly-7o**.

Absorbance and emission studies of **Poly-11** showed several differences when compared to studies of **Poly-4** and **Poly-7**. Due to the very low amount of DTE in **Poly-11**, it was necessary to study the ring-closing reaction at a much higher optical density with respect to the polymer backbone than for the other polymers. As shown in Figure 4-9a, irradiation of a benzene solution of **Poly-11** at 302 nm shows an increase in absorbance at ~ 600 nm and an isobestic point at 340 nm. The slight shift of the polymer backbone absorbance from 440 nm in **Poly-4** to ~ 430 nm in **Poly-11** appears to be of little consequence to the ring-closing reaction.

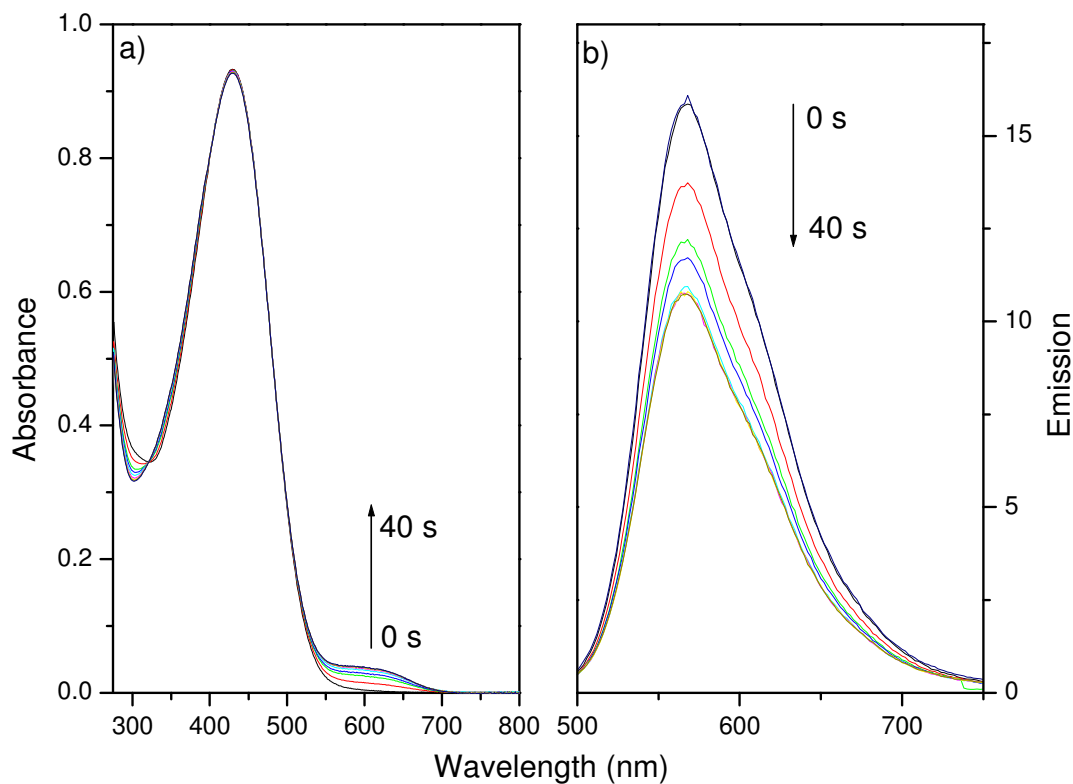


Figure 4-9. (a) UV-vis absorption and (b) emission spectra of the photo-induced ring closing reaction of a C₆H₆ solution of **Poly-11** upon irradiation with a 302 nm lamp.

The emission of **Poly-11** occurs at $\lambda_{\text{max}} = 567$ nm (Figure 4-9b). This falls between the observed λ_{max} values for **Poly-4** and **Poly-7**. The overlap between the emission and the absorbance of the ring-closed form in **Poly-11** is favourable for fluorescence quenching, yet the extent of quenching is highly reduced relative to **Poly-4**. The emission observed at the PSS of the ring-closing reaction is still 68% of the original intensity.

4.3.2 Fluorescence Quenching and Amplification

Fluorescence quenching was observed for **Poly-4** and each of its analogs (**71**, **Poly-7** and **Poly-11**). To measure the extent of fluorescence quenching and to establish the effective amplification of the quenching, each sample was compared to a solution containing the un-tethered precursors to **Poly-4**; **Poly-2** and **DTE-37**. This solution was prepared in concentrations that replicate the optical density of **Poly-4** in solution such that the absorbance spectra for **Poly-2/DTE-37o** and **Poly-2/DTE-37c**, were nearly superimposable with those for **Poly-4o** and **Poly-4c** (Figure 4-10).

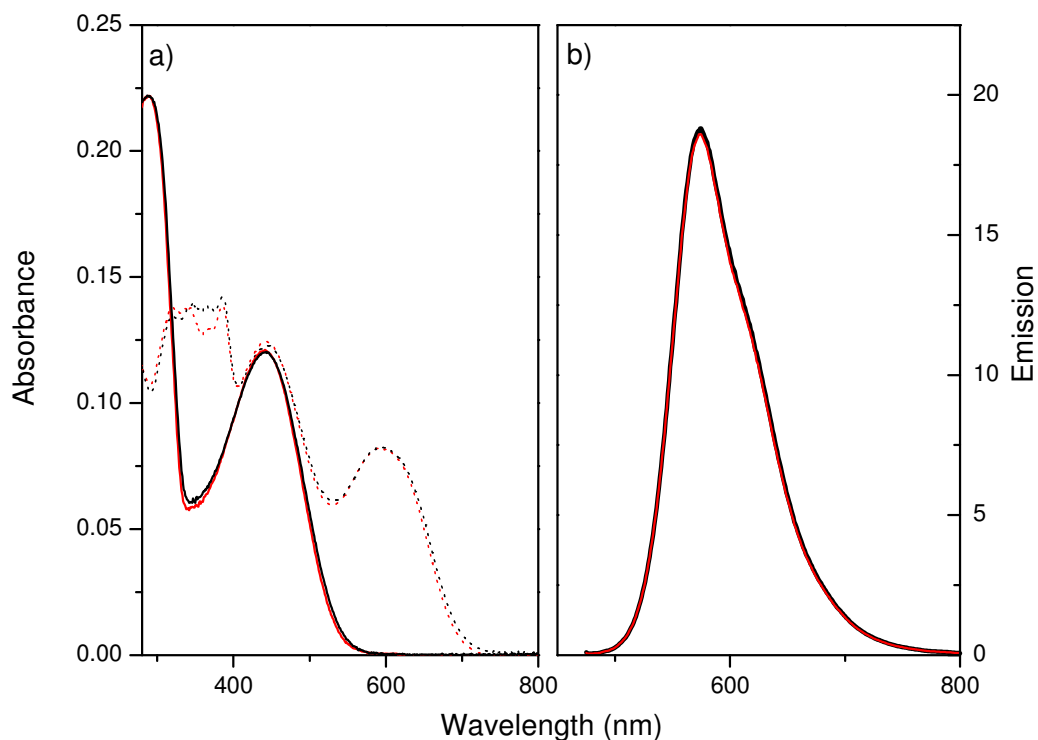


Figure 4-10. (a) Absorption and (b) emission spectra of **Poly-4** (open: black solid lines, closed: black dotted line) and **Poly-2/DTE-37** (open: red solid lines, closed: red dotted line).

The data in Figure 4-11 displays the absorbance values corresponding to the ring-closed systems at 595 nm plotted versus irradiation time. They indicate that both solutions approach the PSS (900 s) at the same rate. The percentage of ring-closed isomer present at the PSS is 96% for both systems as measured using ^1H NMR spectroscopy.

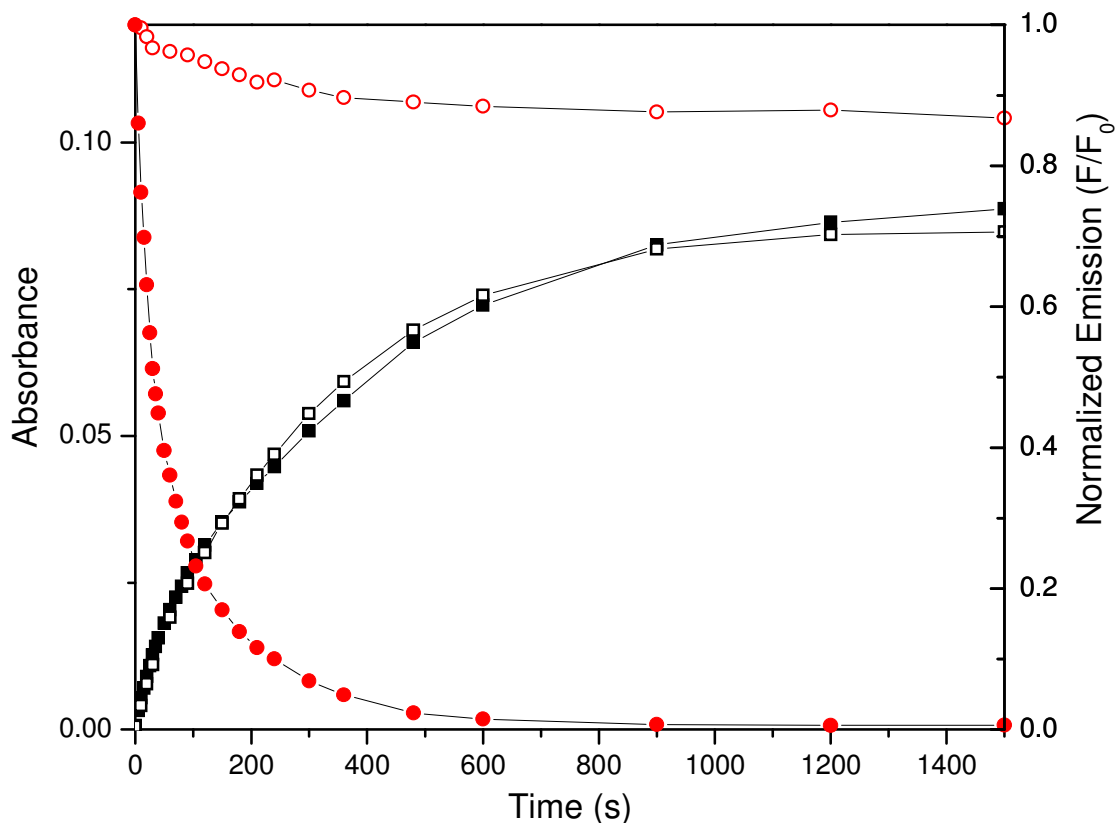


Figure 4-11. Changes in absorbance ($\lambda_{\text{max}} = 595$ nm) of **Poly-4c** (■) and **Poly-2/DTE-37c** (□), and changes in emission ($\lambda_{\text{max}} = 575$ nm) of **Poly-4o** (●) and **Poly-2/DTE-37o** (○) upon approaching the PSS.

Figure 4-11 also reveals that fluorescence quenching by the covalently bound DTE of **Poly-4c** differs dramatically from that of the **Poly-2/DTE-37c** mixture. At the PSS, the emission of **Poly-4** has been quenched 99% relative to the emission intensity of the ring-open isomer. The control solution has only been reduced by 12% of its original intensity. This difference may be studied using a Stern-Volmer analysis. The Stern-

Volmer relationship describes the variations of photophysical (e.g. fluorescence and phosphorescence) intermolecular deactivation processes represented by the equations:



where A is the chromophore and Q is a quencher. In the simplest case, the change in emission is linearly related to the concentration of available quencher. Here, the effective concentration of quencher (closed DTE) is much higher in **Poly-4** than in the solution **Poly-2/DTEc** where the quenching species is not attached.

Quantum yield (Φ) measurements were made to further quantify the extent of fluorescence quenching in **Poly-4** compared to that of the **Poly-2/DTE-37** mixture. The quantum yield decreases from 0.25 for **Poly-4o** to 0.003 for **Poly-4c**. The values measured for **Poly-2/DTE-37o** and **Poly-2/DTE-37c** were 0.31 and 0.19, respectively. These values display a quenching efficiency for **Poly-4** of 99% and only 39% for that of the **Poly-2/DTE-37** mixture.

Closer inspection reveals that the increased quenching efficiency of **Poly-4c** is amplified along the CP backbone. In Figure 4-12, the normalized emission (emission relative to that of the ring-open isomer) is plotted as a function of effective concentration of ring-closed isomer (measured absorbance at 595 nm, normalized to the PSS). In the case of the **Poly-2/DTE-37** mixture there is a nearly linear dependence on the decrease of emission with the related increase in ring-closed DTE concentration. In terms of the Stern-Volmer relationship, this is the behaviour expected for an intermolecular quenching

process. The non-linear dependence seen for **Poly-4** clearly demonstrates the amplification of a low concentration of ring-closing events on the emission of the polymer.

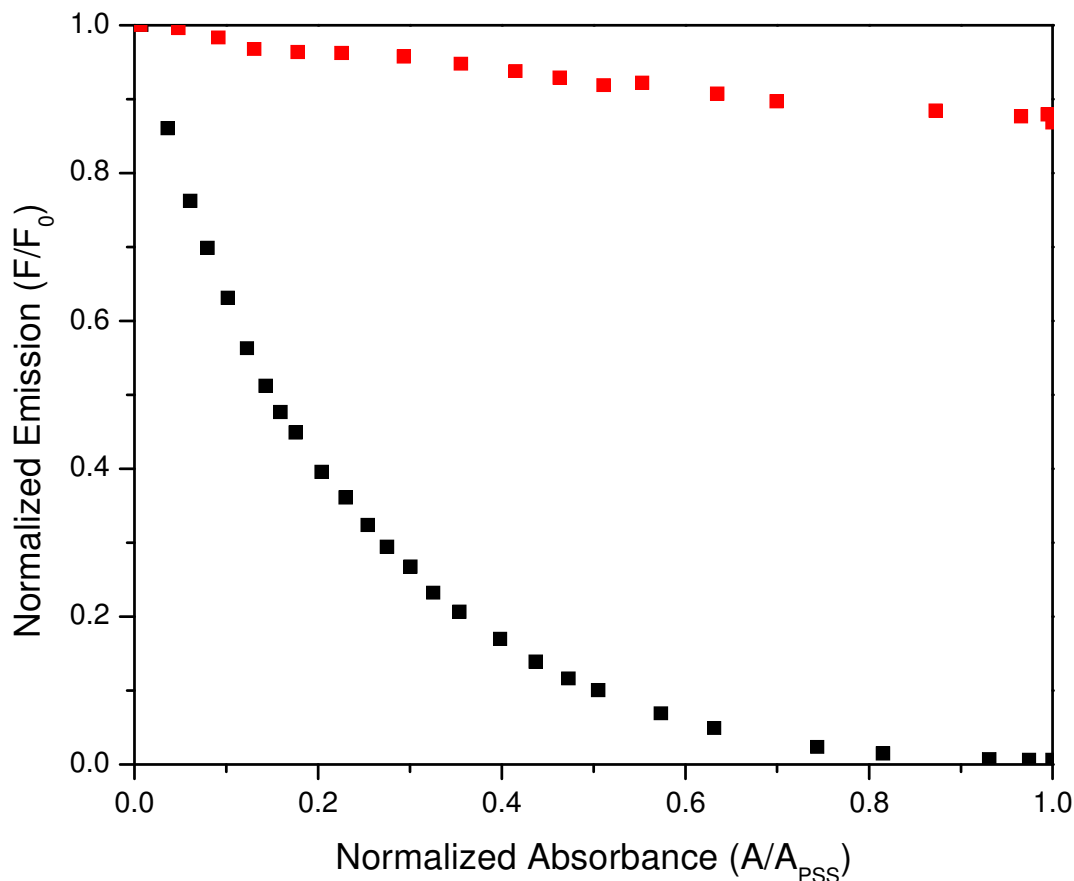


Figure 4-12. Normalized emission, F/F_0 ($\lambda_{\max} = 575$ nm), as a function of normalized absorbance, A/A_{PSS} ($\lambda_{\max} = 595$ nm), for the C_6H_6 solutions of **Poly-4** (■) and **Poly-2/DTE-37** (■).

The amplification is attributed to the rapid migration of initially formed excitons along the polymer backbone rendering further quenching events unproductive. It is expected that at low concentrations of ring-closed DTE, fluorescence quenching would still obey the Stern-Volmer relationship. To verify this, the initial induction period of

fluorescence quenching was examined with shorter irradiation times,²⁹ intended to drive the photo-induced ring-closing reaction to only 4% of the PSS. At this concentration, the ring-closed DTE groups are statistically distributed throughout the polymer chain, where they can quench the fluorescence without interfering or overlapping with each other, affording a ‘cleaner’ effect. As depicted in Figure 4-13 there is a linear relationship between the concentration of the ring-closed DTE and polymer emission intensity.

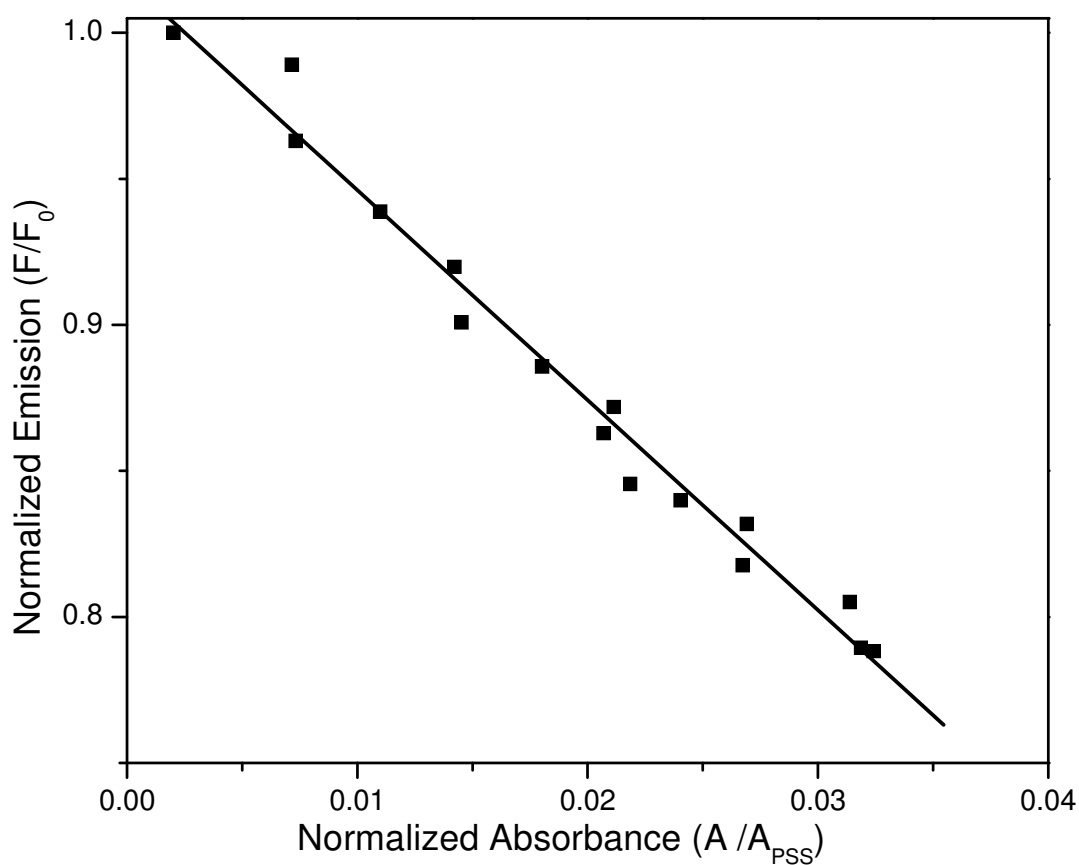


Figure 4-13. Initial induction of fluorescence quenching experienced by **Poly-4** with shorter irradiation times.²⁹

This induction period was used as a measure of the efficiency of the fluorescence quenching along the CP. Taking the average molecular weight (\overline{M}_w) of the polymer chain (16000 g mol⁻¹) determined from SEC, and the molecular weight of the monomer unit determined by ¹H NMR from the ratio of monomers within the chain (2:1; hexyl:DTE), the number of repeat units was estimated. An average chain was determined to contain approximately 15 repeat units, corresponding to 15 DTE moieties within a polymer chain containing ~ 45 thiophene rings. Extrapolation of the data in Figure 4-13 to zero fluorescence (100% quenching) results in a necessary concentration of 14% of the DTE moieties to reach the PSS which correlates to the ring-closing of only two DTE units. Therefore, with two DTE units contributing to 100% fluorescence quenching, the average exciton migration was determined to occur along ~ 20 thiophene units agreeing well with previous estimates.³¹

The comparison between each of the DTE functionalized analogs of **Poly-4** with respect to their individual effectiveness for fluorescence quenching is shown in Figure 4-14, where normalized emission (relative to the emission of the ring-open isomer) is plotted as a function of ring-closed isomer (measured at the absorbance at 595 nm, normalized to the PSS).

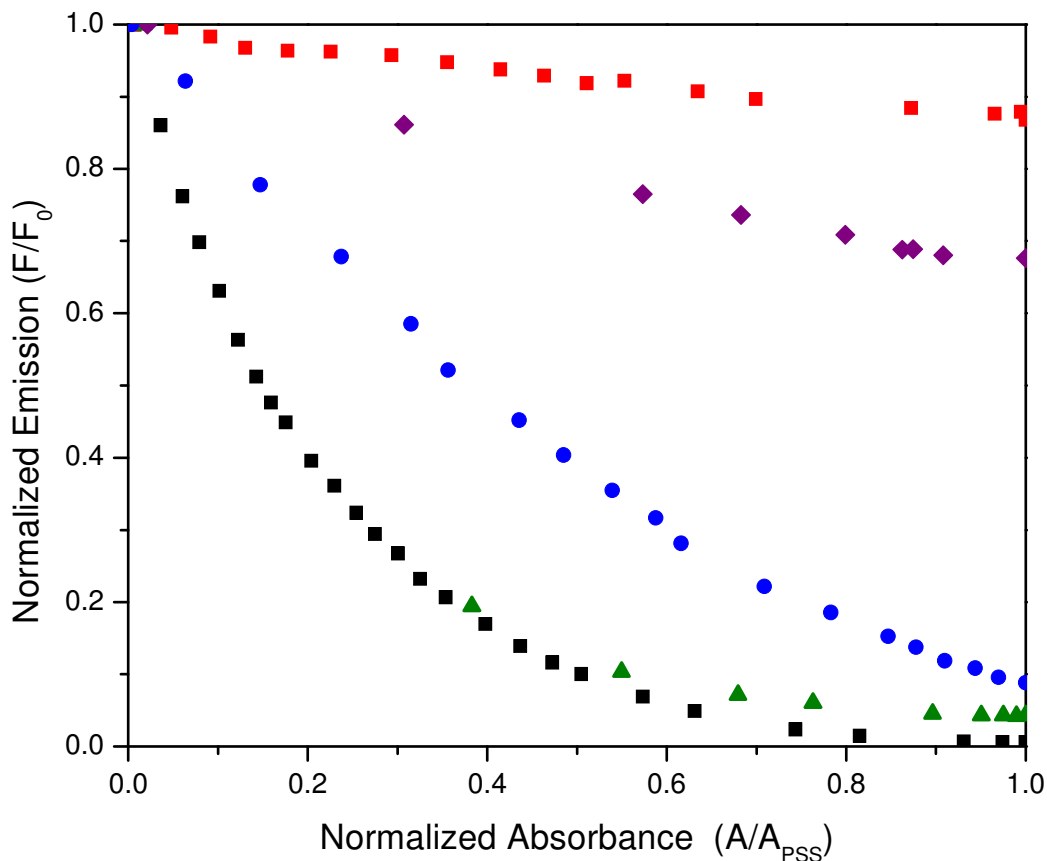


Figure 4-14. Comparison of amplified fluorescence quenching for **Poly-4** (■), **Poly-2/DTE-37** (■), **Poly-7** (▲), **Poly-11** (◆) and **71** (●).

The two extremes of fluorescence quenching are demonstrated by the control solution **Poly-2/DTE-37** with a linear dependence on quencher concentration and **Poly-4**, which demonstrates non-linear or amplified fluorescence quenching. The next most effective quenching system is observed to be **Poly-7** (▲), where (at the PSS) the emission is determined to be 96% quenched. This is to be expected for the polymer whose structure closely resembles the backbone structure of **Poly-4**. However, there is a slight decrease in overall quenching efficiency of **Poly-7** compared to **Poly-4** and this

may relate to the slight decrease in HT regioregularity in the polymer backbone of **Poly-7** leading to a higher degree of breaks in conjugation.

The next most efficient fluorescence quenching is observed in the terthiophene analog, compound **71** (●). The gradual decrease in emission approaches linearity but still trends toward 100% fluorescence quenching. The lack of amplification results from the significantly shorter backbone, which eliminates the necessity for long range exciton migration. The terthiophene species effectively behaves as a solution of monomeric receptors (Figure 4-1) where one DTE moiety can fully quench the fluorescence of the terthiophene oligomer it is tethered to. The quenching efficiency of **71** is higher than that of the control solution **Poly-2/DTE-37** due to the close proximity of a covalently bound DTE unit to the terthiophene backbone. By comparison, the quenching efficiency of **Poly-2/DTE-37** relies on diffusion limited intermolecular quenching.

Finally, the block copolymer **Poly-11** is not observed to reach the fully quenched fluorescent state, reaching only 68% of the original fluorescent intensity. This reduction of fluorescence quenching is believed to be due to the block structure of the polymer. Results from the SEC analysis show that the final average molecular weight of **Poly-11** is approximately 6000 g mol^{-1} . If one assumes a 10:1 ratio of hexyl:DTE content, the average polymer chain contains approximately 30 hexylthiophene units to three DTE moieties. From the average exciton migration length calculated for **Poly-4**, it appears that the average length of **Poly-11** is too long for the excitons at one end of the polymer to reach the other.

4.4 *Conclusions*

Functionalization of a HT regio-regular PT with a pendant DTE photoswitch demonstrates efficient fluorescence quenching via energy transfer from the excited state of the PT backbone to that of the ring-closed DTE absorption. Amplification of fluorescence quenching is observed for **Poly-4** and **Poly-7**, the two analogs with extended conjugation allowing for efficient migration of excitons along the polymer backbone. The migration of excitons along a CP backbone is shown to have a limit in path length, displayed by the inefficient fluorescence quenching of **Poly-11**. This block copolymer has an average chain length approximately 30 thiophene units long which extends beyond the experimentally determined migration length of 20 thiophenes. The linear quenching dependency observed for compound **71** reinforces the need for long range conjugation throughout the length of the polymer backbone in order for an amplified effect to be observed.

4.5 References

1. Thomas, S. W.; Joly, G. D.; Swager, T. M., *Chem. Rev.* **2007**, 107, (4), 1339-1386.
2. Kim, T. H.; Swager, T. M., *Angew. Chem. Int. Ed.* **2003**, 42, (39), 4803-4806.
3. Tang, Y. L. et al., *Macromol. Rapid Commun.* **2006**, 27, (6), 389-392.
4. Huang, H. M. et al., *Angew. Chem. Int. Ed.* **2004**, 43, (42), 5635-5638.
5. Ramachandran, G. et al., *J Fluoresc* **2003**, 13, (5), 427-436.
6. Kim, J.; McQuade, D. T.; McHugh, S. K.; Swager, T. M., *Angew. Chem. Int. Ed.* **2000**, 39, (21), 3868-3872.
7. Wang, B.; Wasielewski, M. R., *J. Am. Chem. Soc.* **1997**, 119, (1), 12-21.
8. Kumaraswamy, S. et al., *Proc. Natl. Acad. Sci. USA* **2004**, 101, (20), 7511-7515.
9. Rininsland, F. et al., *Proc. Natl. Acad. Sci. USA* **2004**, 101, (43), 15295-15300.
10. Ho, H. A.; Béra-Abérem, M.; Leclerc, M., *Chem. Eur. J.* **2005**, 11, (6), 1718-1724.
11. Bernier, S. et al., *J. Am. Chem. Soc.* **2002**, 124, (42), 12463-12468.
12. Ho, H. A. et al., *Angew. Chem. Int. Ed.* **2002**, 41, (9), 1548-1551.
13. Brédas, J. L. et al., *Acc. Chem. Res.* **1999**, 32, (3), 267-276.
14. Schwartz, B. J., *Annu. Rev. Phys. Chem.* **2003**, 54, 141-172.
15. Kim, J.; Levitsky, I. A.; McQuade, D. T.; Swager, T. M., *J. Am. Chem. Soc.* **2002**, 124, (26), 7710-7718.
16. Levitsky, I. A.; Kim, J.; Swager, T. M., *Macromolecules* **2001**, 34, (7), 2315-2319.
17. Zhou, Q.; Swager, T. M., *J. Am. Chem. Soc.* **1995**, 117, (50), 12593-12602.

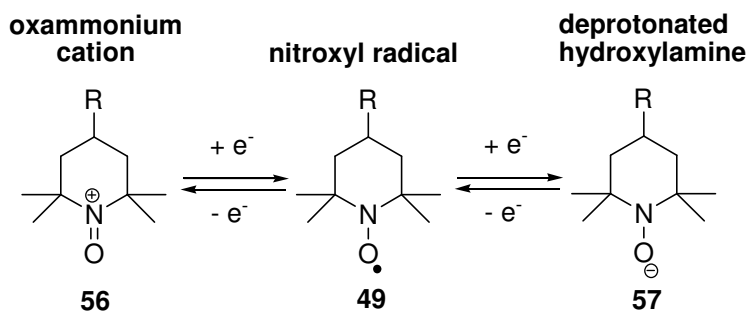
18. Zhou, Q.; Swager, T. M., *J. Am. Chem. Soc.* **1995**, 117, (26), 7017-7018.
19. Allwood, B. L. et al., *J. Chem. Soc., Chem. Commun.* **1987**, (14), 1064-1066.
20. Rose, A.; Lugmair, C. G.; Swager, T. M., *J. Am. Chem. Soc.* **2001**, 123, (45), 11298-11299.
21. Wosnick, J. H.; Liao, J. H.; Swager, T. M., *Macromolecules* **2005**, 38, (22), 9287-9290.
22. Yamaguchi, S.; Swager, T. M., *J. Am. Chem. Soc.* **2001**, 123, (48), 12087-12088.
23. Yang, J. S.; Swager, T. M., *J. Am. Chem. Soc.* **1998**, 120, (46), 11864-11873.
24. Yang, J. S.; Swager, T. M., *J. Am. Chem. Soc.* **1998**, 120, (21), 5321-5322.
25. Zacharias, P. et al., *Angew. Chem. Int. Ed.* **2009**, 48, (22), 4038-4041.
26. Tsujioka, T.; Masui, K.; Ootoshi, F., *Appl. Phys. Lett.* **2004**, 85, (15), 3128-3130.
27. Myles, A. J.; Branda, N. R., *Adv. Funct. Mater.* **2002**, 12, (3), 167-173.
28. Myles, A. J.; Wigglesworth, T. J.; Branda, N. R., *Adv. Mater.* **2003**, 15, (9), 745-748.
29. Finden, J.; Kunz, T. K.; Branda, N. R.; Wolf, M. O., *Adv. Mater.* **2008**, 20, (10), 1998-2002.
30. Chen, T. A.; Wu, X. M.; Rieke, R. D., *J. Am. Chem. Soc.* **1995**, 117, (1), 233-244.
31. Kishino, S. et al., *Phys. Rev. B* **1998**, 58, (20), 13430-13433.

CHAPTER 5 Electrodeposition of TEMPO Functionalized Polythiophene Thin Films*

5.1 Introduction

Organic materials capable of reversibly storing charge are of significant interest for use in devices such as batteries^{1,2} or supercapacitors.³⁻⁷ These materials offer several key advantages over traditional inorganic battery materials. They are low weight, offer mechanical flexibility and are compatible with solution based processing techniques such as spin-coating^{8,9} and ink-jet printing.¹⁰⁻¹² Conjugated polymers (CPs) have been investigated as potential battery materials¹³ as they possess many desirable characteristics for this application: they can be reversibly doped, can be prepared in thin-film form, and can be made soluble via substituents on the polymer backbone. However, CPs often exhibit low doping levels, resulting in small redox capacities, and slow kinetics at the electrode often limit the charging and discharging rates of the resulting device.¹⁴

Scheme 5-1



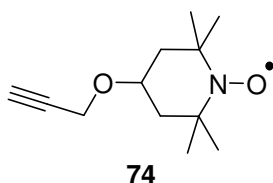
An alternative approach involves the use of redox polymers where discrete moieties, which undergo reversible redox processes, are attached to a polymer backbone

* A version of this chapter will be submitted for publication. Kunz, T. K. and Wolf, M. O., Electrochemical Thin Film Deposition of TEMPO Functionalized Polythiophenes.

5.2 *Experimental*

5.2.1 **General**

All reagents and solvents were used as received except where noted. Tetrahydrofuran (THF) was distilled from Na/benzophenone. Anhydrous dimethylformamide (DMF) was distilled from P₂O₅. Compound **74** was prepared according to the literature.¹⁷

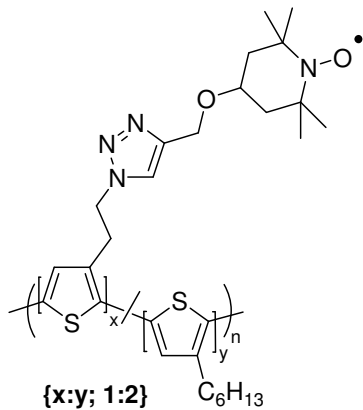


¹H NMR spectra were obtained in CDCl₃ either on a Bruker AV- 400 Inverse or a Bruker AV-400 Direct spectrometer. Chemical shifts are reported in ppm, referenced to residual chloroform (CHCl₃) (δ 7.27). ATR-IR spectra were recorded on a Thermo Scientific Nicolet 6700 FT-IR spectrometer as neat powders or oils. Electronic absorption spectra were obtained on a Varian Cary 5000 UV-vis spectrometer in HPLC grade CH₂Cl₂ and CHCl₃. Fluorescence measurements were made on a PTI Quantamaster spectrometer in the same solvents used for UV-vis measurements. Molecular weight distribution curves of polymers were determined by size exclusion chromatography (SEC) was performed using a Waters SEC equipped with 3 μg-Styrgel columns against polystyrene standards. Polymers were dissolved, filtered and eluted with THF at a flow rate of 1.0 mL/min and monitored with a UV-vis detector (Waters 2487). Data was acquired and analyzed using an IBM personal computer and custom-written software. Electrochemical measurements were conducted on a Autolab PGSTAT12 using either a

Pt disk, ITO plated glass or microporous carbon paper working electrode, Pt mesh counter electrode, and a Ag wire reference electrode. These measurements were made in CH_2Cl_2 passed through an alumina column, acetonitrile (ACN) distilled over molecular sieve (type 3A, 4-8 mesh beads) or propylene carbonate obtained from Aldrich (sure-seal). Unless specified, measurements were referenced against the pseudo-reference Ag wire. Alternatively, an internal reference (decamethylferrocene) was added to correct the measured potentials with respect to saturated calomel electrode (SCE). The 0.1 M [*n*- Bu_4N] PF_6 supporting electrolyte was purified by triple recrystallization from ethanol and dried at 90°C under vacuum for 3 days. Electron Spin Resonance (ESR) spectra were obtained using a Bruker Elexys E-500, X-band (9.5 GHz) spectrometer. Samples were measured as benzene solutions.

5.2.2 Procedures

Synthesis of Poly-12



Poly-2²⁷ (0.0615 g, 0.127 mmol) and acetylene functionalized TEMPO (**74**) (0.0271 g, 0.129 mmol) were dissolved in THF (10 mL) resulting in an orange solution which was degassed with N_2 (20 min). CuI (0.0044 g, 0.023 mmol) was added to the stirring solution in one portion. The reaction mixture was covered in Al foil and the solution was heated to 100 °C. The vigorously stirring solution was left overnight and then cooled to allow precipitation of a purple solid from methanol (600 mL). **Poly-12** was then re-precipitated twice from methanol. Yield: 0.052 g (59%). 1H NMR (400 MHz, $CDCl_3$, δ): 7.01 (br, s), 2.81 (br, s), 1.8 – 1.2 (m), 0.91 (m). ATR-IR (ν , cm^{-1}): 2961, 2923, 2853, 1456, 1376, 1361, 1259, 1219, 1175, 1081, 1015, 863, 795, 669, 569. UV-vis (CH_2Cl_2) λ_{max} : 435 nm. Fluorescence (CH_2Cl_2) λ_{max} : 575 nm. SEC: \overline{M}_w = 13500, \overline{M}_n = 8500, PDI = 1.5.

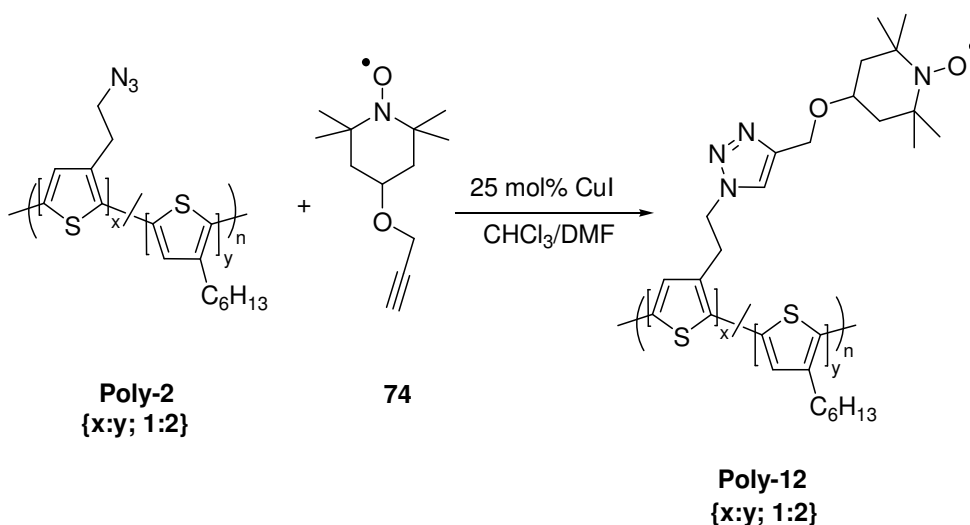
5.3 Results and Discussion

5.3.1 Synthesis and Characterization

The modification of a HT regioregular polymer (prepared through the GRIM polymerization) via attachment of a stable free radical was carried out to investigate the potential charge storage capabilities of a coupled organic redox group and a CP. **Poly-12** was synthesized using Click chemistry to modify a previously prepared polymer, **Poly-2**,²⁷ with an acetylene modified TEMPO radical (**74**) as shown in

Scheme 5-3. Previously,²⁷ the Click reaction was carried out using $\text{CuSO}_4 \cdot 5\text{H}_2\text{O}$ and L-ascorbic acid to generate the active catalyst Cu^{I} from Cu^{II} *in-situ*. It has been demonstrated that nitroxyls of the piperidine series can be oxidized by Cu^{II} in solution.^{28,29} To avoid any complications with the reactivity of the catalyst, Cu(I)iodide was used in place of $\text{CuSO}_4 \cdot 5\text{H}_2\text{O}$ and ascorbic acid.^{17,30} The final polymer was isolated and purified via multiple re-precipitations from methanol.

Scheme 5-3



Poly-12 was characterized by ATR-IR, UV-vis, fluorescence, ^1H NMR, and ESR spectroscopy. In the ATR-IR spectrum, the azide stretching band of **Poly-2** at 2091 cm^{-1} disappears. In addition, there are no acetylene stretches present at 3229 or 2111 cm^{-1} . This suggests that the azide and acetylene starting materials have reacted. TEMPO lacks a distinct IR handle for confirmation of its presence; closer inspection of the fingerprint region of the IR spectra was necessary (Figure 5-1). A stretching band observed at 1361 cm^{-1} is within the characteristic range of the $\text{NO}\cdot$ moiety ($1340\text{--}1390\text{ cm}^{-1}$)^{15,31} and supports the presence of the free radical. Further support of this assignment is obtained from a stretching frequency at 1365 cm^{-1} observed for the TEMPO precursor, **74**, and the lack thereof in **Poly-2**.

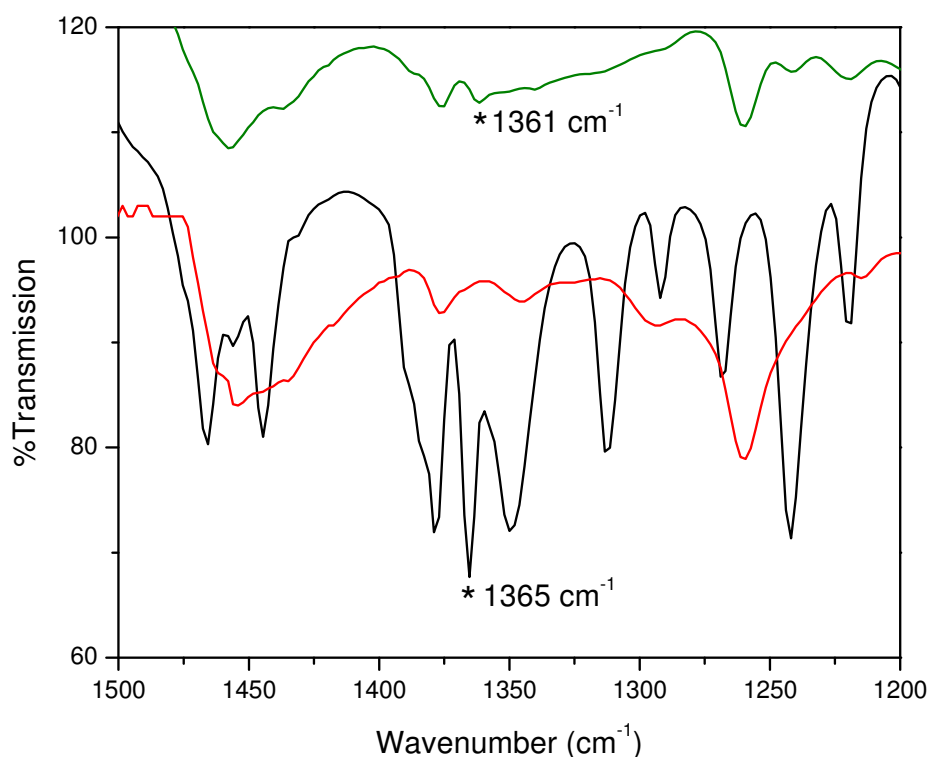


Figure 5-1. IR spectra of **Poly-12** (green), **Poly-2** (red), and **74** (black) displaying the fingerprint region. (*) indicates the $\nu(\text{NO}\cdot)$ stretching frequency.

Absorbance and emission studies were carried out in CH₂Cl₂ solution (

Figure 5-2). The absorbance maximum of **Poly-12** is observed at 436 nm displaying a minimal shift compared to that of **Poly-2** ($\lambda_{\text{max}} = 437$ nm). **Poly-12** also exhibited an emission maximum at 575 nm, directly corresponding to the emission wavelength of **Poly-2**. Interestingly, there is a significant reduction in fluorescence intensity for **Poly-12** compared to that of **Poly-2** when the two compounds were studied in CH₂Cl₂ solutions of the same optical density. The significant emission quenching observed in **Poly-12** can be rationalized by electron transfer between the TEMPO group and the excited state of the polymer backbone. In fact, the TEMPO group is commonly used as a one electron acceptor in fluorescence quenching experiments.^{32,33} The fluorescence has not been completely quenched and is attributed to the concentration of TEMPO groups being too low to fully quench the system.

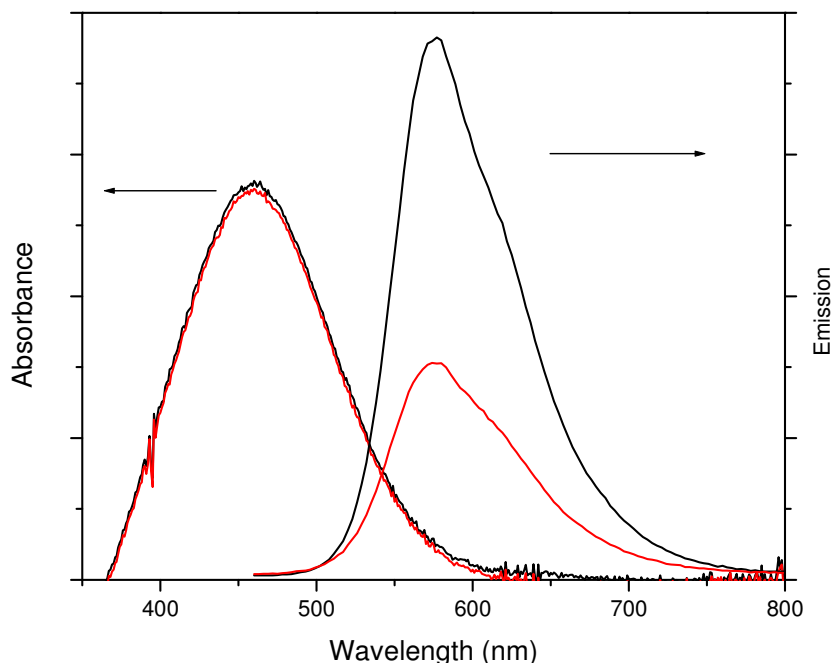


Figure 5-2. Absorption and emission spectra of CH₂Cl₂ solutions of **Poly-2** (black) and **Poly-12** (red).

The ^1H NMR spectrum of **Poly-12** displays significantly broadened signals, as expected for a polymeric radical-containing material.³⁴ The only protons that could be resolved were observed from δ 2.80 to 0.91 are assigned to the protons of the hexyl groups corresponding in chemical shift with similar resonances in **Poly-2**.

5.3.2 Electron Spin Resonance Studies

Systems that contain one or more unpaired electrons result in line broadening in NMR spectroscopy.³⁴ Electron spin resonance (ESR) spectroscopy is a technique used specifically to study such paramagnetic systems. ESR spectroscopy was carried out on **Poly-12** to further confirm the presence of the TEMPO moiety (Figure 5-3). The nitroxide free radical is known to show a triplet hyperfine structure due to the interaction between the nuclear spin of ^{14}N ($I = 1$), and the electron spin of the free radical ($I = 1/2$) according to the equation $2nI + 1$, where n is the number of nuclei and I is the spin state of that nucleus.^{35,36} The ESR spectrum of **Poly-12** in a benzene solution at room temperature shows a triplet centered at 3504 G, characteristic of TEMPO derivatives, confirming that the radical is present in **Poly-12**.³⁷

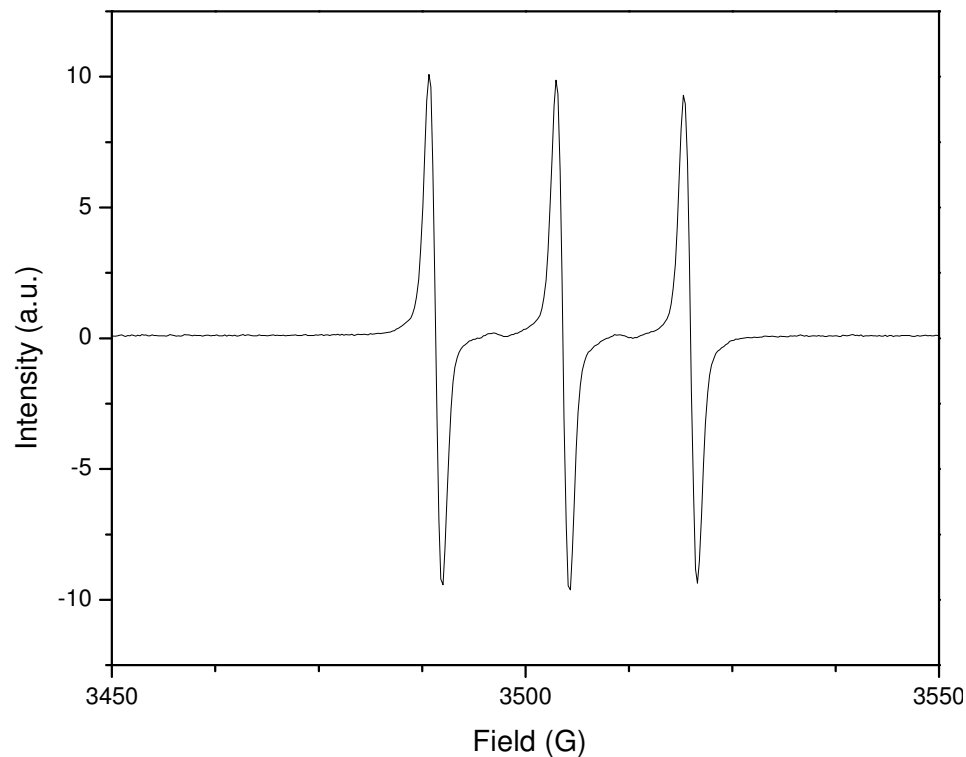


Figure 5-3. X-band ESR spectrum of **Poly-12** in C_6H_6 solution at 22 °C. Modulation Frequency: 20.00 kHz. Modulation Amplitude: 0.02 G. Time Constant: 2.56 s. Gain: 60 dB. Sweep Width: 150.6 G.

5.3.3 Cyclic Voltammetry Studies

Poly-12 was studied using cyclic voltammetry (CV) using indium tin oxide (ITO) coated on glass and high surface area microporous carbon paper working electrodes. In the studies of **Poly-12** carried out on ITO coated glass slides, the first scan (Figure 5-4a) of the voltammogram in CH_2Cl_2 displays an oxidation wave at 1.28 V (vs. Ag wire) due to oxidation of TEMPO with the corresponding reduction wave observed at 1.06 V (vs. Ag wire). Interestingly, sequential scans exhibit increasing current (Figure 5-4b). This behaviour is characteristic of conducting polymer deposition on an electrode and is typically observed in monomers which polymerize electrochemically.

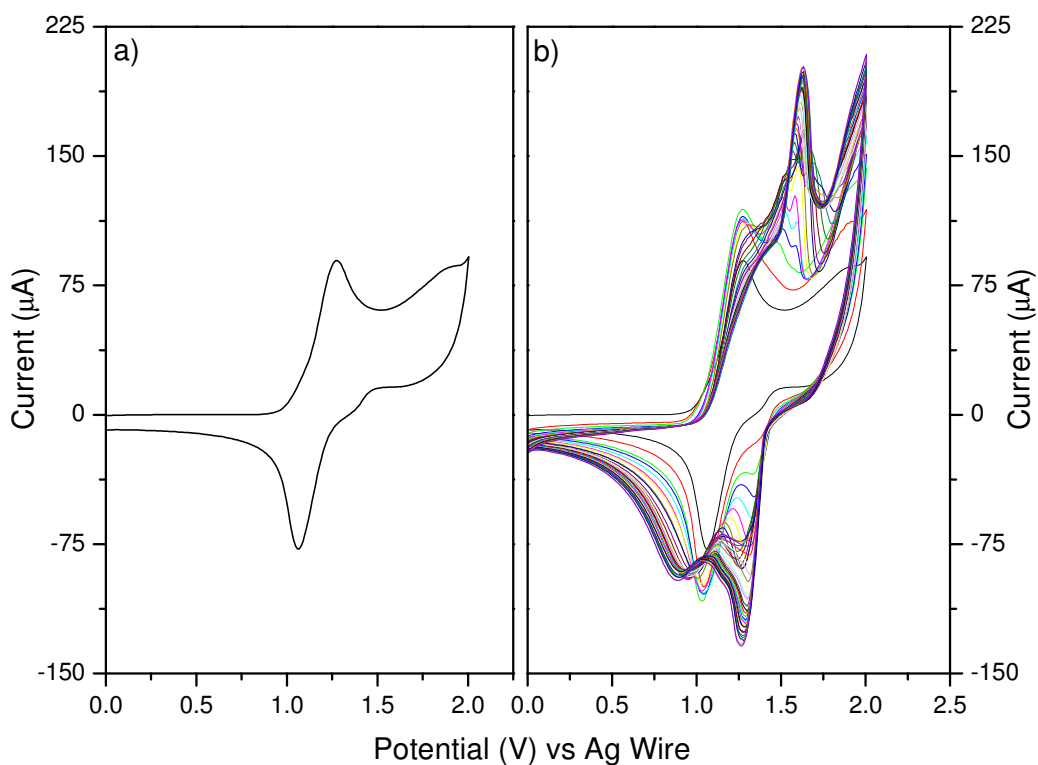


Figure 5-4. (a) Initial scan and (b) polymerization of **Poly-12** on ITO. 0.1 M [*n*-Bu₄N]PF₆ in CH₂Cl₂ on ITO coated glass working electrodes. Scan rate = 50 mVs⁻¹.

This growth phenomenon has not been previously reported for preformed CPs. The same polymer growth was displayed by the precursor polymer **Poly-2**, demonstrating that it was not an isolated effect caused by inclusion of the TEMPO moiety. As seen in Figure 5-5, the redox wave of the TEMPO group seems to overlay the features of the growing polymer, with a noticeable shift of the TEMPO redox wave to higher potential.

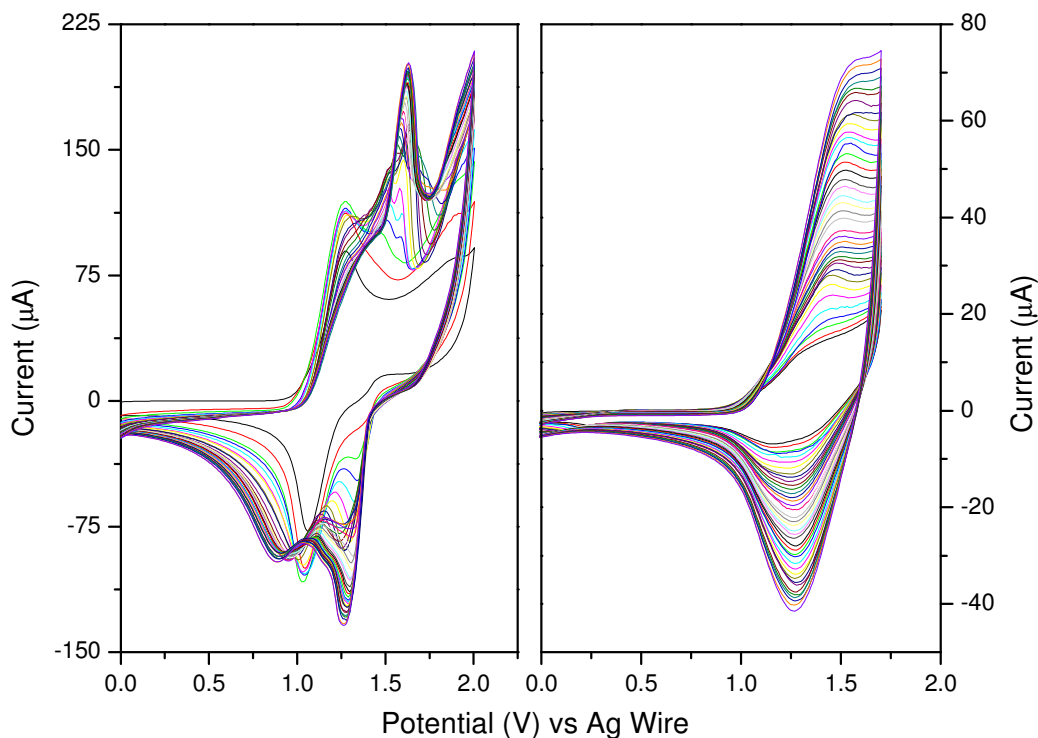


Figure 5-5. Cyclic voltammograms of the growth of **Poly-12** vs. **Poly-2**. 0.1 M [*n*-Bu₄N]PF₆ in CH₂Cl₂ solutions growth on ITO coated glass electrodes. Scan rate = 50 mVs⁻¹.

The film was removed from the polymerization solution, washed with CH₂Cl₂ to remove any extraneous, undeposited polymer, and subsequently studied in polymer-free CH₂Cl₂ solution. Upon applying a potential scan (-0.2 V to 1.8 V) to the thin film electrode, only background current was recorded. A second film was studied in ACN solution in which the current was observed to decrease with sequential scans, indicating loss of the film from the electrode (Figure 5-6). The loss of the film was also confirmed visually with the appearance of a purple halo-like cloud forming around the electrode during the sequential scans.

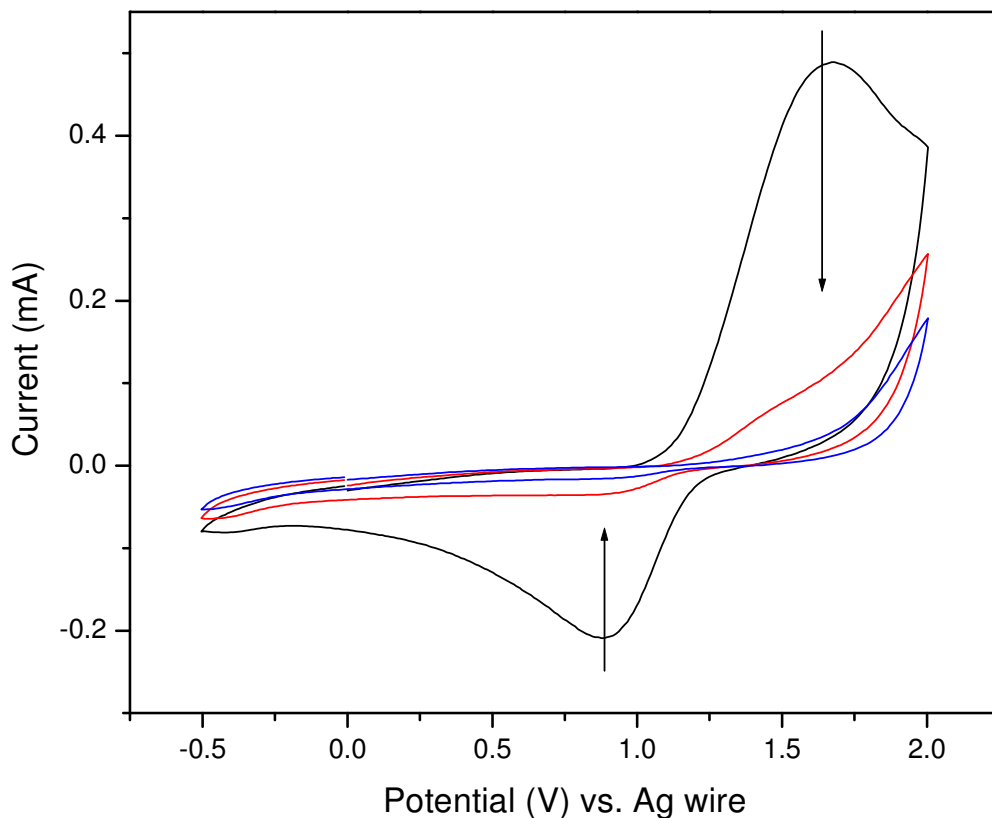


Figure 5-6. Degradation of **Poly-12** on ITO working electrode. 0.1 M $[n\text{-Bu}_4\text{N}]\text{PF}_6$ in ACN. Scan rate = 100 mVs^{-1} .

Similar redox features and film instability were observed for the thin films of **Poly-12** deposited on carbon paper electrodes when studied in both CH_2Cl_2 and ACN. The oxidation and reduction waves of the TEMPO groups were observed at 0.91 V and 0.85 V (vs. SCE) on carbon paper, respectively. Due to the larger surface area of the carbon paper electrode, passivation of the electrode surfaces didn't occur until a higher number of scans had been reached allowing for a greater mass of polymer to be deposited. This subsequently provided enough additional mass to allow for microanalysis weight measurements to be performed. Deposited polymer masses were obtained in the range of 0.5 to 1.2 mg.

The carbon paper electrodes were studied in a propylene carbonate solution, where the deposited polymer films of **Poly-12** were stable enough for additional measurements. Unfortunately, the ITO samples seemed to degrade in this solvent as well. The thin film of **Poly-12** on the carbon paper electrode was subjected to several potential scans at various speeds (Figure 5-7). A linear increase in peak current as a function of increasing scan rate demonstrates that the redox behaviour of TEMPO is reversible and exhibits rapid electron transfer kinetics.³⁸

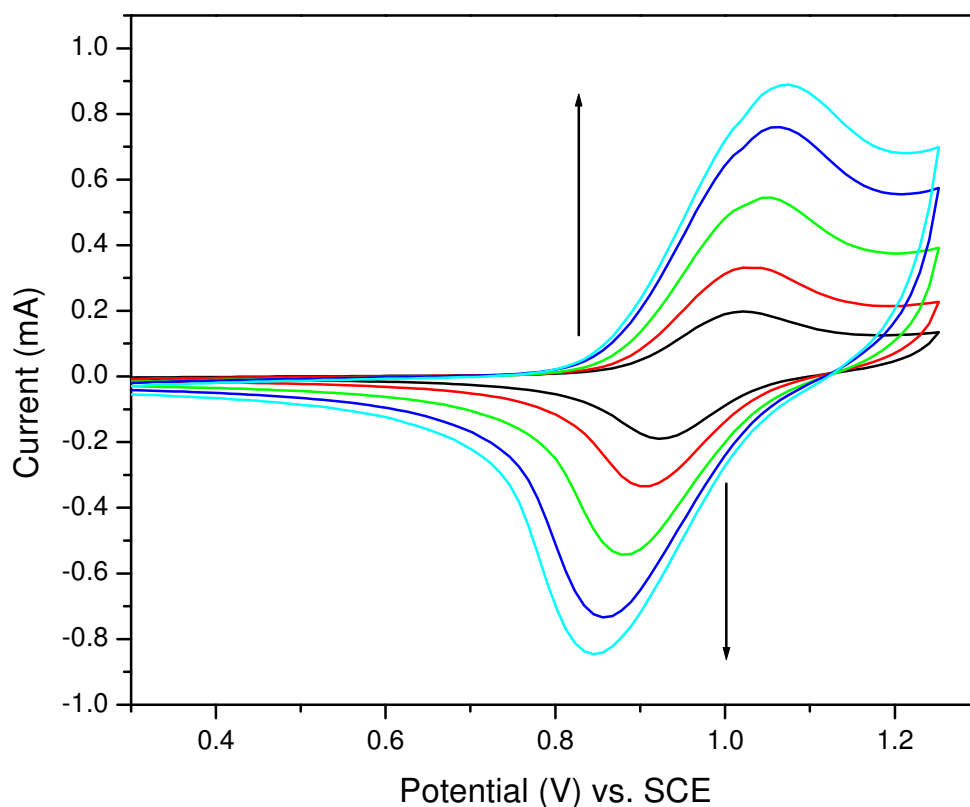


Figure 5-7. Cyclic voltammogram of **Poly-12** on carbon paper with increasing scan rate (Propylene carbonate, mVs⁻¹): 25, 50, 100, 150, 200.

5.3.4 Capacity and Charge/Discharge Studies

The samples of **Poly-12** deposited on carbon paper electrodes were used to measure the capacity of the polymer films. Integration of the CV curve along the oxidation scan from 0.0 to 1.5 V yields a measure of the amount of charge that can be stored in the material over that potential range. The theoretical capacity (C ; in A h kg^{-1}) is determined from the molecular weight required per exchangeable unit charge in the polymer according to Eq. 5-1:

$$C(\text{Ah/kg}) = \frac{N_A \times e}{3600 \times \left(\frac{\text{MW}}{1000} \right)} \quad \text{Eq. 5-1}$$

where $N_A \times e$ is the Faraday constant ($96,487 \text{ C mol}^{-1}$), MW is the equivalent mass of the polymer in grams, and defined as the molecular weight of the repeating unit divided by the number of electrons exchanged or stored within it.^{39,40} The theoretical capacity of **Poly-12** is calculated to be 76.5 A h kg^{-1} assuming that the TEMPO group can store one electron and the thiophene backbone can store one electron per three thiophene rings (the repeat unit determined from $^1\text{H NMR}$ of **Poly-2**).^{13,41-43} The value determined for **Poly-12** from the experimental data is 2.3 A h kg^{-1} (averaged over several samples). In contrast, samples of electrochemically synthesised PT have been observed to display a specific charge as high as 52 A h kg^{-1} .¹³ These results are contrary to the expected improvement in properties afforded by the rr-PT backbone.

For a more critical evaluation of the capacitance of the polymer film, galvanostatic charge and discharge cycles were carried out. The deposited film was

placed in a polymer free solution and with a constant applied current the potential is scanned in both a positive and negative direction within the potential range of charge storage. Figure 5-8 displays the charge/discharge curves from scans at 0.1 mA, cycled between 0.8 and 1.2 V for **Poly-12**. The amount of charge being stored in the film is calculated in terms of Farads per gram ($F g^{-1}$). For several samples of **Poly-12** grown on carbon paper electrodes, the curves led to specific capacities in the range of $\sim 0.8 F g^{-1}$. By way of comparison, the charge and discharge cycles carried out on **Poly-2**, delivered values an order of magnitude higher at $11.3 F g^{-1}$. Multiple samples were prepared and studied, and in all of these samples **Poly-12** displayed consistently lower values than those of **Poly-2**.

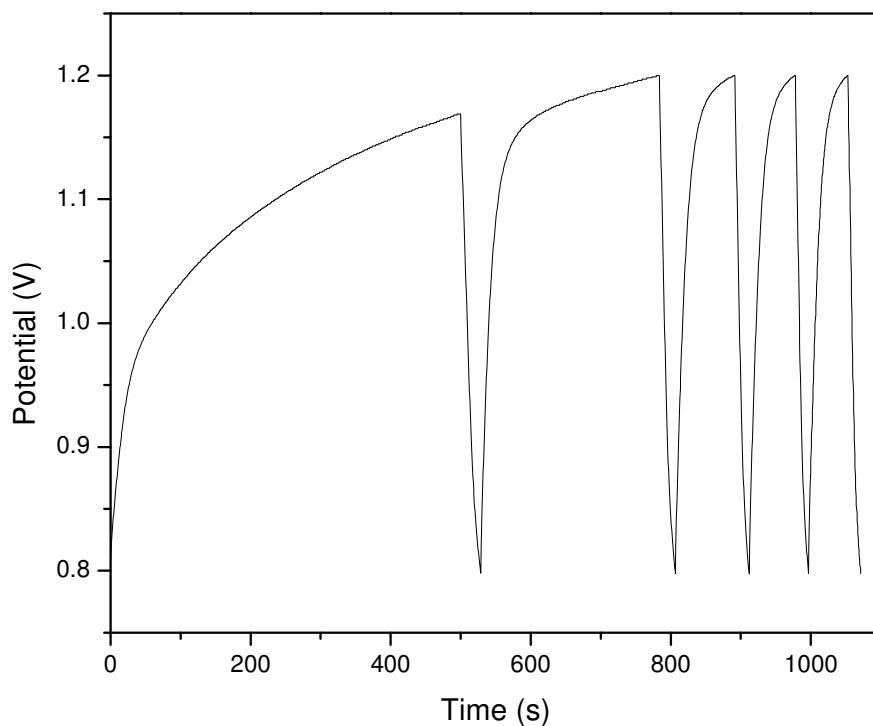


Figure 5-8. Typical galvanostatic charge-discharge curve of **Poly-12** scanned at 0.1 mA in propylene carbonate with 0.1 M $[n\text{-Bu}_4\text{N}]\text{PF}_6$ supporting electrolyte. Scanned between 0.8 – 1.2 V.

5.3.5 Backbone Oxidation

A dramatic decrease of polymer electroactivity was observed after the first cycle of the galvanostatic charge-discharge experiment, with continued degradation observed for each sequential scan (Figure 5-8). Each of the samples of **Poly-12** exhibited this same behaviour. This pronounced degradation and the unsatisfactory specific charge and capacity measurements obtained for **Poly-12**, led to investigations into the possible causes of degradation. A potential explanation lies in the possibility of breaks in the conjugation along the polymer chain. This may be the result of mechanical strain provoked by the ions during insertion and deinsertion⁴⁴ or chemical attack by the solvent, doping ions or water contained in the electrolyte.⁴⁵ Several investigations have also been carried out into the reactivity of singlet oxygen generated during UV irradiation causing degradation of PT backbones via chain breaking and disruption to the conjugation.^{46,47} It is proposed that TEMPO, a known oxidizing agent for the oxidation of alcohols, may be contributing to the accelerated oxidation of the PT backbone.

Recovery of the polymer from the solutions of **Poly-12** and **Poly-2** used for electrochemistry allowed study by both ATR-IR and UV-vis spectroscopies, which offered some insight into the nature of the film degradation. As seen in the ATR-IR spectra (Figure 5-9a), there is a distinct new stretching frequency located in the spectrum of **Poly-12** after the 'polymerization' (black) that is not present before (green) at 1725 cm^{-1} . In Figure 5-9b, comparing the recovered sample of **Poly-12** (black) to **Poly-2** (red), it can clearly be observed that **Poly-2** is not experiencing the same degradation as the 1725 cm^{-1} band is not present.

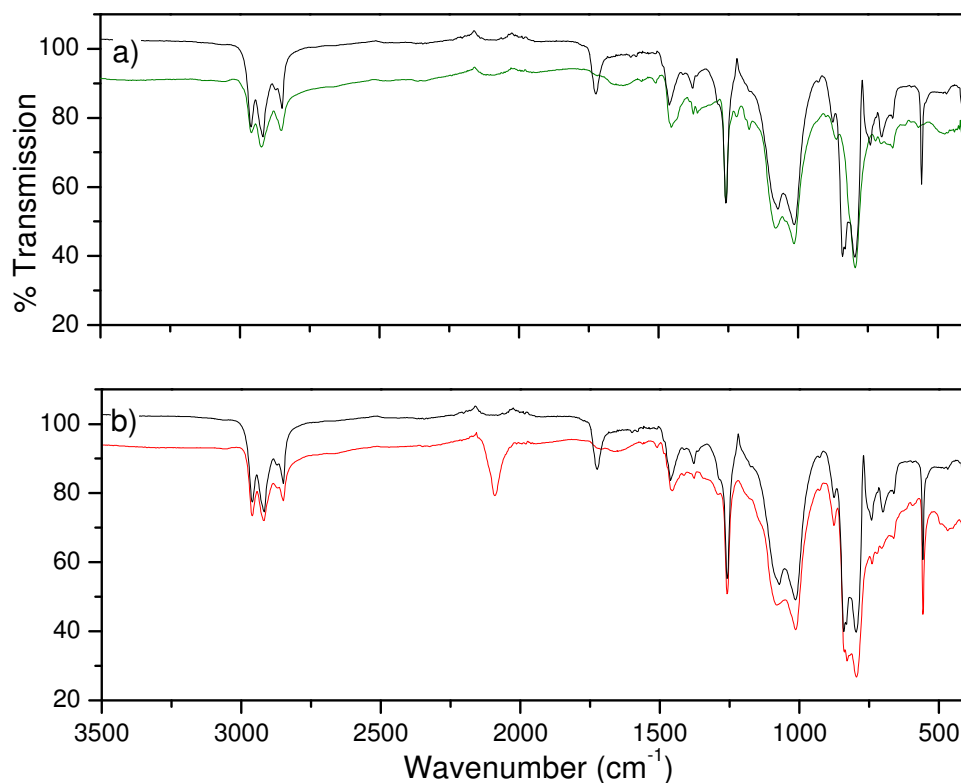
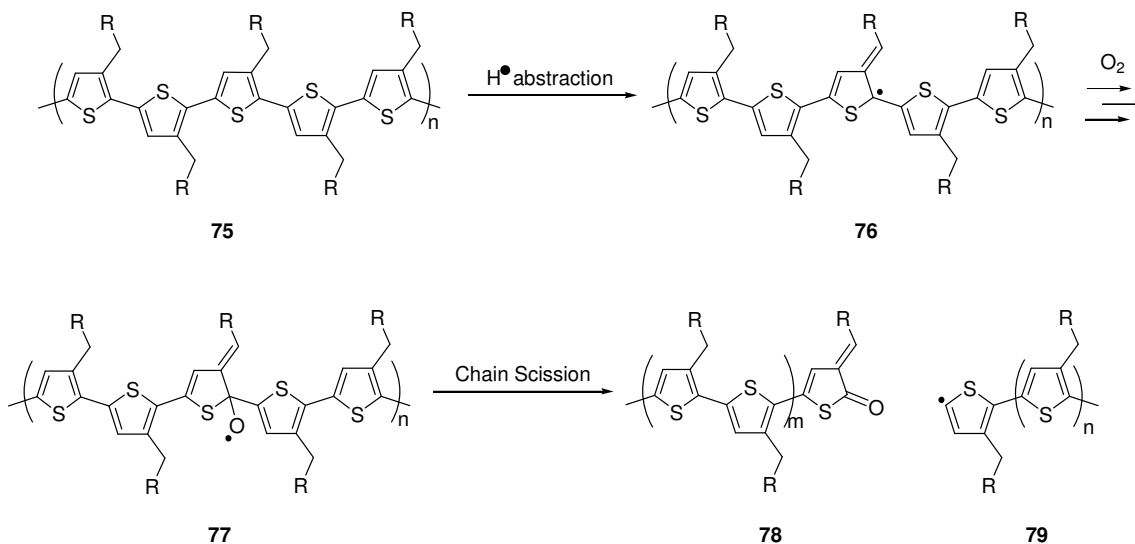


Figure 5-9. ATR-IR spectra of (a) **Poly-12** before (black) and after (green) isolation from the CV solution and (b) **Poly-12** (black) and **Poly-2** (red) isolated from the polymerization reaction.

The stretching frequency located at 1725 cm^{-1} is in the characteristic range of a carbonyl stretch ($\nu_{\text{C=O}}$; $1700\text{-}1800\text{ cm}^{-1}$) and strongly suggests oxidation of the polymer backbone. There are several possible mechanisms that could lead to the formation of a carbonyl group within a PT backbone.^{46,48,49} The polymer backbone may be susceptible to hydrogen abstraction from the TEMPO, and in the presence of oxygen the polymer backbone is oxidized. Scheme 5-4 outlines a potential mechanism for the formation of carbonyl groups leading to chain scission and reduced conjugation. UV-vis spectroscopy

also displayed a blue shift in the maximum absorbance (436 to 430 nm), directly related to a reduction in π -conjugation along the polymer backbone.

Scheme 5-4



Despite the lack of conductivity available from the polymer backbone, the TEMPO groups should still have demonstrated some charging behaviour. It is possible that as the conductivity of the polymer is reduced, the TEMPO groups farthest from the electrode are rendered inaccessible due to a lack of conjugation throughout the polymer. This compounds the effect of the disrupted conjugation, contributing to the disappointing measured specific charge of **Poly-12**.

5.4 Conclusions

A polymer prepared via GRIM polymerization was functionalized with the stable free radical TEMPO. This new material was anticipated to display improved charging and discharging capabilities for applications towards organic based batteries. The performance of the thin films in specific capacity and charge/discharge experiments was determined to be less than optimal. Further investigations suggest that the TEMPO group may be contributing to oxidation of the backbone of **Poly-12**. The appearance of a new stretching frequency in the ATR-IR spectrum at 1725 cm^{-1} indicates the formation of a carbonyl group, a characteristic feature of oxidized PT.^{48,49} The disruption in conjugation caused by chain scission effectively decreases the polymers ability to conduct and store charge corroborating the low capacitance measurements of only 0.8 F g^{-1} .

It was demonstrated that the pre-formed **Poly-12** and **Poly-2** were deposited on electrode surfaces such as carbon during electrochemical cycling; this is a new method of depositing soluble CPs onto active electrodes. Deposition of polymers having known structures (i.e. HT regioregularity) onto electrode surfaces provides a direct correlation between structure-property relationships observed for the surface bound species. This understanding may help improve synthetic strategies towards the desired electrochemical properties of conjugated organic materials.

5.5 References

1. Suga, T. et al., *Adv. Mater.* **2009**, 21, (16), 1627-1630.
2. Suga, T.; Konishi, H.; Nishide, H., *Chem. Commun.* **2007**, (17), 1730-1732.
3. Patra, S.; Munichandraiah, N., *J. Appl. Polym. Sci.* **2007**, 106, (2), 1160-1171.
4. Marchioni, F.; Yang, J.; Walker, W.; Wudl, F., *J. Phys. Chem. B* **2006**, 110, (44), 22202-22206.
5. Laforgue, A.; Simon, P.; Sarrazin, C.; Fauvarque, J. F., *J. Power Sources* **1999**, 80, (1-2), 142-148.
6. Hussain, A. M. P.; Kumar, A., *J. Power Sources* **2006**, 161, (2), 1486-1492.
7. Laforgue, A.; Simon, P.; Fauvarque, J. F., *Synth. Met.* **2001**, 123, (2), 311-319.
8. DeLongchamp, D. M. et al., *Chem. Mater.* **2005**, 17, (23), 5610-5612.
9. Cui, H. N.; Teixeira, V.; Zhang, J.; Lee, H., *Thin Solid Films* **2006**, 515, (1), 301-306.
10. Wood, V. et al., *Adv. Mater.* **2009**, 21, (21), 2151-2155.
11. Jahn, S. F. et al., *Langmuir* **2009**, 25, (1), 606-610.
12. Aernouts, T. et al., *Appl. Phys. Lett.* **2008**, 92, (3), 33306 (1-3).
13. Novák, P.; Müller, K.; Santhanam, K. S. V.; Haas, O., *Chem. Rev.* **1997**, 97, (1), 207-281.
14. Oyaizu, K.; Nishide, H., *Adv. Mater.* **2009**, 21, (22), 2339-2344.
15. Rozantsev, E. G.; Sholle, V. D., *Synth. Int. J. Method. Synth. Org. Chem.* **1971**, (4), 190-202.
16. Ma, Z.; Bobbitt, J. M., *J. Org. Chem.* **1991**, 56, (21), 6110-6114.

17. Gheorghe, A.; Matsuno, A.; Reiser, O., *Adv. Synth. Catal.* **2006**, 348, (9), 1016-1020.
18. Luo, J. T.; Pardin, C.; Lubell, W. D.; Zhu, X. X., *Chem. Commun.* **2007**, (21), 2136-2138.
19. Wang, X. L.; Liu, R. H.; Jin, Y.; Liang, X. M., *Chem. Eur. J.* **2008**, 14, (9), 2679-2685.
20. Krishna, M. C. et al., *J. Med. Chem.* **1998**, 41, (18), 3477-3492.
21. Krishna, M. C. et al., *Proc. Natl. Acad. Sci. USA* **1992**, 89, (12), 5537-5541.
22. Búcsiová, L.; Yin, M. Z.; Chmela, Š.; Habicher, W. D., *J. Macromol. Sci., Pure Appl. Chem.* **2008**, 45, (9), 761-768.
23. Chen, X. W. et al., *Macromol. Rapid Commun.* **2007**, 28, 1792-1797.
24. Takahashi, Y. et al., *Polym. J. (Tokyo, Jpn.)* **2008**, 40, (8), 763-767.
25. Oyaizu, K.; Suga, T.; Yoshimura, K.; Nishide, H., *Macromolecules* **2008**, 41, (18), 6646-6652.
26. Nishide, H. et al., *Electrochim. Acta* **2004**, 50, (2-3), 827-831.
27. Finden, J.; Kunz, T. K.; Branda, N. R.; Wolf, M. O., *Adv. Mater.* **2008**, 20, (10), 1998-2002.
28. Rozantsev, E. G.; Sholle, V. D., *Synth. Int. J. Method. Synth. Org. Chem.* **1971**, (8), 401-414.
29. Aurich, H. G., Nitroxides. In *Nitrones, nitronates and nitroxides*, Patai, S., Rappoport, Z., Eds. John Wiley & Sons: Chichester, 1989; Vol. 2, pp 313-370.
30. Gheorghe, A. et al., *Synlett* **2006**, (17), 2767-2770.
31. Morat, C.; Rassat, A., *Tetrahedron* **1972**, 28, (3), 735-740.

32. Jang, K. S.; Ko, H. C.; Moon, B.; Lee, H., *Synth. Met.* **2005**, 150, (2), 127-131.
33. Laferrière, M.; Galian, R. E.; Maurel, V.; Scaiano, J. C., *Chem. Commun.* **2006**, (3), 257-259.
34. Banwell, C. N.; McCash, E. M., Electron Spin Resonance Spectroscopy. In *Fundamentals of Molecular Spectroscopy*, 4 ed.; McGraw-Hill Publishing Company: Berkshire, 1994; pp 245-256.
35. Banwell, C. N.; McCash, E. M., Infra-Red Spectroscopy. In *Fundamentals of Molecular Spectroscopy*, 4 ed.; McGraw-Hill Publishing Company: Berkshire, 1994; pp 55-98.
36. Inorganic Spectroscopic Methods. Brisdon, A. K., Ed. Oxford University Press: New York, 1998; p 20.
37. Whisnant, C. C.; Ferguson, S.; Chesnut, D. B., *J. Phys. Chem.* **1974**, 78, (14), 1410-1415.
38. Electrochemical Methods: Fundamentals and Applications. 2 ed.; Bard, A. J.; Faulkner, L. R., Eds. John Wiley & Sons: Hoboken, 2001.
39. Chen, J. et al., *J. Power Sources* **2006**, 159, (1), 708-711.
40. Passiniemi, P.; Osterholm, J. E., *Synth. Met.* **1987**, 18, (1-3), 637-644.
41. Stenger-Smith, J. D., *Prog. Polym. Sci.* **1998**, 23, (1), 57-79.
42. Brédas, J. L. et al., *Acc. Chem. Res.* **1999**, 32, (3), 267-276.
43. Holzer, W. et al., *Chem. Phys.* **1997**, 224, (2-3), 315-326.
44. Wang, J. X., *Electrochim. Acta* **1994**, 39, (3), 417-429.
45. Wang, J. X., *Electrochim. Acta* **1997**, 42, (16), 2545-2554.
46. Manceau, M. et al., *Polym. Degrad. Stab.* **2009**, 94, (6), 898-907.

47. Manceau, M.; Rivaton, A.; Gardette, J. L., *Macromol. Rapid Commun.* **2008**, 29, (22), 1823-1827.
48. Holdcroft, S., *Macromolecules* **1991**, 24, (17), 4834-4838.
49. Abdou, M. S. A.; Holdcroft, S., *Macromolecules* **1993**, 26, (11), 2954-2962.

CHAPTER 6 Conclusions and Future Work

6.1 *General Conclusions*

In this thesis, a series of rr-PT derivatives were prepared, functionalized post-polymerization, and characterized by NMR spectroscopy, ATR-IR spectroscopy, solution absorption/emission spectroscopy, and CV. The optical and electronic properties of the functionalized polymers were investigated to understand the effect of the attached pendant groups on the PT backbone. Detailed conclusions are presented and discussed within each chapter; general conclusions in reference to the initial objectives and in light of current research in the field are presented herein.

The relevance of the research presented in this thesis is evident from numerous applications of CPs for organic based devices,^{1,2} and in particular, rrP3AT that are synthesized via GRIM conditions in order to afford a high density of HT couplings.³⁻¹⁵ In this research, a parent PT copolymer was synthesized via GRIM polymerization conditions, which reliably and efficiently generated a regioregular polymer with extended conjugation related to the ordered structure of the backbone.

Organic electronics are developed and improved through our understanding of the structure-property relationships that extend to the bulk properties of the overall system. Generation of a diverse library of functional polymers, each with identical average chain length, polydispersity, and backbone structure is beneficial to build and expand this knowledge. Post-polymerization modification of a single reactive precursor is a useful method towards this goal.¹⁶ The Huisgen 1,3-dipolar cycloaddition reaction was used in this study to successfully attach several structurally dissimilar pendant groups to a

common parent PT precursor, reinforcing the utility of this reaction for post-polymerization modifications.

The choice of pendant groups studied in this thesis was made based on the desire to prepare materials with *in-situ* tuneable properties. The ability for a material to interconvert between two distinguishable states is especially desirable when the ability to reach both states is brought about through an environmental stimulus such as light or electrical current.¹⁷⁻²⁰ This thesis describes the attachment of two pendant groups that display different states upon stimulation with photons or electrons, which in turn may influence and modify the properties of the bulk polymer.

In the study of DTE functionalized PT, the ring opening/closing reaction of the DTE reversibly quenched the fluorescence of the conjugated backbone.²¹ The significance of this finding was the amplified nature with which the photo-induced ring closing reaction quenched the polymer fluorescence. Amplified fluorescent polymers are particularly interesting for the sensitivity they exhibit upon interaction with trace amounts of analyte.^{22,23} Modification of the DTE backbone to incorporate gated photochromic reactivity, and thus access on-off sensor applications, is discussed *vide infra*.

In the study of TEMPO functionalized PT, the anticipated high charge storage capability of the material was not achieved. Instead, the system was observed to physically degrade during CV studies. The TEMPO pendant group is a known oxidant for conversion of alcohols to aldehydes and ketones²⁴⁻²⁹ and the TEMPO group was contributing to oxidation of the PT backbone. Alternatively, it was determined that the PT backbone could be electrodeposited onto a carbon paper electrode. This facilitates a route to deposit thin polymer films on various conductive substrates with predefined

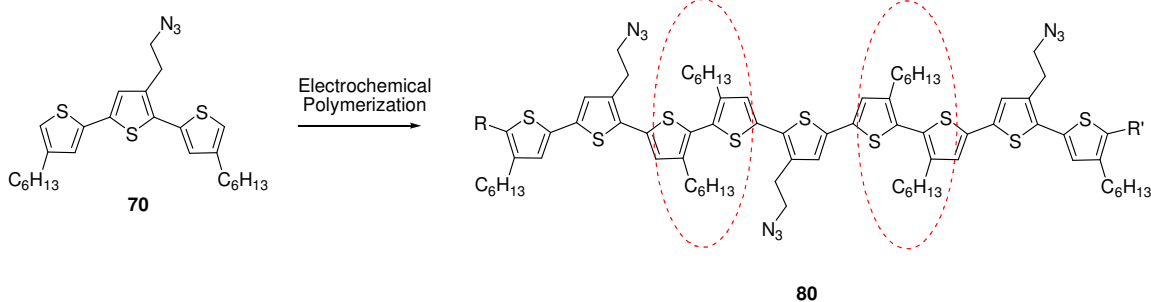
molecular structure, a currently unknown process for conventional electropolymerized species.

In conclusion, the work presented in this thesis has reinforced the beneficial application of post-polymerization functionalization. Click chemistry proved to be a simple and efficient method to generate a library of diverse functional rr-PT copolymers. This research has also expanded the family of rr-PT with a variety of functional pendant groups that can be used to further modify polymer properties *in-situ*. Additionally, the materials prepared in this work, demonstrate promising functionality for further development towards novel organic electronic applications.

6.2 *Suggestions for Future Work*

There are several potential new areas of study stemming from these results. In connection with the attempts to generate a conductive thin film from TEMPO functionalized PT, it may be interesting to first generate the polymer film and subsequently attach the TEMPO group. This may be achieved through several approaches. The first approach would be to electropolymerize the azide functionalized terthiophene (**70**) onto an electrode. The electropolymerization of terthiophene derivatives is generally easier to accomplish than polymerization of the monomer species due to a lower oxidation potential. As well, the azide group has been shown to withstand the experimental conditions of an electrochemical polymerization and would be available for subsequent Click modifications with TEMPO acetylene (**74**).³⁰ This would, however, lead to a significant number of HH/TT couplings (Scheme 6-1), decreasing conjugation along the backbone, and consequently decreasing the conductivity and charge storage capability of the material.

Scheme 6-1



A second approach would be to prepare a thin polymer film of the azide functionalized PT (**Poly-2**) via spin coating, drop casting, or via the electrochemical deposition demonstrated in Chapter 5, and perform the Click reaction on this surface. Click reactions are known to be tolerant of a large variety of solvents,³¹ therefore, solubilization of the film after deposition could easily be avoided with the proper solvent choice. It may also be interesting to apply a variation of the Click reaction recently demonstrated by Stoddard *et al.*, in which they were able to direct-write coupling reactions between an acetylene and azide using a copper coated AFM tip.³² This process was carried out on an azide terminated self assembled monolayer (SAM) on a silicon surface. Such an approach would not only provide a better understanding of the density of TEMPO groups present at the surface, but should eliminate oxidation and therefore maintain the extended HT regioselectivity of **Poly-2**.

Another interesting avenue of future work would be the use of the amplified fluorescence quenching afforded by the ring closing reaction of DTE functionalized PT (**Poly-4**) for application in an "On-Off" organic sensor.¹⁷ This would require gated photochromic reactivity, a property through which the irradiation of any given wavelength of light does not induce colour changes unless an additional external

stimulant (heat,³³ light of a different wavelength,^{34,35} or chemical^{36,37}) is present. As a sensor, the DTE would have to be modified to only allow ring-closing reaction upon binding of an analyte of interest (Figure 6-1). The benefit of the amplified fluorescent quenching demonstrated by **Poly-4**, would be that only minimal concentrations of analyte would need to bind to result in 100% quenching and essentially turn off the polymer fluorescence.

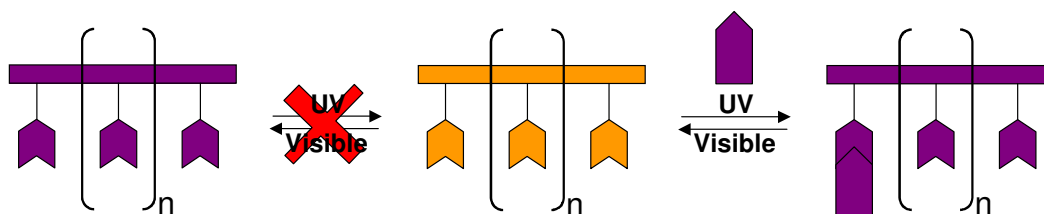
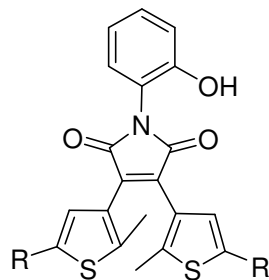


Figure 6-1. Schematic of a gated sensor based on DTE photoinduced ring-closing fluorescence quenching in which DTE (👉) can only undergo the ring-closing reaction upon binding of the analyte (👈).

Irie *et al.* have recently prepared a chemically gated DTE derivative (**81**, Chart 6-1) which was demonstrated to undergo typical photochromic reactions only upon esterification of the hydroxyl group.³⁸ In the synthesis proposed below (Scheme 6-2), this DTE derivative could be modified to allow tethering to **Poly-2** via the Click reaction. It should follow that upon esterification of the hydroxyl group, the allowed ring closing reaction of the DTE moiety would initiate fluorescence quenching along the polymer chain, thus acting as a On-Off sensor.

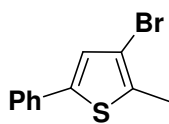
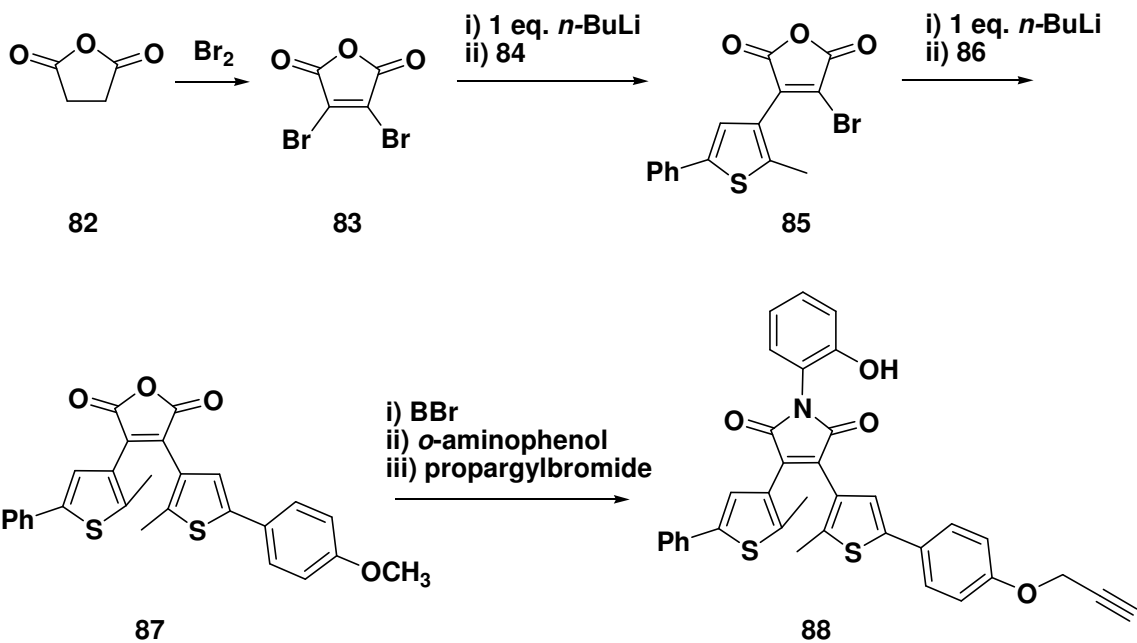
Chart 6-1



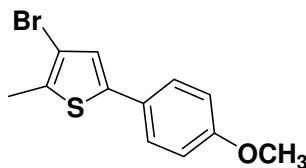
81

R = CH₃, Ph

Scheme 6-2



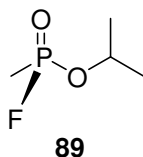
84



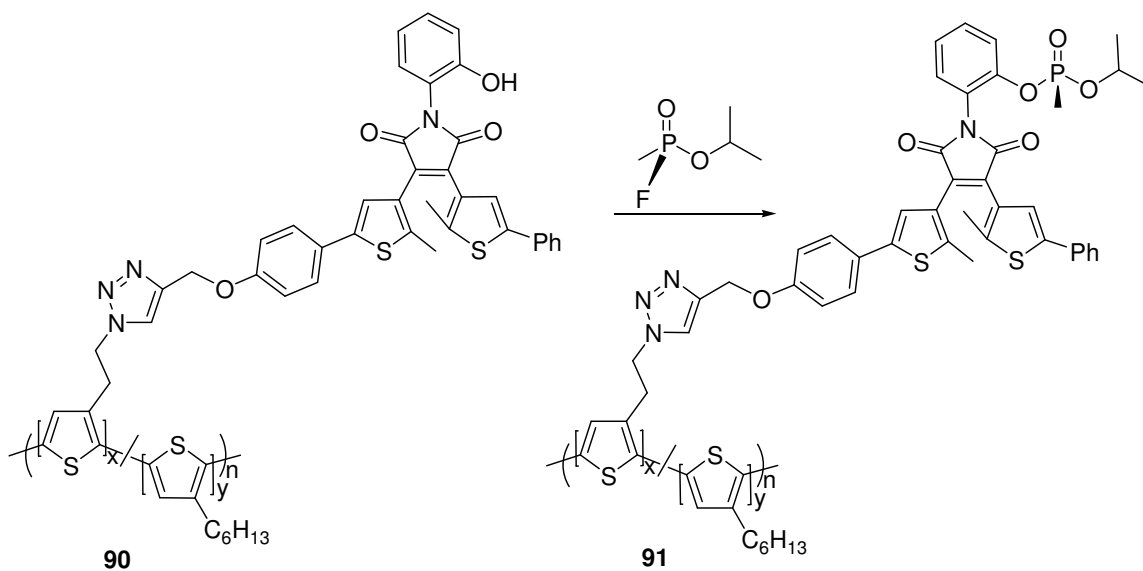
86

An interesting application of this material would be to act as a sensor for the highly toxic fluorinated phosphonate sarin (Chart 6-2).³⁹ It is reported that even very low concentrations can be fatal and it is estimated to be approximately 500 times more toxic than cyanide. Once heavily used as a chemical weapon this nerve agent still leaks from existing residual chemical stockpiles.⁴⁰ Safety concerns associated with these leaks could benefit from such a sensor. It is proposed that upon reaction with compound **90**, trace quantities of sarin would permit photo-induced ring-closing and thus quench polymer fluorescence (Scheme 6-3).

Chart 6-2



Scheme 6-3



6.3 References

1. Friend, R. H. et al., Applications of Conducting Polymers. In *Handbook of Conducting Polymers*, 2 ed.; Skotheim, T. A., Elsenbaumer, R. L., Reynolds, J. R., Eds. Marcel Dekker: New York, 1998; pp 823-1073.
2. Handbook of Thiophene-Based Materials: Applications in Organic Electronics and Photonics. Perepichka, I. F.; Perepichka, D. F., Eds. John Wiley & Sons: Chichester, 2009; Vol. 2.
3. Han, Y. K.; Lee, Y. J.; Huang, P. C., *J. Electrochem. Soc.* **2009**, 156, (4), K37-K43.
4. Zoombelt, A. P. et al., *Thin Solid Films* **2008**, 516, (20), 7176-7180.
5. Zhang, Y.; Tajima, K.; Hirota, K.; Hashimoto, K., *J. Am. Chem. Soc.* **2008**, 130, (25), 7812-7813.
6. Zhang, Q. L.; Cirpan, A.; Russell, T. P.; Emrick, T., *Macromolecules* **2009**, 42, (4), 1079-1082.
7. Xue, C. H.; Luo, F. T.; Liu, H. Y., *Macromolecules* **2007**, 40, 6863-6870.
8. Richard, F. et al., *Macromol. Rapid Commun.* **2008**, 29, (11), 885-891.
9. Ouhib, F. et al., *Macromolecules* **2008**, 41, (24), 9736-9743.
10. Ouhib, F. et al., *Thin Solid Films* **2008**, 516, (20), 7199-7204.
11. Ouhib, F. et al., *J. Polym. Sci., Part A: Polym. Chem.* **2008**, 46, (22), 7505-7516.
12. Miyanishi, S.; Tajima, K.; Hashimoto, K., *Macromolecules* **2009**, 42, (5), 1610-1618.
13. Li, Y. W. et al., *J. Polym. Sci., Part A: Polym. Chem.* **2008**, 46, (12), 3970-3984.

14. Chang, Y. T.; Hsu, S. L.; Su, M. H.; Wei, K. H., *Adv. Funct. Mater.* **2007**, 17, 3326-3331.
15. Bricaud, Q.; Cravino, A.; Leriche, P.; Roncali, J., *Sol. Energy Mater. Sol. Cells* **2009**, 93, (9), 1624-1629.
16. Gauthier, M. A.; Gibson, M. I.; Klok, H. A., *Angew. Chem. Int. Ed.* **2009**, 48, (1), 48-58.
17. de Silva, A. P. et al., *Chem. Rev.* **1997**, 97, (5), 1515-1566.
18. Collin, J.-P.; Kern, J.-M.; Raehm, L.; Sauvage, J.-P., Metallo-Rotaxanes and Catenanes as Redox Switches: Towards Molecular Machines and Motors. In *Molecular Switches*, Feringa, B. L., Ed. Wiley-VCH GmbH: Weinheim, 2001; pp 249-280.
19. Irie, M., Photoswitchable Molecular Systems Based On Diarylethenes. In *Molecular Switches*, Feringa, B. L., Ed. Wiley-VCH GmbH: Weinheim, 2001; pp 37-61.
20. Lukas, A. S.; Wasielewski, M. R., Approaches to a Molecular Switch Using Photoinduced Electron and Energy Transfer. In *Molecular Switches*, Feringa, B. L., Ed. Wiley-VCH GmbH: Weinheim, 2001; pp 1-35.
21. Finden, J.; Kunz, T. K.; Branda, N. R.; Wolf, M. O., *Adv. Mater.* **2008**, 20, (10), 1998-2002.
22. Adhikari, B.; Majumdar, S., *Prog. Polym. Sci.* **2004**, 29, (7), 699-766.
23. Thomas, S. W.; Joly, G. D.; Swager, T. M., *Chem. Rev.* **2007**, 107, (4), 1339-1386.
24. Gheorghe, A. et al., *Synlett* **2006**, (17), 2767-2770.

25. Gheorghe, A.; Matsuno, A.; Reiser, O., *Adv. Synth. Catal.* **2006**, 348, (9), 1016-1020.
26. Luo, J. T.; Pardin, C.; Lubell, W. D.; Zhu, X. X., *Chem. Commun.* **2007**, (21), 2136-2138.
27. Ma, Z.; Bobbitt, J. M., *J. Org. Chem.* **1991**, 56, (21), 6110-6114.
28. Sheldon, R. A.; Arends, I., *Adv. Synth. Catal.* **2004**, 346, (9-10), 1051-1071.
29. Wang, X. L.; Liu, R. H.; Jin, Y.; Liang, X. M., *Chem. Eur. J.* **2008**, 14, (9), 2679-2685.
30. Bu, H. B. et al., *Chem. Commun.* **2008**, (11), 1320-1322.
31. Binder, W. H.; Kluger, C., *Curr. Org. Chem.* **2006**, 10, (14), 1791-1815.
32. Paxton, W. F.; Spruell, J. M.; Stoddart, J. F., *J. Am. Chem. Soc.* **2009**, 131, (19), 6692-6694.
33. Irie, M.; Eriguchi, T.; Takada, T.; Uchida, K., *Tetrahedron* **1997**, 53, (36), 12263-12271.
34. Murakami, M. et al., *J. Am. Chem. Soc.* **2004**, 126, (45), 14764-14772.
35. Uchida, M.; Irie, M., *J. Am. Chem. Soc.* **1993**, 115, (14), 6442-6443.
36. Irie, M.; Miyatake, O.; Uchida, K.; Eriguchi, T., *J. Am. Chem. Soc.* **1994**, 116, (22), 9894-9900.
37. Matsui, F. et al., *Chem. Lett.* **1994**, (10), 1869-1872.
38. Ohsumi, M.; Fukaminato, T.; Irie, M., *Chem. Commun.* **2005**, (31), 3921-3923.
39. Wikipedia, The Free Encyclopedia Home Page.
http://en.wikipedia.org/wiki/Main_Page. Sarin. <http://en.wikipedia.org/wiki/Sarin>
(accessed Aug 20 2009).

40. Drogin, B. Clock Ticks Down on a Deadly Chemical Stockpile. *Los Angeles Times*, Aug 23 2009, <http://www.latimes.com/news/nationworld/nation/la-na-chemical23-2009aug23,0,2941213.story> (accessed Aug 20 2009).